Characterization and prediction of ephemeral gully erosion in Wallonia

Alexandre Maugnard

Thèse présentée en vue de l'obtention du titre de Docteur en Sciences Agronomiques et Ingénierie Biologique

March 2015

Université Catholique de Louvain
Earth and Life Institute - Environmental Sciences
Louvain-la-Neuve
Belgique

THESIS EXAMINING BOARD

SUPERVISOR

Prof. C. Bielders (UCL, Belgium)

JURY PRESIDENT

Prof. M. Vanclooster (UCL, Belgium)

JURY MEMBERS

Prof. P. Defourny (UCL, Belgium)
Prof. A. Degré (ULg, Belgium)
Prof. J. Poesen (KUL, Belgium)
Mr. D. Torri (CNR, Italy)
Dr. K. Vandaele (Watering van Sint-Truiden, Belgium)

Acknowledgements

Cela m'a toujours paru difficile d'écrire des remerciements. Non pas qu'ils soient superflus, bien loin s'en faut, mais plutôt que cela me semble un exercice délicat. Cependant, puisqu'il en est ainsi, je me lance…

Parmi les personnes qui ont contribué à l'achèvement de cette thèse, il y a bien sûr celles qui m'ont conseillé, aidé et épaulé dans mon entourage professionnel. Il y a en premier lieu mon promoteur. Je tiens donc à remercier chaleureusement Charles pour sa confiance et son aide. Je n'aurais pu souhaiter de meilleur promoteur. J'ai apprécié ta rigueur, ta franchise, tes conseils avisés et la dimension humaine de ton encadrement. Je tiens également à remercier les membres de mon comité d'accompagnement et/ou jury à savoir Pierre Defourny, Aurore Degré, Jean Poesen, Dino Torri et Karel Vandaele. Vous m'avez tous permis d'améliorer ce document par vos remarques pertinentes. Je voudrais aussi remercier Marnik de m'avoir fait le plaisir d'accepter la présidence du jury. Il y a ensuite de nombreuses personnes qui ont participé à la réussite de cette thèse de près ou de loin. Merci donc à mes collègues du GERU, contemporains et passés, pour ces quelques 6 années où j'ai été heureux de venir m'assoir devant mon ordinateur. Merci également à mes joyeux collègues de la Direction du Développement Rural du SPW pour cette chaleureuse ambiance de travail. Je tiens à ce propos à remercier spécialement la DDR pour son financement. Je remercie également mes collègues GISERiens qui ont tous contribué à cette thèse. Enfin, il y a, non des moindres, les amis et la famille qui au jour le jour et de par leur soutien ont fait que cette lourde tâche se concrétise. Parmi ces personnes je pense en particulier à Caroline, Lila, Samuel et Zacharie.

Contents

Acknowledgements	i
Contents	iii
List of Figures	vii
List of Tables	xii
List of abbreviations and variables	xiv
1 Context and objectives	**1**
1.1 Background	3
1.2 Research needs	4
1.3 Objectives	7
1.4 Outline of the thesis	7
2 Literature review	**11**
2.1 Definition of gully erosion and gully types	13
2.2 Ephemeral gully erosion in agricultural settings	15
2.3 Remote sensing techniques to study ephemeral gully erosion	17
2.4 Ephemeral gully initiation points and topographic threshold	19
2.5 Factors controlling ephemeral gully end	22
2.6 Prediction of ephemeral gully occurrence	24
3 Material and methods	**27**
3.1 Study sites and related gully databases	29
3.1.1 Characteristics and spatial variability of ephemeral gully erosion	31
3.1.2 Temporal variability of ephemeral gully erosion	36
3.1.3 Uncertainty assessment of ephemeral gully erosion when using aerial photographs and prediction of ephemeral gully erosion	37
3.2 Gully databases creation	38
3.2.1 Gully identification and digitizing	38
3.2.2 Gully classification	38
4 Uncertainty assessment of ephemeral gully identification, characteristics and topographic threshold when using aerial photographs in agricultural settings	**41**
4.1 Introduction	43
4.2 Material and methods	46
4.2.1 Ephemeral gully identification and gully digitizing	46
4.2.2 Ephemeral gully classification	48

4.2.3 Ephemeral gully characteristics 49
4.2.4 Topographic thresholds 49
4.3 Results 51
4.3.1 Ephemeral gully characteristics and classification 51
4.3.2 Location of the ephemeral gully heads 56
4.3.3 Topographic threshold analysis 57
4.4 Discussion 62
4.4.1 Ephemeral gully characteristics and classification 62
4.4.2 Location of the ephemeral gully heads 66
4.4.3 Topographic threshold analysis 66
4.5 Conclusions 73

5 Characteristics and spatio-temporal variability of ephemeral gully erosion in Wallonia 75
5.1 Introduction 77
5.2 Material and methods 77
5.3 Results and discussion 78
5.3.1 Characteristics of ephemeral gullies in the study sites 78
5.3.2 Assessing the recurrence of ephemeral gully erosion 83
5.4 Conclusions 85

6 Analysis of the topographic threshold for the initiation of ephemeral gullies 87
6.1 Introduction 89
6.2 Material and methods 91
6.3 Results and discussion 92
6.3.1 Comparisons of the thresholding methods 92
6.3.2 Regional differences in the topographic thresholds 97
6.3.3 Comparison with topographic thresholds from other areas 101
6.3.4 Temporal stability of the topographic threshold 104
5.4 Conclusions 107

7 What factors cause ephemeral gullies to end? 109
7.1 Introduction 111
7.2 Material and methods 112
7.2.1 Databases used 112
7.2.2 Characterization of the main factors controlling ephemeral gully ending points 113
7.2.3 Critical slope and topographic thresholds 113
7.2.4 Probabilistic approach to predict gully ending points controlled by topography 114
7.3 Results 115
7.3.1 Regional variability of the main factors controlling ephemeral gully ending points 115
7.3.2 Topography-controlled ephemeral gully ending points 118

7.3. Vegetation-controlled ephemeral gully ending points 125
7.3.4 Linear element- and headland-controlled ephemeral gully ending points 127
7.4 Discussion 129
7.4.1 Topography-controlled ephemeral gully ending points 129
7.4.2 Vegetation-controlled ephemeral gully ending points 132
7.4.3 Ephemeral gully ending points controlled by linear landscape elements and headlands 132
7.4.4. Regional variability of the main factors controlling ephemeral gully ending points 133
7.5 Conclusions 134

8 How effective are hydraulic and topographic indicators at predicting the occurrence of ephemeral gullies in agricultural settings? 137
8.1 Introduction 139
8.2 Material and methods 141
8.2.1 Study area and gully database 141
8.2.2 Baseline data 142
8.2.3 Calculation of the topographic and hydraulic indicators 142
8.2.4 Performance assessment of the topographic and hydraulic indicators to predict ephemeral gully location 146
8.2.5 Calibration and validation of the best indicator to predict ephemeral gully location 149
8.3 Ephemeral gully erosion indicators tested 151
8.3.1 Topographic indicators 151
8.3.2 Runoff volume 151
8.3.3 Peak discharge 155
8.3.4 Stream power 156
8.3.5 Flow velocity 156
8.3.6 Unit stream power 158
8.3.7 Flow shear stress 159
8.4 Results 160
8.4.1 Calibration of the λ parameter of the NRCS Curve Number method 160
8.4.2 Performance assessment of the topographic and hydraulic indicators to predict ephemeral gully location 161
8.4.3 Calibration and validation of the best indicator to predict ephemeral gully location 167
8.5 Discussion 172
8.5.1 Performance assessment of the topographic and hydraulic indicators to predict ephemeral gully location 172
8.5.2 Calibration and validation of the best indicator to predict ephemeral gully location 174
8.6 Conclusions 176

9 Conclusions **177**
9.1 Main findings of the thesis 179
9.2 Main recommendations for policy 182
9.3 Perspectives for future research 184

Appendix – Derivation of Equation 8-16 **187**

References **191**

List of publications **205**

Summary **207**

List of Figures

1-1: Thesis flowchart……. 9

2-1: Topographic thresholds (solid lines) for a fictive dataset defined using the A) Patton & Schumm (1975) method based on the lowermost points, B) Vanwalleghem et al. (2005a) method as the translation of the orthogonal regression (dotted line) until the lowermost point while keeping the slope constant, C) Vandekerckhove et al. (1998) method as the lower limit of the 95 % confidence interval (dashed lines) of the orthogonal regression (dotted line) and D) Torri and Poesen (2014) method based on a *b* value (Equation 2-1) of 0.38 and the lowermost points……..21

3-1: Location of the study sites in Wallonia. 1) Loamy area, 2) Famenne, 3) Jurassic area, 4) Condroz/Loamy area, 5) Red dashed zone was located in Loamy area…….....32
3-2: Types of ephemeral gullies identified in the present study. (A) Type 1: gullies located on a well-defined runoff flow concentration axis (Picture: GISER); the contour lines on the scheme indicate that the gully is on a thalweg. (B) Type 2: slope gullies located on a slope without apparent flow concentration axis (Picture: GISER). (C) Examples of Type 3 gully. On the scheme, gully resulted from flow concentration due to a bank. On the picture (Bielders, C.), gullies formed in a wheel track. Arrows indicate the water flow direction…..39

4-1: (a) Gully with deposition fan; (b) deposition at the end of furrows against the headland and field border; (c) recurrent linear objects with a near constant spacing and width, probably corresponding to wheel tracks or caused by a problem with the drilling machine……..48
4-2: Number of gullies per gully type identified by each of the 11 operators…….52
4-3: Sum total length of gullies as a function of the operator and the gully class. The table below the graph reports mean gully length and standard deviation as a function of the operator……...……52
4-4: Mean standard distance of the gully head locations as a function of the gully type, for gullies identified by at least six operators……..57
4-5: Mean standard distance of the gully head locations as a function of the number of operators who identified them……..57

4-6: Topographic threshold for gully initiation calculated for each of the 11 operators by the five different methods: PS75, VW05, VDK98, DT14 and QR. The bold dashed line represents the threshold calculated for the compound dataset (gullies identified by at least six operators).....58
4-7: Relation between the number of gullies in a given dataset and the lowest quantile that could be used for deriving the topographic threshold line through quantile regression. Each point corresponds to a different operator……..60
4-8: Slope and contributing area values at the gully heads of all Type 1 gullies. The size of the symbol is related to the number of operators who identified a given gully. Filled symbols relate to gullies whose contributing areas were not crossed by a road whereas open symbols relate to gullies whose contributing areas were crossed by a road……61
4-9: Four objects digitized as gullies which are not gullies: (a) deposition in the furrows crossing a depression, (b) flow concentration axis without erosion signs, (c) diffuse erosion, (d) rills…….65
4-10: Relation between the number of gullies in a dataset and the *a* value (Equation 2-1) of the topographic threshold line derived by quantile regression. Each point corresponds to a different operator……...68
4-11: Topographic thresholds derived by quantile regression (solid lines), the method of Vandekerckhove et al. (1998) (dashed lines) and the method of Torri and Poesen (2014) (dotted lines) for the 11 operator datasets (Op.) as well as for the compound dataset (≥ 6) consisting of all gullies identified by at least six operators and whose contributing areas are not crossed by a road. Regression coefficients are shown in Table 4-3…..70

5-1: Daily precipitation from April to July in (A) 1999, (B) 2006 and (C) 2009 in study site #4……..……....84

6-1: Comparison of different thresholding methods for a fictional dataset. A) Patton & Schumm (1975) method: multiple thresholds may exist. B) Patton & Schumm (1975) method: sensitivity to extreme values. The three lines are drawn after excluding 0 (solid line), 1 (dashed line) or 2 (dotted line) extreme data points (closed symbols). C) Methods based on orthogonal regression. Solid line: orthogonal regression. Dashed line: translation of orthogonal regression until the lowermost point while keeping the slope constant (Vanwalleghem et al., 2005a). Dotted line: lower limit of the 95 % confidence interval of the orthogonal regression (Vandekerckhove et al., 1998). D) Torri and Poesen method (2014): constant slope...……..…….……..90
6-2: Differences between the contributing area values obtained by hand delineation on a contour map (CAh, reference value) and the contributing area obtained from the flow accumulation raster values (CAf). The latter were obtained by searching for the largest flow

accumulation value within a given radius around the gully head location.....92
6-3: Five thresholding methods applied to the gully head datasets from (A) the Loamy area, (B) the Famenne and (C) the Jurassic area. The quantile regression is calculated for α = 0.06, 0.17, and 0.13 for the three areas, respectively. These values correspond to the most extreme quantiles for which the regression parameters can be estimated with acceptable precision. Note that for the Loamy area, the Patton and Schumm (1975) threshold and the Torri and Poesen (2014) threshold overlap. For the Famenne, the Patton and Schumm (1975) threshold and the Vanwalleghem et al. (2005a) threshold overlap.…….94
6-4: Estimates of *a* and *b* parameters of the topographic threshold (Eq. 2-1) using quantile regression, for quantiles comprised between 0.01 and 0.5 (solid lines) for the Loamy area (A and B), the Famenne (C and D) and the Jurassic area (E and F). Dotted lines are the 90% confidence intervals. The dashed vertical lines mark the most extreme quantile for which the confidence intervals of both regression parameters can be estimated with acceptable precision……..96
6-5: Relation between the highest quantile which can be used with acceptable precision for quantile regression and the number of gullies in each dataset, for the six datasets used in this study……...97
6-6: Comparison of the best values of (A) *a* (intercept) and (B) *b* (slope) parameters of the topographic threshold (Eq. 2-1) for the study sites #1 to #3 (Figure 3-1). The best values were obtained by quantile regression for the highest possible quantile for which the 90% confidence interval can be extracted with acceptable precision estimated. Vertical bars correspond to the 90% confidence intervals computed with the rank-score test method……...98
6-7: Estimates of *a* and *b* parameters of the topographic threshold (Eq. 2-1) using quantile regression, for quantiles comprised between 0.01 and 0.5 (solid lines) for area #4 (Figure 3-1) for 1999 (A and B), 2006 (C and D) and 2009 (E and F). Dotted lines are the 90% confidence intervals. The dashed vertical lines mark the most extreme quantile for which the confidence intervals of both regression parameters can be estimated with acceptable precision…….105
6-8: Topographic threshold determined with the quantile regression method for area #4 (Figure 3-1) for three different years. Quantile α = 0.07 for 1999 (PPNC), 0.06 for 2006–2007 and 0.13 for 2009–2010)…….106
6-9: Comparison of the best values of a (A) and b (B) parameters of the topographic threshold (Eq. 2-1) for area #4 (Figure 3-1) for three different years. The best values were obtained by quantile regression for the highest possible quantile for which the 90% confidence interval could be estimated with acceptable precision. Vertical bars correspond to the 90% confidence…….....107

7-1: Examples of gully ending points controlled by (1) topography, (2) change in vegetation cover (in this case, from sugar beet to grassland), (3) linear element (here, road associated with a bank) and (4) headland. Dashed lines indicate ephemeral gullies and crosses indicate their ending points……116
7-2: Relations between (1) the proportion of vegetation- and linear element-controlled gully ending points and the mean size of cultivated fields; (2) the proportion of linear element-controlled gully ending points and the density of linear elements present alongside cropland. Each round symbol corresponds to an agricultural area. Data from the Condroz/Loamy area are split by year…….....117
7-3: Distributions of slope values for gully ending point grid cells and gully grid cells in the four study regions. Vertical dashed lines correspond to the critical slope thresholds…….....119
7-4: Topographic thresholds for topography-controlled ending points (continuous lines) and for gully initiation (dashed lines; Chapter 6) and critical slope thresholds for topography-controlled ending points. The quantiles α = 0.95, 0.76 and 0.97 were used for ending point topographic thresholds of the Loamy area, the Jurassic area and the Condroz/Loamy area, respectively. For initiation topographic thresholds, quantiles α = 0.06, 0.17, 0.13 and 0.05 of the Loamy area, the Famenne, the Jurassic area and the Condroz/Loamy area…….120
7-5: Logistic regressions applied to the datasets of the Loamy (Eq. 7-1) and Condroz/Loamy areas (Eq. 7-2). Dot symbols are gully grid cells whereas round symbols correspond to observed topography-controlled gully ending points……...123
7-6: Distributions of the topographic parameters used for the logistic regression in the Loamy area……...124
7-7: Distribution of slope values at gully ending points controlled by vegetation as a function the vegetation type in the Loamy and Condroz/Loamy areas……..126

8-1: Semi-circular cross-section of a concentrated flow axis and associated parameters……..…….....145
8-2: The study area divided into the 14 aerial photographs extents. Zones #3, #8 and #12 were used for to compare the topographic and hydraulic indicators. The remaining zones were then used to validate the most relevant indicator…….147
8-3: Examples of ROC Curves. Bold line: perfect ROC curve (AUC = 1), all the positives can be separated from the negatives. Dashed line: No discrimination between positives and negative (AUC = 0.5). ROC curves can vary between those two extreme situations such as the dotted line (AUC = 0.75)……149
8-4: Best threshold value of the indicator to discriminate between gullied and ungullied grid cells……..…….150

8-5: Relation between the observed runoff volumes and those simulated using the NRCS Curve Number method with λ estimated using Equation 8-28. The dashed line corresponds to the 1:1 line……161
8-6: Rescaled topographic indicators and runoff volume, peak discharge and unit stream power in zone #12 (Figure 8-2)……162
8-7: Rescaled flow velocity indicators (V_1 and V_2, respectively A and B; Equations 8-13 and 8-20), rescaled unit stream power indicators (U_1 and U_2, respectively C and D; Equations 8-21 and 8-22) and rescaled flow shear stress indicators (Ts_1 and Ts_2, respectively C and D; Equations 8-23 and 8-24), in zone #12 (Figure 8-2)..……...……...163
8-8: ROC curves depending on the topographic and hydraulic indicators and their relative AUC. Note that the curves related to the peak discharge and the flow velocity (V_2) perfectly overlap…….……...165
8-9: Runoff volumes and observed ephemeral gullies in the calibration area (zones A) #3,B) #8 and C)#12; Figure 8-2).……168
8-10: Distributions of the runoff volume for ungullied and gullied grid cells in the calibration area (zones #3, #8 and #12; Figure 8-2)….....169
8-11: Runoff volumes and observed ephemeral gullies in three zones of the validation area (zones A) #2,B) #13 and C)#0; Figure 8-2)……171

A-1: Relation between log(H) and log($\frac{Q*n}{S^{0.5}}$) for a radius of 1000 m…..189
A-2: Relation between the a coefficient and the semi-circular cross section radius……190
A-3: Relation between the b coefficient and the semi-circular cross section radius……190

List of Tables

3-1: Thesis objectives, and related gully databases and study sites. The aerial photographs datasets are also mentioned……..……..30
3-2: Study sites and aerial photographs used…….33
3-3: Distributions of soil textures and rock fragment contents in volume across the four study sites used for the characterization of ephemeral gully erosion……..35

4-1: Distribution of the 259 digitized ephemeral gullies per gully class as a function of the number of operators that identified a given gully. [1]: Ephemeral gullies located on a well-defined runoff flow concentration axis (Type 1), [2]: Ephemeral gullies located on planar hillslope sections without apparent flow concentration axis (Type 2), [3]: Ephemeral gullies resulting from linear elements (Type 3), [1 or 2], [2 or 3], [1 or 3]: Ephemeral gullies which were classified about equally by the operators in two different classes (see text)……..……...55
4-2: Distribution among the three ephemeral gully types of the ephemeral gullies dominantly classified as Type 1, as a function of the number of operators that identified a given gully. The distribution reflects the classification of each gully by each individual operator. Only ephemeral gullies digitized by at least six operators are considered……...56
4-3: Values of the *a* and *b* coefficients of the topographic threshold lines (Equation 2-1) for each of the 11 operator datasets and five thresholding methods. Only Type 1 ephemeral gullies whose contributing areas are not crossed by roads were considered. The quantile α used for the quantile regression method is also shown. The compound dataset corresponds to all Type 1 gullies identified by six operators or more and whose contributing areas are not crossed by roads……59
4-4: Re-interpretation by the lead author of the nature of the 103 objects identified as gullies by a single operator……...64

5-1: Distribution of the number of gullies by type (Figure 3-2) and their mean length (mean ± SD) for each study site…...…….79
5-2: Frequency and density of ephemeral gullies per acreage of agricultural land or cropland for each study site.……..80
5-3: Frequency and density of gullies for different crop types…….....82

6-1: *a* and *b* parameters of the topographic thresholds (Eq. 2-1) obtained by the Patton and Schumm (1975) method, the Torri and Poesen (2014) method, the orthogonal regression method as implemented by

Vandekerckhove et al. (1998) or Vanwalleghem et al. (2005a), and the quantile regression method……..100
6-2: Parameters *a* and *b* of the topographic thresholds (Eq. 2-1) for ephemeral gullies reported by various studies. The parameters were obtained by the method of Patton and Schumm (1975) (PS) or the orthogonal regression method (OR, Vandekerckhove et al., 1998 or Vanwalleghem et al., 2005a)……...102

7-1: Total number and proportion of the different factors causing gullies to end in the 4 study areas……116
7-2: Mean local slope (± standard deviation; SD) and critical slope threshold of topography-controlled gully ending points as a function of the agricultural area……...119
7-3: Confusion matrices when classifying observed gully or gully ending point grid cells using the critical slope threshold or the topographic threshold for each agricultural area. NO E = gully grid cell excluding ending points, E = gully ending point……..……121
7-4: Distribution of vegetation types observed at the downstream end of the plot border for vegetation-controlled gully ending points…..…….125
7-5: Effect of vegetation transitions on the end of ephemeral gullies…..…127
7-6: Types of linear elements controlling gully ending in the four study areas…….128
7-7: Density of different linear landscape elements present alongside cropland in the four study areas……..…….128

8-1: List of gully erosion indicators and required parameters…….....143
8-2: Confusion matrix to compare the predicted ungullied and gullied grid cells to the "true" ungullied and gullied grid cells when defining a threshold value above which gullying is expected. c, d, e and f can be expressed either in terms of number of grid cells, or as a percentage of the total number of grid cells……...148
8-3: Parameters used to adjust the CN value for each grid cells (Equation 8-9) depending on the crop type and the hydrological soil group……...154
8-4: Watersheds and rainfall-runoff volume data used for the calibration of the λ parameter of the NRCS Runoff Curve Number method…….155
8-5: AUC values and associated p-value of the test AUC < > 0.5.…….164
8-6: P-values resulting from to the two by two comparison tests for significant differences of the AUC values……...166
8-7: Threshold values and AUC of the related ROC curves……...169
8-8: Probability of gully occurrence depending on the runoff volume in the calibration area…….……170
8-9: Probability of gully occurrence in the validation area based on the runoff volumes classes defined at Table 8-6……...170

List of abbreviations and variables

a	Coefficient of the topographic threshold equation [-]
A	Contributing area [ha]
A_{m1}	Wetted cross section for a semi circular cross section [m²]
A_{m2}	Wetted cross section for a rectangular cross section [m²]
A_s	Unit contributing area [$m^2\ m^{-1}$]
AUC	Area Under Curve
B	Exponent of the topographic threshold equation [-]
c	Number of true positives
c_1	coefficient [-]
c_2	coefficient [-]
C_c	Cover crop percentage [%]
C_r	Crusting stage [-]
CN	Curve Number [-]
CN_{bare}	Curve Number for a bare soil [-]
CN_{max}	Maximum Curve Number [-]
CN_{min}	Minimum Curve Number [-]
CN_w	Weighted Curve Number [-]
d	Number of false positives
d_{50}	Median sediment diameter [m]
D_c	Detachment rate [$kg\ m^{-2}\ s^{-1}$]
e	Number of false negatives
f	Number of true negatives

g	Gravitational acceleration [m s^{-2}]
H_1	Water depth [mm]
H_2	Water depth [mm]
H_r	Runoff depth [mm]
I	Topographic index [m^b]
I_a	Initial abstraction [mm]
k	Constant [-]
K_c	Soil erodibility [s m^{-1}]
l	Flow length [m]
n	Gauckler-Manning coefficient [-]
n_a	Part of the Gauckler-Manning coefficient related to vegetation, obstructions and surface irregularities [-]
n_b	Part of the Gauckler-Manning coefficient related to grain size [-]
n_s	Part of the Gauckler-Manning coefficient related to soil roughness [-]
n_v	Part of the Gauckler-Manning coefficient related to vegetation [-]
p	Constant [-]
P	Wetted perimeter [m]
Pl	Rainfall depth [mm]
PPNC	Plans Photographiques Numériques Communaux
Q	Discharge [m^3 s^{-1}]
Q_p	Peak discharge [m^3 s^{-1}]
r	Radius [m]
ROC	Receiving Operating Characteristics
S	Slope gradient [m m^{-1}]
S_{CN}	Maximum potential retention [mm]
t_c	Time of concentration [s]

U_1	Unit stream power [m s^{-1}]
U_2	Unit stream power [m s^{-1}]
V_1	Flow velocity [m s^{-1}]
V_2	Flow velocity [m s^{-1}]
V_r	Runoff volume [m^3]
W	Gully width [m]
Y	land slope [%]
λ	I_a/S_{CN}
Υ	Specific weight of water [N m^{-3}]
Ω	Stream power [W m^{-2}]
Θ	Angle [rad]
τ	Shear stess [N m^{-2}]
τ_c	Critical shear stress [N m^{-2}]
τ_{s1}	Flow shear stress acting on soil [N m^{-2}]
τ_{s2}	Flow shear stress acting on soil [N m^{-2}]
ω’	Runoff energy rate per unit bed area [W m^{-1}]
ω_c’	Critical runoff energy rate per unit bed area [W m^{-1}]

1 Context and objectives

1.1 Background

Gullies are channels caused by water erosion during concentrated runoff. Such channels are considered to be gullies if their cross section is at least 929 cm² or 1 ft² (Hauge, 1977). Gullies are generally wider, deeper and longer than rills and often recur at the same location. Gullies that can be partially or totally erased and filled by tillage operations are called ephemeral gullies. Ephemeral gully erosion deserves special attention because it is responsible for large soil losses and hampers agricultural traffic. It also causes severe damage to crops both in the gullied area as well as in the sediment deposition fan at the downstream end of the gully. It contributes to sedimentation in ponds and increases the silting rate of water bodies. Depending on rainfall and site conditions, soil loss rates between 1 and 65 t ha^{-1} yr^{-1} have been reported in Europe for ephemeral gully erosion (Casali et al., 2000; Poesen et al., 2006). According to Poesen et al. (2003), the contribution of ephemeral gully erosion to total sediment production ranged from 10% to 83% in Europe. Ephemeral gully erosion is a widespread phenomenon on agricultural land in Belgium. For instance, 71% of the farmers affected by erosion problems in the silt-loam region of Wallonia had to deal with rills and gullies (Bielders et al., 2003). For small catchments less than 300 ha in size in central Belgium, up to 80% of the total soil loss by water erosion may result from ephemeral gullying (Vandaele et al., 1997). According to Vanwalleghem et al. (2005a), a single ephemeral gully in the Loess belt of central Belgium causes damage by incision to 186 m² of land, on average. This concentrated form of water erosion increases the hydrological connectivity in watersheds and enhances the export of sediment produced in inter-gully areas (Stall, 1985). This leads to an increase in the risk of muddy floods, silting up of rivers and reservoirs, and degradation of surface water quality by suspended sediment and associated contaminants. More than

half of the Walloon municipalities were exposed at least once to flooding by runoff from agricultural land between 1990 and 2000 (Bielders et al., 2003), a phenomenon that is frequently, though not always, associated with gullying in upstream areas (Evrard et al., 2007). According to Verstraeten et al. (2006), the total annual cost of muddy floods to private properties in the affected areas in Flanders equals €5.5-16.5 million. For these reasons, the Walloon administration decided to fund a research program[1] to reduce soil erosion and mitigate the off-site risks. A part of this research program is dedicated to gully erosion.

1.2 Research needs

Although ephemeral gully erosion is known to be a widespread phenomenon in certain areas of Wallonia, it has not been studied so far in this region. There is therefore a need to assess the extent of the phenomenon and its spatio-temporal variability. Furthermore, a better knowledge of the environmental contexts leading to ephemeral gully initiation would help decision makers, field engineers and farmers target sites with a high risk of gully erosion where mitigation measures should be taken. Many studies have focused on topographic criteria to identify the contexts that may trigger gully erosion (e.g., Montgomery and Dietrich, 1992; Vandaele et al., 1996; Vandekerckhove et al., 1998; Wu and Cheng, 2005, Gutierrez et al., 2009). They suggest that a topographic threshold exists that allows differentiating topographic contexts for which gully initiation is unusual from contexts for which gully initiation is possible. Different methods have been used to define the topographic threshold (e.g., Patton and Schumm, 1975; Vandekerckhove et al., 1998, Vanwalleghem et al., 2005a), but all are based on the relationship between the drainage area and the slope at the gully initiation point. The

[1] Convention GISER « Gestion intégrée sol-érosion-ruissellement »

topographic threshold has been shown to vary across different study sites because it is sensitive to environmental conditions (e.g., Vandaele et al., 1996). So far, no information is available for Wallonia regarding the topographic conditions leading to gully erosion.

As compared to the contexts leading to gully initiation, much less attention has been paid to the factors causing gullies to end. However, information about the factors causing gullies to end would improve our understanding of the role of gullies in overland flow connectivity and may prove useful to promote land use patterns or practices that limit gully length. It is well recognized that gully deposition is frequently due to a decrease of the transport capacity resulting from a lowering of slope gradient or a widening of the concentrated flow cross section (e.g. Toy et al., 2002). For this reason, the use of a critical slope has been proposed to identify locations where the sediment eroded during gullying is deposited (e.g., Nachtergaele et al., 2001). Some authors also proposed to use a topographic threshold to identify the location prone to gully deposition (e.g., Vandekerckhove et al., 2000). Besides topographic controls, gullies can also end as a result of changes in vegetation cover or soil shear strength (Beuselinck et al., 2000). As for gully initiation, no information is currently available across Wallonia regarding the factors that cause gullies to end. Information on land use transitions or crop transitions forcing gullies to end may, in particular, be very useful to make recommendations regarding the spatial organization of land use and crops in watersheds sensitive to gullying. It could also provide useful information regarding the effectiveness of grass strips or hedges at stopping gullies. Besides the characterization of the environmental contexts causing gullies to initiate or to end, different approaches have been proposed in order to predict the risk of gully occurrence and their trajectories in various environmental contexts. These approaches include topographic indicators, statistical

approaches and physically-based modelling of concentrated soil erosion processes. Such prediction tools are needed at the Walloon scale to identify sensitive areas and could serve as decision support tools to maximize the returns from investments by land managers (regional or local administrations, public environmental associations, environmental experts,…) in the prevention of gully erosion. It could also allow taking into account the risk of ephemeral gully erosion and the associated potential damage in land planning projects. However, to the best of our knowledge there has been no attempt to compare the various indices of gully erosion risk on a common dataset and hence little is known regarding their relative performance in identifying areas prone to gullying.

For a proper characterization and prediction of ephemeral gully erosion at the regional scale, a large dataset of ephemeral gullies is required. Even though field-based approaches should ideally serve as reference to characterize ephemeral gully erosion, such methods are generally too time consuming and costly. This is because of the often low spatial density of ephemeral gullies (e.g., approx. 0.13 km of ephemeral gullies per km² in Australia; Hughes et al., 2001), which implies working over large study areas so as to obtain reliable estimates of gully characteristics. Furthermore, ephemeral gully erosion is, by essence, a short-lived phenomenon which prevents retrospective analyses. Information on ephemeral gully erosion is therefore often extracted from aerial imagery using remote sensing techniques. Interpretation of aerial photographs remains the most widely used technique (e.g., Nachtergaele and Poesen, 1999; Martinez-Casasnovas, 2003). This may, however, lead to substantial errors or biases due to human subjectivity (Lunetta et al., 1991), which have to be assessed.

1.3 Objectives

The overall goal of this thesis is to characterize and predict the occurrence of ephemeral gully erosion in Wallonia. More specifically, we seek to provide an answer to several specific scientific questions (Figure 1-1):

1) What is the uncertainty associated with ephemeral gully characteristics when aerial photographs are used for studying ephemeral gully erosion, and what is the impact of this uncertainty on the topographic threshold for ephemeral gully initiation?

2) What are the extent and characteristics of ephemeral gullies in Wallonia? What is the spatial and temporal variability of ephemeral gully erosion?

3) What is the variability of the topographic threshold for ephemeral gully initiation across various agricultural areas in Wallonia and over the years?

4) What are the main factors controlling where ephemeral gullies end?

5) What is the best indicator for predicting ephemeral gully occurrence based on the data readily available at Walloon scale?

1.4 Outline of the thesis

After this **first chapter** presenting the general context of the research and the research needs, a **second chapter** is dedicated to a state of the art regarding ephemeral gully erosion. **Chapter three** presents the study sites and the general methodology used to create the gully databases.

The use of photo interpretation to identify and to characterize ephemeral gullies is assumed to lead to operator-dependent errors (linear features wrongly interpreted as ephemeral gullies, uncertainty regarding the location of the incision point, inaccuracies during delineation of the ephemeral gullies, ...). For this reason, **chapter four** is dedicated to the uncertainty assessment of ephemeral gully identification, characteristics and topographic threshold when using aerial photographs. Because ephemeral gully erosion is expected to vary across Wallonia due to the diversity of topographic contexts, soil conditions and land use, ephemeral gullies have been characterized (type, length…) across three contrasting agricultural areas located in Wallonia in **chapter five.** Furthermore, a retrospective analysis of ephemeral gully erosion has been performed for one of the study sites to assess the temporal variability of the phenomenon. In **chapter six**, the current thresholding methods used for characterizing the contexts prone to ephemeral gully initiation are compared. A new thresholding method is proposed. The spatial variability of the resulting topographic thresholds across the three agricultural areas and its stability over time are assessed. **Chapter seven** aims at characterizing and quantifying the factors controlling where ephemeral gullies end. Their spatial variability is assessed across different agricultural areas of Wallonia. The relevance of using a critical slope threshold and a topographic threshold to predict ephemeral ending points is assessed. **Chapter eight** deals with the prediction of ephemeral gully erosion. Because the literature provides little guidance as to the best indicator for predicting gully erosion, several topographic and hydraulic indicators of increasing complexity are compared. **Chapter nine** summarizes the main findings of this research work and highlights the perspectives.

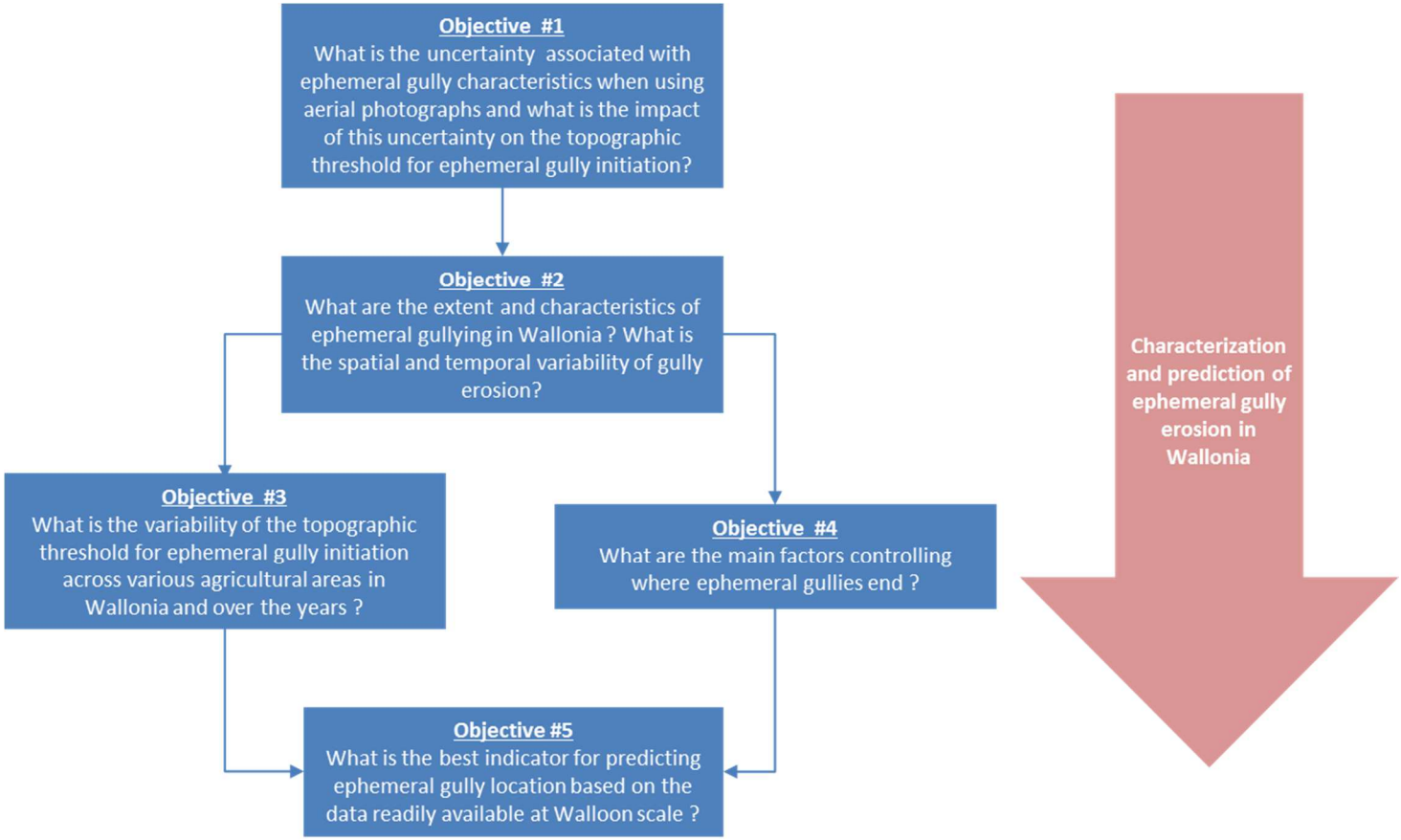

Figure 1-1: Thesis flowchart.

2 Literature review

2.1 Definition of gully erosion and gully types

Gully erosion is defined as the erosion process whereby runoff water accumulates and often recurs in channels and, over short periods, removes soil from these channels to considerable depths (Poesen et al., 2003). Gully forms where there is sufficient magnitude and duration of concentrated surface runoff to initiate and sustain erosion and flow channelization (Thorne et al., 1986). According to Bocco (1991), it initiates when a threshold is transgressed due to either a decrease in the resistance of the materials or an increase in the erosivity of the runoff, or both.

Channels caused by concentrated runoff water are considered to be gullies if the cross section is at least 929 cm^2 or 1 ft^2 (Hauge, 1977). If not, channels are considered to be rills. Gullies can be classified depending on several factors (Poesen et al., 2011): gully form (linear, bulbous, dendritic, trellis, parallel, and compound) (Ireland et al., 1939), gully position in the landscape (valley-floor, valley-side, valley-head) (Brice, 1966), shape of the gully cross-section or the material in which the gully developed (Imeson and Kwaad, 1980). Gullies are also often classified depending on their permanent or ephemeral nature.

Permanent gullies are deep channels that cannot be obliterated by conventional tillage (Poesen and Govers 1990). They range from 0.5 m to 25 to 30 m depth (Soil Science Society of America, 2001). In Belgium, permanent gullies are often associated with banks. They form where a wash line, a rill or an ephemeral gully crosses a sunken road bank or lynchet (Poesen and Govers., 1990). They are quite rare because, according to Verstraeten et al. (2006), land consolidation programs have removed many sunken lanes and lynchets, notably in many areas of the Belgian Loess belt.

However, old permanent gullies can still be observed under forest. Vanwalleghem et al. (2003) mapped 43 old permanent gullies whose mean depth was 1.26 m and mean width was 8.09 m in the Meerdal forest in Flanders. Near Leuven, Vanwalleghem et al. (2005b) described an 18th century gully of up to 3.5 m deep and 4.5 to 5.5 m wide. These gullies are considerably deeper and larger than the present-day shallow ephemeral gullies forming yearly under cropland.

Ephemeral gullies are usually smaller channels located in dry valleys. Depending on their size they can either be easily filled by normal tillage or require larger tillage implements to bring the soil in. They can form repeatedly at or near the same location on a yearly basis because the surface topography of the field is not modified appreciably (Casali et al., 2000). Ephemeral gullies usually form at the end of the winter or early spring. During winter ephemeral gullies result from a slow erosion process related to successive rainfall events with moderate depth and intensity on wet sealed soil (Nachtergaele et al., 2001). In the early spring, ephemeral gullies usually result from a single high intensity event on soil with low vegetation cover. These gullies, also called summer gullies, are often shallow and wide. Vanwalleghem et al. (2005a) reported a 2.2 m mean width at the gully head and a 0.1 m depth (i.e. thickness of the seedbed) for ephemeral gullies located in the Flemish Loess belt. Winter gullies were deeper (0.36 m on average) but narrower (0.52 cm on average). Besides being driven by topography, some ephemeral gullies can also form along linear landscape elements causing flow concentration such as parcel borders, field roads or plough furrows (Vandaele et al., 1996).

2.2 Ephemeral gully erosion in agricultural settings

Ephemeral gully erosion is a widespread phenomenon across the world. Significant soil losses due to ephemeral gully erosion have been reported mainly in the USA and Europe. Poesen et al. (2006) made an inventory of soil loss rates in different parts of the world for both ephemeral and permanent gullies. The contribution of gully erosion rates to the total sediment yield caused by water erosion has been shown to range from 10% up to 94%. According to Casali et al. (2000), who compiled data for the USA, the ratio of ephemeral gully erosion to rill and sheet erosion reached up to 274% depending on the states, with an average of 78%. Gully erosion was responsible for 13 t^{-1} ha^{-1} y^{-1} of soil losses on average while soil losses due to rill and sheet erosion were almost 21 t^{-1} ha^{-1} y^{-1} on average based on data compiled by Casali et al. (2000) for the USA, Australia and Europe. Poesen et al. (1996) reported that, on average, 44% of the total sediment produced in intensively cultivated small catchments with loess derived soils was due to ephemeral gully erosion, but this ratio increased to 80% or more in Mediterranean areas with stony soils. Other studies stressed the significant contribution of ephemeral gully erosion to total soil erosion, ranging from 20% to 100% of total soil losses in agricultural watersheds (Bennett et al., 2000; De Santisteban et al., 2005, 2006).

In Belgium all the studies focusing on ephemeral gully erosion have so far been performed in the Loess belt of Flanders (e.g., Poesen and Govers 1990; Vandaele and Poesen, 1995; Vandaele et al., 1996, 1997; Desmet et al., 1999; Nachtergaele et al., 2001, 2002; Nachtergaele and Poesen, 1999, 2002; Vanwalleghem et al., 2005a). Vandaele et al (1997) and Nachtergaele and Poesen (1999) showed that ephemeral gully erosion rates ranged from 0.8 t^{-1}

$ha^{-1}\ y^{-1}$ to 13.2 $t^{-1}\ ha^{-1}\ y^{-1}$ over a 6-month period based on aerial photographs. According to Verstraeten et al. (2006), for rain events with a return period of 1-10 years, gully erosion can be held responsible for 20-80% of total soil losses in Flanders. No data are available for Wallonia.

The above overview highlights that ephemeral gully erosion rates as well as the contribution of gully erosion to total erosion can be highly variable. This may result from differences in environmental conditions (climate, land use, soil types…). Data from Central Belgium compiled by Vandaele (1996) indicate that the contribution of gully erosion to total sediment production for a given catchment decreases with increasing return period of the rain event (Poesen et al., 1996). The contribution of gully erosion to total sediment production is therefore higher in Belgium during winter compared to spring or summer characterized by more intense rainstorms (Vandaele and Poesen, 1995). According to Poesen et al. (2006), soil loss rates by gully erosion are also affected by both spatial and temporal scale. They highly depend on the size of the study area. At the runoff plot scale, interrill and rill erosion dominate and soil loss rates by gully erosion always equal 0%. When the study areas exceeds a critical value (approx. 1 to 10 ha), gully erosion becomes the dominant sediment-producing process. The reasons given by Poesen et al. (2006) are that (i) gully erosion mostly operates at catchment scale, (ii) most sediment produced by interrill and rill erosion in uplands is often deposited at the foot of hill slopes or in depressions within the landscape and therefore does not reach the outlet. Fluctuations in soil loss rates by gully erosion can also be due to the temporal scale. Trimble (1999) reported that the contribution of gully erosion to total soil loss varied from 18% to 36% for three different periods covering several decades and explained these fluctuations by changes in land use. Poesen et al. (2002) compared soil loss rates by gully erosion during one wet winter with gully erosion rates at the medium time scale (i.e. 3-20 years) in the Iberian

Peninsula. They concluded that soil loss rates by gully erosion increase when the time scale increases.

Ephemeral gully erosion causes disturbances both on-site and off-site. First, gullying leads to important and irreversible soil losses at the location where they formed and contribute to a loss of agronomic value of the soil. It also causes severe damage to crops and induces an increase of workload for farmers when they have to fill in or smooth out gullies. Furthermore, Poesen et al. (2006) indicate that the infilled soil material can usually be easily eroded again by subsequent storms. By increasing the connectivity in the landscape, the development of ephemeral gullies also enhances the sediment delivery to downstream sites (Poesen et al., 2002). They therefore aggravate off-site effects such as muddy floods (e.g. Evrard et al., 2007) and pollution of watercourses by sediment (e.g. Valentin et al., 2005) and associated contaminants (e.g. Verstraeten et al., 2006). For instance, Wantzen (2006) stressed a highly significant reduction in density, biomass and taxon richness of the benthic invertebrates in watercourses caused by siltation due to gullying. Due to the large amount of soil transported, gullies also contribute to diminish the water retention capacity of retention ponds by gradually filling them with soil (Verstraeten and Poesen, 1999).

2.3 Remote sensing techniques to study ephemeral gully erosion

Nachtergaele and Poesen (1999) noted that the major problem with ephemeral gully erosion research is the collection of reliable data. They indicated that the most obvious way to gather data on ephemeral gully erosion is by what can be called ‘an after event field survey’. However the area that can be covered is often very small due to the labor intensive nature

of field surveys and the temporary nature of the ephemeral gullies. In addition, because of the low spatial density of gullies, the number of gullies that can be documented in this way is generally very low. For this reason, remote sensing-based techniques have increasingly been used for the assessment of gully erosion. Despite the increasing availability of very high resolution (< 1 m) satellite imagery, aerial photographs remain the most widely used type of imagery for assessing gully characteristics and the environmental drivers of gully erosion (e.g., Daba et al., 2003; Martinez-Casasnovas, 2003; Parkner et al., 2006; Kakembo et al., 2009) or eroded volume resulting from ephemeral gully erosion (Vandaele et al. 1997, Nachtergaele and Poesen, 1999). This is because very high resolution satellite imagery has become available only in very recent years, and at a high cost to users. Hence, aerial photographs are often the only available source of low cost, very high resolution imagery covering vast tracts of territory. Aerial photographs are also the only option when historical data are needed, as is the case for diachronic studies.

Analysis of remote sensing imagery has been performed through techniques ranging from manual photo interpretation (e.g., Smith, 1943; Langran, 1983) to object-oriented analysis (e.g., Knight et al., 2007; Shruthi et al., 2011). Because the quality of current automated gully detection and delineation schemes is moderate at best, and their applicability is restricted to the area used for calibration and validation, gully identification and delineation on images is still done manually in most studies.

2.4 Ephemeral gully initiation points and topographic threshold

According to Poesen et al. (2002), gully initiation and development of gullies result from a concentrated flow intensity that must be large enough and must last long enough (i) to overcome the resistance to detachment and transport of the topsoil by concentrated flow and (ii) to scour a channel with a cross-section equal to or exceeding the square foot criterion. However, very few studies have attempted to measure critical hydraulic conditions for incipient gullying under field conditions, mainly because of logistical constraints (Poesen et al., 2011). Instead, many studies have focused on the critical environmental conditions for gullying such as the topographic threshold. The latter one has been proposed as a simple means for characterizing the topographic contexts that may lead to gully initiation. According to Schumm (1979), for an area of uniform geology, land use and climate, a critical valley slope exists above which a valley floor is unstable and may be gullied. For gullied valley floors, Patton and Schumm (1975) analyzed the relationship between drainage area and slope at the gully incision point in order to identify the gullying threshold. This approach has been widely used since then (e.g., Montgomery and Dietrich, 1992; Vandaele et al., 1996; Vandekerckhove et al., 1998, 2000; Vanwalleghem et al., 2005a ; Wu and Cheng, 2005, Gutierrez et al., 2009).

Several methods have been used so far for defining the topographic threshold. Patton and Schumm (1975) drew a straight line manually through the lowermost points in a log-log scatter plot of slope vs. contributing area at the gully incision point (Fig.2-1A). A second method is based on orthogonal regression and was applied by Vandekerckhove et al. (1998) and

Vanwalleghem et al. (2005a). After having determined the regression parameters, Vanwalleghem et al. (2005a) modified the intercept of the line while keeping the same slope such that all points would fall on or above the line except for extreme values (Fig.2-1B) Vandekerckhove et al. (1998) relied on the lower 95% confidence interval of the orthogonal regression line to position the threshold (Fig.2-1B). Whatever the method used, the threshold equations can be expressed by Equation 2-1:

$$S = a\ A^{b} \qquad (2\text{-}1)$$

where S and A are the slope [$m.m^{-1}$] and contributing area [ha] at the gully head, respectively, a is a coefficient and b an exponent. In a log-log plot, a corresponds to the intercept of the threshold line and b to its slope. Recently, Torri and Poesen (2014) proposed on new thresholding based on the use of a constant b value (Equation 2-1) of 0.38. The threshold line is then fitted through the lowermost points. This method is based on the finding that the b value is quite similar across a range of environments.

The topographic threshold has been shown to vary depending on the gully types and the environmental conditions. Indeed according to Morgan (1979), gully erosion is the result of the interaction among: 1) volume, velocity and type of runoff, 2) susceptibility of soils to erosion, and 3) land use and agricultural practices. Hence, besides slope and contributing area, soil, climate and land use factors may affect the threshold line. These factors mostly affect the intercept of the threshold line, whereas it was shown that the slope of the line is much less variable across regions (e.g., Vandaele et al., 1996). Torri and Poesen (2014) showed that the intercept of the topographic threshold is lower for croplands than for rangelands, pastures or forests, and that it can be predicted using soil and vegetation characteristics,

based on the NRCS Runoff Curve Number values and on surface rock fragment cover.

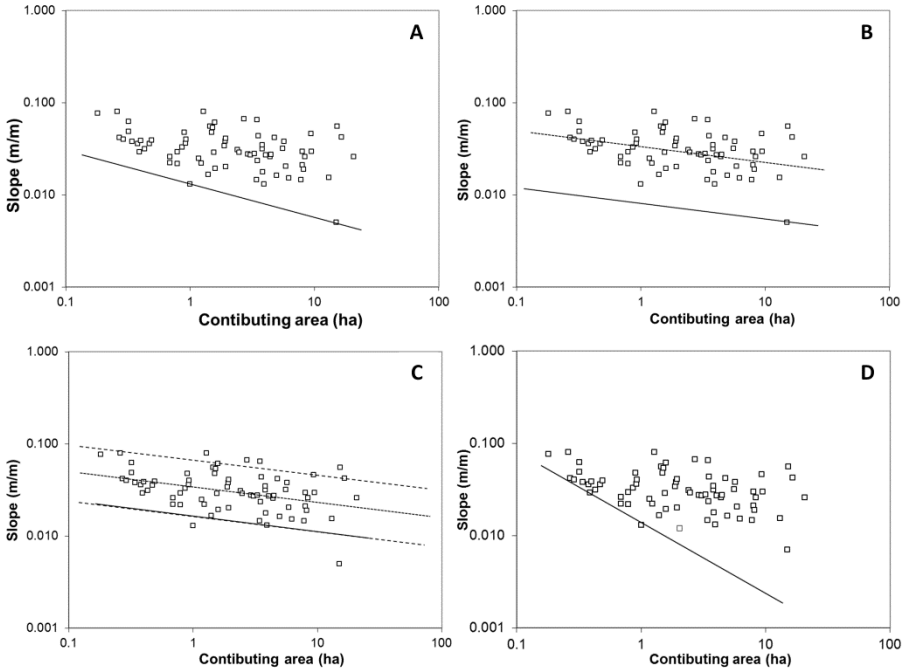

Figure 2-1: Topographic thresholds (solid lines) for a fictive dataset defined using the A) Patton & Schumm (1975) method based on the lowermost points, B) Vanwalleghem et al. (2005a) method as the translation of the orthogonal regression (dotted line) until the lowermost point while keeping the slope constant, C) Vandekerckhove et al. (1998) method as the lower limit of the 95 % confidence interval (dashed lines) of the orthogonal regression (dotted line) and D) Torri and Poesen (2014) method based on a b value (Equation 2-1) of 0.38 and the lowermost points.

Some of the variability across studies may also result from differences in data collection (e.g., field data vs. data derived from maps or images; accuracy of the field methods; differences in data or image resolution; Vandaele and Poesen, 1995) as well as from the use of different thresholding methods as discussed above. Besides the lack of standardization of methods used for defining the topographic threshold for gully initiation, a major drawback of the concept is that it provides no insight into the probability of

occurrence of gullying when the threshold is exceeded. Above the threshold, topographic conditions are such that gullying may occur, though not necessarily so. Most studies focusing on the prediction of gully initiation points stressed the large scatter of the observation data points, typically allowing to predict about 70-80% of the channel heads correctly (Poesen et al., 2011). As a matter of fact, the threshold line is most useful for identifying areas where gullying is highly unlikely to occur.

2.5 Factors controlling ephemeral gully end

According to Poesen et al. (2003), gullies usually end where the sediment transport capacity of the concentrated overland flow drops and/or where the erosion resistance of the topsoil increases sharply. An increase in soil erosion resistance can be induced by changes in vegetation cover (Beuselinck et al., 2000). It can also be due to an increase in rock fragment cover or changes in tillage practices along the gully trajectory (Knapen et al., 2007a). A drop in transport capacity can be caused by several factors. Because transport capacity is in part proportional to slope gradient and flow rate, a lowering of slope gradient or a widening of the concentrated flow cross section can trigger sediment deposition (Toy et al., 2002). An increase of the hydraulic roughness, due to changes in vegetation cover or obstacles such as embankments along the gully trajectory, can also lead to a decrease of the transport capacity.

When the gully end is slope-controlled, it has been suggested that a critical slope exists below which sedimentation occurs. De Ploey (1984) proposed a colluviation model in which the critical slope angle depends on the sediment concentration in overland flow, the unit flow discharge and the median grain size. In the Belgian Loess Belt, areas prone to deposition are characterized by a critical slope threshold of 2 to 4% (Poesen et al., 1998; Beuselinck et

al., 2000). Vandekerckhove et al. (2000) and Nachtergaele et al. (2001) showed that the critical slope threshold for sediment deposition is strongly dependent on the characteristics of the transported material and on the surface conditions of the sedimentation area such as the percentage vegetation cover, the surface roughness or the stoniness. Because the critical slope for sedimentation depends on flow discharge (De Ploey, 1984), topographic thresholds based on land slope and contributing area values have been proposed (e.g., Vandekerckhove et al., 2000). Above the topographic threshold line sedimentation is never observed, whereas below the threshold line deposition may occur (though not necessarily so).

The spatial organization of land use within agricultural catchments also affects ephemeral gully ending. Beuselinck et al. (2000) pointed out that up to 28% of ephemeral gully deposits in the Belgian Loam Belt were triggered at field borders due to changes in vegetation roughness. In the spring, grassland or winter wheat act as vegetation barriers. According to the same study, vegetation-controlled deposition occurs at significantly higher slope gradients than slope-controlled sediment deposition.

Roads are known to affect gullying (Desmet et al., 1999), but other linear elements such as banks, ditches, hedges or tillage direction are also expected to affect the location of ephemeral gully ending points. Though some studies attempted to take linear elements into account to explain gully location or susceptibility (Conoscenti et al., 2014; Dube et al., 2014, Makanzu Imwangana et al., 2014), only few studies have assessed their impact on ephemeral gully ending points (Takken et al., 1999).

2.6 Prediction of ephemeral gully occurrence

One way to predict the occurrence of ephemeral gully erosion is to start with defining the initiation points of the ephemeral gully, and then to derive the ephemeral gully path by routing the water from the initiation point until conditions are met for deposition (Nachtergaele et al., 2001). For instance, Chaplot et al. (2005) successfully predicted occurrence and length of ephemeral gullies in Laos, over a 10-m cell, using a flow velocity threshold to identify gully incision points and a threshold change in slope gradient for sedimentation. Besides this first approach, various methods have been used to map the risk of gullying based on the delineation of areas where critical conditions for gullying are met. These conditions include simple topographical indices, physically-based modeling of gully erosion processes and empirical multivariate approaches. For instance, Gutierrez et al. (2009) used multivariate adaptive regression splines based on topography, vegetation cover and climate to model the occurrence of permanent gullies in rangelands in Spain. Eustace et al. (2011) used a set of 17 variables related to soil, topography and vegetation to model gully presence with random forest technique in Australia.

Topographical indices typically combine local slope, upstream drainage area and sometimes local planform curvature, and are assumed to be proportional to the stream power of the flow (e.g. Thorne et al., 1986). Desmet et al. (1999) showed that the location of gullies is mostly controlled by the contributing area while incipient gully incision is rather controlled by slope gradient. Satisfactory results were obtained using this method for small catchments ranging from 7.5 ha to 252 ha (Moore et al., 1988; Desmet et al., 1999; Jetten et al., 2006, Momm et al., 2012).

Souchère et al. (2003) proposed an expert-based model for predicting gully location and volume. Factors impacting flow velocity or soil resistance such as land use, plant cover percentage, roughness and soil crusting stage were considered. Many existing physically-based erosion models allow for the estimation of soil losses by gullying (CREAMS; Knisel, 1980, GLEAMS; Knisel, 1993, EGEM; Merkel et al., 1988; Woodward, 1999, WEPP; Flanagan and Nearing, 1995) but only few are capable of predicting the location of gullies. Gully location is generally required as user input.

Poesen et al. (2003) argued that gullies develop only if concentrated flow intensity during a rainfall event exceeds a threshold value. Horton (1945) first proposed the concept of a threshold tractive force for particle entrainment and transportation. According to Bryan (2000) and Knapen et al. (2007b), many simple hydraulic indices are related directly to this critical tractive force such as water depth, peak discharge, flow velocity, flow shear stress, effective shear stress, shear velocity, stream power, unit stream power or effective stream power. Such hydraulic indices can also be combined with the related, soil-specific critical value (e.g. critical shear stress…) into "excess models". Knapen et al. (2007b) reviewed such models (e.g. excess shear stress; Eq. 2-2, Foster; 1982 or excess stream power; Eq.2-3, Elliot and Laflen, 1993):

$$D_c = K_c(\tau - \tau_{cr})^b \qquad (2\text{-}2)$$

$$D_c = K_c(\omega' - \omega'_{cr}) \qquad (2\text{-}3)$$

In Eq.2-2, the soil detachment rate, D_c [kg m^{-2} s^{-1}] is proportional to the soil erodibility K_c [s m^{-1}], the shear stress applied by the flow τ [Pa] and the critical shear stress τ_{cr} [Pa], and *b* is an exponent. In Eq.2-3, ω'[W m^{-1}] is the

runoff energy rate per unit bed area defined by Eq.2-4 while K and ω_{cr}' represent the soil resistance to concentrated flow erosion.

$$\omega' = \gamma g Q W^{-1} \qquad (2\text{-}4)$$

where Υ = specific weight of water [N m^{-3}], g = gravitational acceleration [m s^{-2}], Q = discharge [m^3 s^{-1}] and W = gully width [m].

Because the detachment rate may decrease with increasing sediment concentration some prediction models also include the transport capacity (e.g. EUROSEM, Morgan et al., 1992). However, Knapen et al. (2007b) recommended the use of simple hydraulic parameters for practical applications because of their straightforwardness. Bryan (2000) stressed that hydraulic parameters that were effective in some studies, proved irrelevant in others, and in many cases, the information needed to determine whether differences were real or artifacts of experimental procedures was not available. According to Knapen et al. (2007b), which gathered R-square values for linear regression analysis between detachment capacity and various hydraulic indicators for the 33 soils of the WEPP model dataset, stream power, shear stress and peak discharge were the most relevant indicators. Bryan (2000) stressed that flow velocity and unit stream power were also consistently useful hydraulic indicators to predict soil detachment by concentrated overland flow.

3 Materials and methods

3.1 Study sites and related gully databases

To achieve the objectives of the thesis, it was necessary to document a large number of gullies for different agricultural areas across Wallonia. For this purpose, aerial photographs were used since they offer a practical means to characterize a large number of ephemeral gullies considering their low spatial density. Aerial photographs also allowed studying the temporal variability of the phenomenon using different aerial photograph datasets for the same location. Color aerial orthophotographs provided by the Walloon administration were used. Three sets of photographs were available at the beginning of the thesis: PPNC (Plans Photographiques Numériques Communaux; 40 cm resolution), 2006–2007 (50 cm resolution), and 2009–2010 (25 cm resolution). PPNC is a mosaic of photographs acquired between 1994 and 2001. Three gully databases covering 5 study sites were created to meet the objectives of the thesis (Table 3-1).

Given the elongated shape of gullies, the critical width for a gully to be detected was expected to be almost equivalent to the aerial photographs' resolution, that is to say 25 to 50 cm depending on the set of photographs. . Based on the study of Vanwalleghem et al. (2005a) for 123 gullies in the Loamy area of Belgium, it should be sufficient to allow detecting most summer gullies, both deep (> 0.8 m depth; mean width at gully head = 0.9 m) and shallow (< 0.8 m depth; mean width at gully head = 2.2 m), as well as deep winter gullies (mean width at gully head = 2.8 m). With a mean width of 0.52 m at the gully head, the number of shallow winter gullies may be substantially underestimated.

Table 3-1: Thesis objectives, and related gully databases and study sites. The aerial photographs datasets are also mentioned.

Gully database number	Objective(s)[2]	Region number[1]	Agricultural area	Aerial photographs dataset(s)
1	#2 and #3: Extent, characteristics and spatial variability of ephemeral gully erosion and topographic threshold for ephemeral gully initiation #4: Factors controlling ephemeral gully ending points	1, 2, 3	Loamy Area, Famenne, Jurassic area	2006-2007
2	#2 and #3: Temporal variability of ephemeral gully erosion and topographic threshold for ephemeral gully initiation #4: Factors controlling ephemeral gully ending points	4	Condroz / Loamy area	PPNC (1999), 2006-2007, 2009-2010
3	#1: Uncertainty assessment of ephemeral gully identification, characteristics and topographic threshold for gully initiation when using aerial photographs #5: Comparisons of prediction methods for ephemeral gully location	5 (red dashed area)	Loamy area	2006-2007

[1] Refers to Figure 3-1

[2] Refers to Figure 1-1

3.1.1 Characteristics and spatial variability of ephemeral gully erosion

A first gully database was created in order to assess the extent, the characteristics and the spatial variability of ephemeral gullying across Wallonia. The database was also used to assess the spatial variability of the topographic thresholds for ephemeral gully initiation and to assess the factors controlling ephemeral gully ending point locations. The 2006–2007 aerial photographs were used because it was the only dataset covering the whole of Wallonia for the same year at the beginning of the present study. Selection of the study sites was based on four different criteria. 1) Each study site had to be located in major yet contrasting agricultural areas of Wallonia in terms of soil, land use and topography. 2) Aerial photographs had to be available for the period between mid-May and the beginning of July to observe gullies developed in fields with either winter or summer crops when winter crops have not yet been harvested and all summer crops have been planted. 3) Each study site had to be large enough to allow detection of 50–100 gullies. 4) The dates of acquisition of aerial photographs had to be as similar as possible within and across study sites. Based on these criteria, three study sites located in the Loamy area, the Famenne and the Jurassic area were selected (sites #1 to #3; Figure 3-1). The aerial photographs covered ca. 25,000 to 29,000 ha in each study site (Table 3-2).

The Loamy area (#1) draws its name from the dominant soil type which is silt loam soil derived from Quaternary aeolian loess deposits (Table 3-3). In the study site, about 10% of the soils have a rock fragment content ranging from 5 to 15% in volume (Table 3-3). This is higher than observed in the whole of the Loamy area where only 2% of the soils have a rock fragment content > 5%.

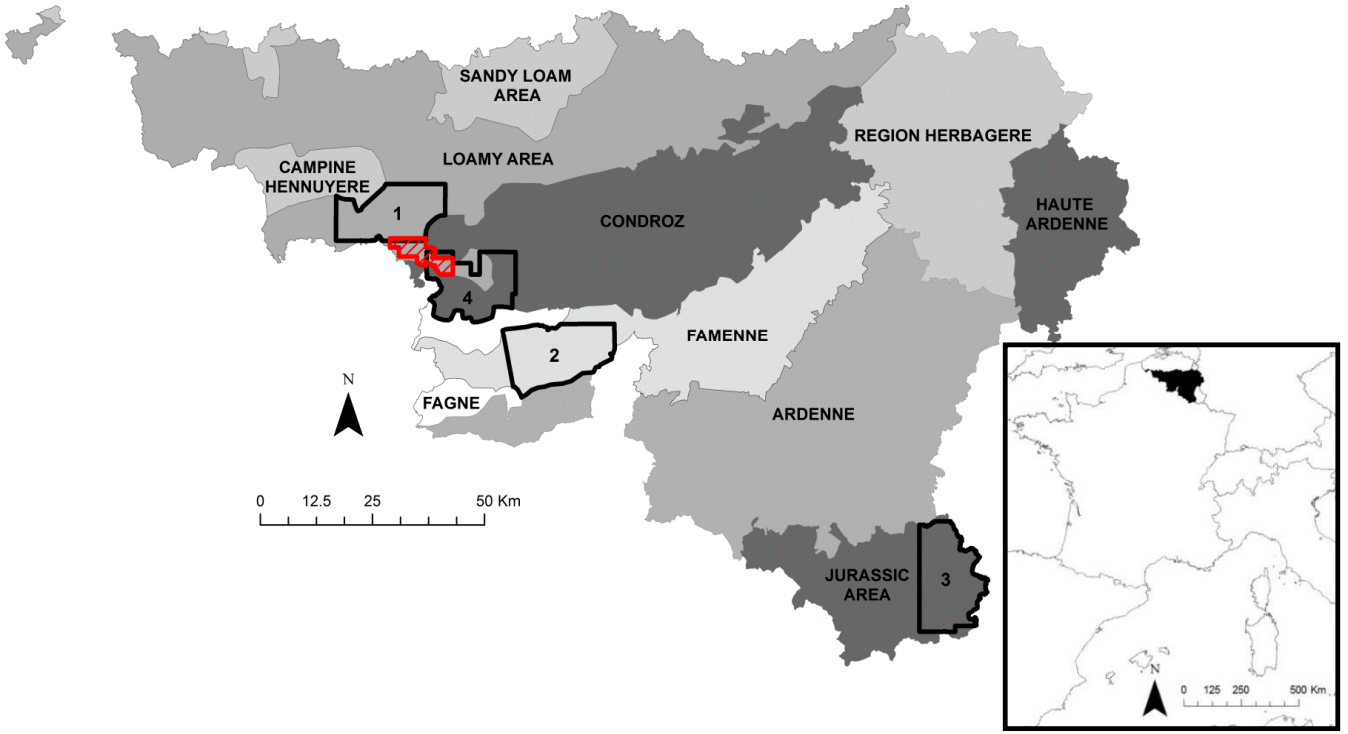

Figure 3-1: Location of the study sites in Wallonia. 1) Loamy area, 2) Famenne, 3) Jurassic area, 4) Condroz/Loamy area, 5) Red dashed zone was located in Loamy area.

Table 3-2: Study sites and aerial photographs used

Region Number[1]	Agricultural area	Pixel resolution	Dates of acquisition	Total area	Cultivated area[3]	Summer / Winter crop parcels ratio[2]	Grassland acreage	Mean size of cultivated parcels[3]	Mean slope of cultivated parcels
			dd/mm/yyyy	**ha**	**ha**	**%**	**ha**	**ha**	**%**
1	Loamy Area	50 cm	02/07/2006	24654	13917	46 / 54	3734	3.15	3.59
2	Famenne	50 cm	17/06/2006 02/07/2006	29161	3737	42 / 58	8157	2.73	4.98
3	Jurassic Area	50 cm	10/06/2006	27939	4398	45 / 55	7444	1.90	6.29
4	Condroz/Loamy area	40 cm	29/07/1999	20963	10058	38 / 62	5607	3.72	4.03
		50 cm	02/07/2006		10743	36 / 64	6056	3.77	4.04
		25 cm	23/05/2009		11024	34 / 66	6077	4.38	3.98
5 (red dashed area)	Loamy area	50 cm	02/07/2006	5235	3296	68 / 32	714	4.42	3.30

[1]Refers to Figure 3-1

[2] Summer crops = mainly sugar beet, potato and maize

[3] Cultivated parcels = agricultural land except grassland and grass strips

Nevertheless, the soils are highly suitable for industrial crop production (wheat, sugar beet, potato, maize, …). Hence, the Loamy area is characterized by a large proportion of cropland and a fairly large average size of cultivated parcels almost equally distributed between summer and winter crops (Table 3-2). The study site is further characterized by a gently undulating relief with vast plateaus dissected by some valleys. Average annual precipitation is around 800 mm and is fairly equally distributed throughout the year. The mean erosivity of precipitation is 680 MJ mm ha^{-1} h^{-1} yr^{-1} (Sohier et al., 2009). The Loamy area is particularly exposed to muddy floods according to Bielders et al. (2003). All municipalities in the study site #1 were hit by muddy floods 2 to more than 10 times over the period 1991-2001. The Famenne (#2) is a depression dug into shale located between the Condroz and the Ardenne. It consists of undulating plateaus separated by vast flat depressions. Many soils have a stony silt loam texture and almost 40% of soils have rock fragment content more than 15% in volume (Table 3-3). However crops are mainly located on silt loam soils with a rock fragment content less than 5% in volume. Annual precipitation is around 950 mm and highest during spring and summer. The mean erosivity of precipitation is 850 MJ mm ha^{-1} h^{-1} yr^{-1}. Cropland occupies less than 15% of the total acreage. The agricultural acreage is mainly grassland. Crops were almost equally distributed between summer and winter crops. The mean size of cultivated parcels and the mean slope are intermediate between those of the Loamy and Jurassic areas (Table 3-2). Among the different agricultural areas studied, the Famenne is the least exposed to muddy floods. The study site #2 comprises municipalities where muddy floods never occurred or occurred 2 to 5 times over the period 1991-2001 (Bielders et al., 2003). The Jurassic area (#3) is characterized by a rugged relief with steep slopes. Geological substrates consist of sandstone, shale and limestone. Annual precipitation is approximately 1100 mm and rainfall is the highest during spring and summer. The mean erosivity of precipitation is 1360 MJ mm ha^{-1} h^{-1} yr^{-1}.

Table 3-3: Distributions of soil textures and rock fragment contents in volume across the four study sites used for the characterization of ephemeral gully erosion.

	Loamy area Study site #1[1]		Famenne Study site #2		Jurassic area Study site #3		Condroz / Loamy area Study site #4	
Soil texture	Study site[2]	Cropland[3]	Study site	Cropland	Study site	Cropland	Study site	Cropland
Silt loam	83.6%	84.1%	30.9%	64.8%	17.3%	16.7%	67.3%	77.6%
Loam	4.4%	3.3%	0.2%	0.2%	12.3%	16.0%	1.2%	1.1%
Stony silt loam	10.6%	11.9%	47.6%	27.6%	22.7%	31.0%	30.8%	20.2%
Sandy loam	0.4%	0.3%	-	-	11.0%	8.8%	0.1%	0.1%
Sand	-	-	-	-	3.9%	30.0%	-	-
Clay loam	1.0%	0.4%	21.0%	7.3%	26.8%	26.2%	0.6%	1.0%
Clay	-	-	0.3%	0.1%	6.0%	1.3%	-	-
Rock fragment content	Study site	Cropland	Study site	Cropland	Study site	Cropland	Study site	Cropland
0 - 5%	89.2%	87.8%	52.2%	72.1%	75.8%	68.5%	69.3%	79.8%
5 - 15 %	0.5%	0.5%	8.1%	5.8%	2.6%	2.4%	0.0%	0.0%
15 - 50 %	10.2%	11.6%	39.3%	22.0%	21.1%	28.4%	30.7%	20.2%
> 50 %	-	-	0.4%	0.1%	0.2%	0.6%	0.0%	0.0%
No data	0.1%	0.1%	-	-	0.3%	0.1%	-	-

[1]Refers to Figure 3-1

[2] Distributions on the whole study sites

[3] Cultivated parcels = agricultural land except grassland and grass strips

Soils are varied but mostly have either stony silt loam or clay loam texture (Table 3-3). The clay content of clay loam soils ranges from 20 to 35%. Almost 30% of the cultivated parcels are located on soils with a rock fragment content more than 15% in volume. Cropland occupies less than 20% of the total acreage. The agricultural acreage is dominated by grassland. Crops were almost equally distributed between summer and winter crops. The mean size of cultivated parcels is the lowest but the mean slope is the highest of the three study sites. Muddy flood are less frequent in the Jurassic area (#3) than in the Loamy area (#1). However, municipalities in the study site were exposed to muddy floods 2 to 10 times over the period 1991-2001 (Bielders et al., 2003). Although the Condroz and the Sandy loam area are also major agricultural areas in Wallonia (Figure 3-1), they were not included in the present study since no set of photographs meeting the above criteria were available. The agricultural areas in eastern Wallonia (Ardenne, Haute Ardenne, and Région Herbagère) were not retained because land use almost exclusively consisted of grassland and forests for topographical and climatic reasons.

3.1.2 Temporal variability of ephemeral gully erosion

A second gully database was created in order to assess the recurrence of ephemeral gully erosion as well as the temporal variability of the topographic threshold for ephemeral gully initiation. The database was also used to assess the factors controlling the location of ephemeral gully ending points. A study site was delineated across the Loamy area and Condroz (#4; Figure 3-1), conditioned by the above mentioned criteria and the availability of the three aerial photograph datasets (PPNC, 2006-2007 and 2009-2010). In the Condroz, soils are mainly silt loam but are much stonier than in the Loamy area (Table 3-3). Almost 20% of the cultivated parcels are located on soils with a rock fragment content more than > 15%. The mean size of cultivated parcels as well as their mean slope are comparable to those of the Loamy area.

The proportion of grassland is slightly more important in the Condroz than in the Loamy area (Table 3-2). As for the Loamy area, the Condroz is particularly exposed to muddy floods (Bielders et al., 2003). The study site #4 is occupied by municipalities where muddy floods occurred 2 to more than 10 times over the period 1991-2001.

3.1.3 Uncertainty assessment of ephemeral gully erosion when using aerial photographs and prediction of ephemeral gully erosion.

The third ephemeral gully database was created to assess the extent to which ephemeral gully characterization as well as the topographic threshold for their initiation is operator-dependent when relying on photo-interpretation. Eleven Masters- or PhD-level operators actively involved in projects dealing with soil erosion on agricultural land were asked to digitize and classify gullies on cropland in a zone located in the Loamy area (#5 - red dashed area; Figure 3-1 and Table 2-1). The size of the study site was set such that it would encompass a sufficient number of gullies (50-100) yet require a reasonable amount of time for the digitizing work (2h-3h). The exact location of the zone was determined by the availability of aerial photographs for a time window comprised between May and July. The characteristics of the study site were similar to site #1 (Figure 3-1) in terms of rainfall and soils. However, cropland occupied more than 80% of the agricultural acreage. Furthermore, crops were mainly summer crops (68%; table 3-2). Mean size of cultivated parcels and mean slope were similar to those in the Loamy area (#1) and Condroz/Loamy area (#2). Because each gully can be associated with a level of uncertainty, the database was also used to assess the performance of methods to predict ephemeral gully occurrence.

3.2 Gully databases creation

3.2.1 Gully identification and digitizing

Gullies were digitized on the aerial photographs viewed at the preferred 1:2,500 scale in ArcGIS software. The scale was a compromise between working time and easiness to locate gullies. Indeed, a 1:5,000 scale would have allowed working faster but would also have increased the risk of missing short or narrow gullies. On the contrary, a 1:1,000 scale would have facilitated ephemeral gully identification but the digitizing work would have been much more time consuming.

Given that only cropland was considered and that such land is tilled in its entirety at least once a year, it was assumed that all gullies were ephemeral gullies. In order to assist with gully identification, additional information was used, i.e., a topographic map with contour lines (IGN, 1:10,000 scale), a map of flow accumulation derived using the 10-m resolution digital elevation model (DEM) and the Steepest Path tool of ArcGIS Spatial Analyst.

3.2.2 Gully classification

Gullies were classified into one of three types (Figure 3-2): (1) those located on a well-defined runoff flow concentration axis, i.e., dry valley, (2) those located on slopes without an apparent runoff flow concentration axis, and (3) those resulting from an anthropogenic linear element such as parcel borders, field roads, plough furrows, wheel tracks or ditches. In contrast to Type 3, Types 1 and 2 are natural gullies and tend to be perpendicular to the contour lines. The distinction between Types 1 and 2 is strongly dependent on the resolution of the DEM and hence somewhat arbitrary.

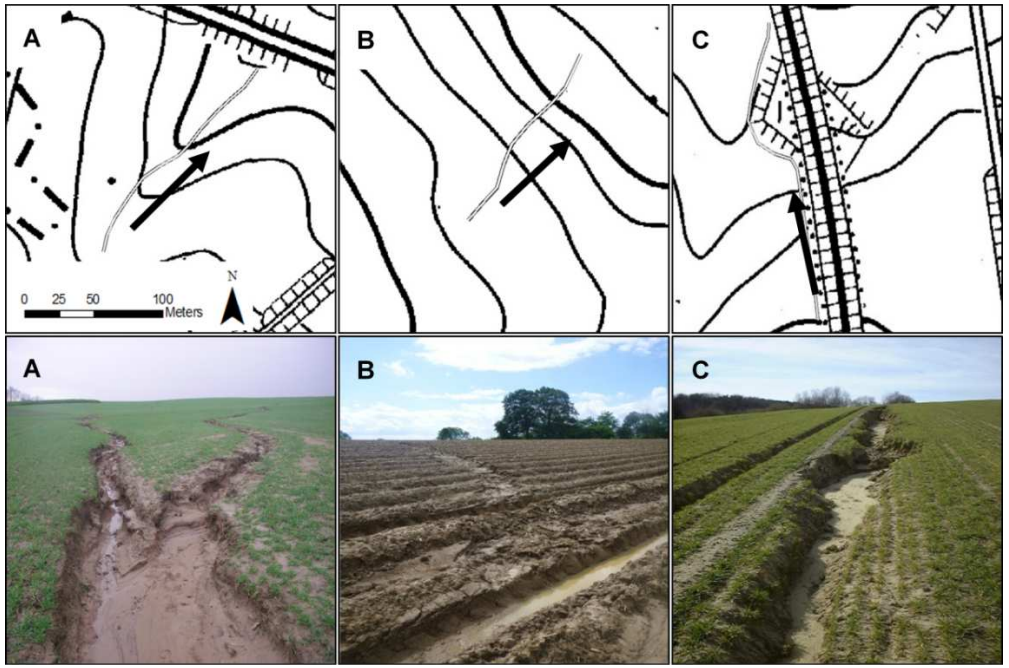

Figure 3-2: Types of ephemeral gullies identified in the present study. (A) Type 1: gullies located on a well-defined runoff flow concentration axis (Picture: GISER); the contour lines on the scheme indicate that the gully is on a thalweg. (B) Type 2: slope gullies located on a slope without apparent flow concentration axis (Picture: GISER). (C) Examples of Type 3 gully. On the scheme, gully resulted from flow concentration due to a bank. On the picture (Bielders, C.), gullies formed in a wheel track. Arrows indicate the water flow direction.

4 Uncertainty assessment of ephemeral gully identification, characteristics and topographic threshold when using aerial photographs in agricultural settings[1]

[1] Based on: *Maugnard, A., Cordonnier, H., Degré, A., Demarcin, P., Pineux, N. and Bielders, C. L. (2014), Uncertainty assessment of ephemeral gully identification, characteristics and topographic threshold when using aerial photographs in agricultural settings. Earth Surf. Process. Landforms, 39: 1319–1330. doi: 10.1002/esp.3526.*

4.1 Introduction

The manual photo-interpretation of aerial photographs to characterize ephemeral gully may lead to substantial errors or biases due to human subjectivity (Congalton et al., 1991). Indeed, whatever the application, it has been well documented that some subjectivity is unavoidable whenever human decisions are taken during the image analysis process (e.g., Legros et al., 1996; Philipson, 1997 in Thierry and Lowell, 2001; Pasquallini et al., 2001; Leckie et al., 2003; Powell et al., 2004; Baveye et al., 2010; Zhou et al., 2010). Any manual photo-interpretation work should therefore incorporate an assessment of the potential impact of this subjectivity on data quality.

It may appear at first that the growing efforts to develop automated approaches to identify and delineate gullies (see, e.g., Eustace et al., 2011; Shruthi et al., 2011) will obliterate the need to assess the impact of operator subjectivity. However, even automated schemes very often depend on manually-derived data. Indeed, automated schemes require training and validation datasets, which are commonly acquired through manual digitizing when field data are not obtainable (Eustace et al., 2011; Shruthi et al., 2011). This is especially common for large scale studies of ephemeral gullies formed on cropland that rely on commercial imagery, because the delay between the acquisition date of the imagery and their publication is often greater than the life span of the ephemeral gullies, which is of the order of a few months (until tillage operations erase them). A proper evaluation of the quality of such automated schemes should therefore also encompass an assessment of the uncertainties introduced in the reference datasets due to human subjectivity.

Besides the identification of gullies per se, operator subjectivity may also affect their delineation, which in turn may affect other characteristics such as estimated gully length, for instance. Classification of digitized gullies (see,

e.g., Poesen et al., 2002 for a review of gully classification schemes) may also be operator-dependent, as this relies on an interpretation by the operator of the factors that triggered the formation of the observed gully. It is also expected that human subjectivity in gully detection will affect the topographic threshold. Since the topographic threshold is based on the land slope and water catchment area values, the computation of the threshold will be affected by the accuracy with which the operator can locate the gully heads on the aerial photographs. Particularly for ephemeral gullies located in cropland, it is sometimes difficult to identify a clear incision point (e.g., the gully may have developed out of one or several rills), which further requires a subjective decision as to where the gully starts. Finally, ephemeral gullies may in some cases be caused by features such as plow furrows or wheel tracks, in which case they should be excluded from the topographic threshold calculation since their formation was not driven by topographic factors only. Consequently, any misclassification of gullies may lead to the rejection or, on the contrary, the inclusion of certain gullies, and hence affect gully statistics. Misclassification as well as uncertainty regarding the gully head location may also affect the topographic threshold analysis for gully initiation. The different thresholding methods exposed in Chapter 2 and Figure 2-1 may be more or less operator dependent. The topographic threshold drawn with the Patton and Schumm (1975) method is very sensitive to the accuracy of gully head location and the resulting slope and contributing area values, because in many cases the threshold depends on only two points. It is also sensitive to extreme values. Because it relies on least squares minimization, the Vanwalleghem et al. (2005a) method is more robust. The slope of the threshold may be only little sensitive to the operator yet the position of the threshold remains sensitive to extreme values because it depends on the lowermost points. The Vandekerckhove et al. (1998) method corrected this deficiency by positioning the threshold at the lower limit of the 95% confidence interval of the orthogonal regression. However, the confidence interval tends to increase, and

hence the threshold tends to be positioned lower, when the dataset size is small or the correlation between the slope and the contributing area is weak, both of which may be affected by misclassification or uncertainty in gully head location. Saito et al. (2010) recently applied quantile regression (Koenker and Bassett, 1978) to identify rainfall intensity–duration thresholds for landslides. The estimates of this statistically-based method have been shown to be robust to the presence of outliers (John and Nduka, 2009). The resulting topographic threshold may be therefore less sensitive to the operator.

To our knowledge, the sensitivity of gully characterization and topographic threshold analysis to the operator has never been assessed. Besides its importance for estimating the uncertainty associated with gully characteristics and topographic thresholds, such information would also help in the interpretation of differences observed across studies because a non-negligible part of the observed differences may be due to human subjectivity when identifying and delineating gullies. Better knowledge of the uncertainty associated with the reference datasets would also help develop more robust automated gully detection procedures.

The aims of this chapter were therefore (i) to assess the extent to which ephemeral gully characterization (number, sum total length, location of the gully heads, gully classification) is operator dependent when relying on manual interpretation of aerial photographs, and (ii) to assess the impact of the operator on the topographic threshold line as a function of the thresholding method used. To achieve these objectives, 11 skilled operators were asked to digitize gullies in a delineated area using aerial photographs and to classify them following a standardized methodology. The resulting 11 datasets were then compared in terms of ephemeral gully numbers and characteristics, as well as in terms of their impact on the analysis of the topographic threshold. The study area was located in the loess belt of Wallonia (Belgium), which is

known to be prone to ephemeral gullying and hence offered favorable conditions for the present study (e.g., Poesen et al, 1990; Vandaele and Poesen, 1995; Nachtergaele et al., 2002).

4.2 Material and methods

The gully database #3 (Table 3-1), resulting from digitizing and the classification of gullies in the Loamy area (#5; Figure 3-1) by 11 Masters- or PhD-level operators actively involved in projects dealing with soil erosion on agricultural land, was used. The color aerial photographs used were taken in 2006 at 5800 m height and were orthorectified. The pixel resolution was 0.5 m. As discussed in the Materials and methods chapter it should allow detecting most summer gullies based on the study of Vanwalleghem et al. (2005a) for 123 gullies in the Loamy area of Belgium. It should also be sufficient to deep winter gullies but shallow winter gullies may be substantially underestimated.

4.2.1 Ephemeral gully identification and gully digitizing

In order to assess the impact of operator subjectivity on ephemeral gully identification, a standardized methodology was defined and explained to the 11 operators. Three sources of information were provided within a GIS software: aerial photographs, National Geographic Institute (IGN) topographic maps with contour lines (scale 1:10,000), and a map which highlights all water flow concentration axes with contributing areas > 1 ha, derived from a 10-m resolution DEM. This is the highest resolution DEM currently available at regional level. All land that was not cropland was hidden by means of a mask. The recommended scale for viewing was 1:2,500 but the operators were allowed to use all the available scales to identify and delineate ephemeral gullies.

Each operator was provided with a decision tree, which was formulated so as to allow the user to discriminate between ephemeral gullies and other linear features which could be confused with gullies. These were illustrated by one or several pictures depending on the case. The operators had to look for linear continuous objects contrasting with their proximal environment, e.g., bare soil areas or fresh green growth within fields cultivated with winter or summer crops. Whatever the shape of the object, if there was a deposition fan at the downstream end, it was considered a gully and the operator had to digitize it (Figure 4-1a). If the object had a sinuous shape over at least part of its total length and if no deposition was observed at the downstream end, the operator was required to make sure that it was not a former trail or road based on the IGN map. If not, the object was considered a gully and had to be digitized. If the object was straight over its entire length without any deposition at the downstream end, the operator had to check two cases. First he had to check whether the object overlapped with a field border or the headland and was oriented perpendicular to the main tillage direction. If true, the object probably corresponded to a wide deposition area formed at the bottom end of successive furrows or in a plough furrow against the headland (Figure 4-1b), and it should not be digitized. Second, if the object had a near constant width and was recurrent in the field with near constant spacing, it probably corresponded to wheel tracks, furrows, patterns caused by drainage pipes or a heterogeneous vegetation cover due to a problem with the drilling machine (Figure 4-1c). In these cases, the object should not be digitized. In all other cases, i.e., isolated objects without apparent deposition fan at their lower end but whose width generally increases downstream, the operator was required to digitize the object as it probably corresponded to ephemeral gullies formed in a wheel track, at a field border or next to a bank.

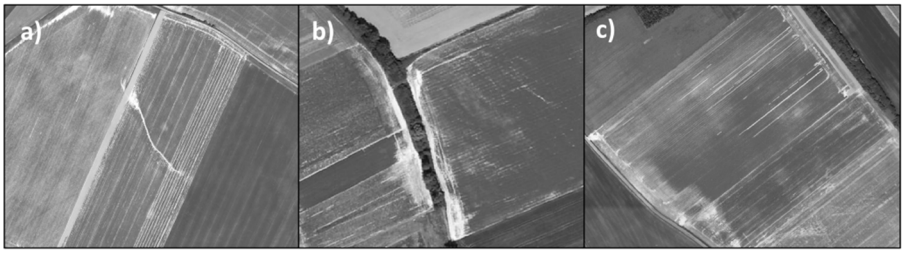

Figure 4-1: (a) Gully with deposition fan; (b) deposition at the end of furrows against the headland and field border; (c) recurrent linear objects with a near constant spacing and width, probably corresponding to wheel tracks or caused by a problem with the drilling machine.

The operators were asked to draw a line from the ephemeral gully head to the gully end. When the gully head was located in a diffuse erosion area, the gully head had to be located at the centroïd of this area. Likewise, when the end of the ephemeral gully corresponded to a large deposition fan, operators were asked to locate the end of the gully at the centroïd of the fan. Discontinuous ephemeral gullies had to be digitized as separate gullies. Operators had no time limit to perform the digitizing and no oversight was provided during digitizing beyond the initial explanatory phase.

4.2.2 Ephemeral gully classification

The operators were asked to classify each ephemeral gully into one of the three types defined in Chapter 3 (Figure 3-2). To help classify the ephemeral gullies, the operators could use the contour line map and the map of flow concentration axes as well as the Steepest Path Tool of ArcGIS®. The latter allows determining the flow path, starting from any point on a map. If the ephemeral gully head was the result of flow accumulation due to a linear element such as a field border, a headland or a wheel track, then the gully had to be classified as Type 3. Else if the ephemeral gully was located on a runoff flow concentration axis, which could be checked by means of the help tools, then it had to be classified as Type 1. Else the ephemeral gully had to be

classified as Type 2, after checking that the gully was perpendicular to the contour lines, that it did not coincide with a runoff flow concentration axis and that the Steepest Path tool showed parallel paths for different points clicked in the proximity of the gully head.

4.2.3 Ephemeral gully characteristics

The total number of ephemeral gullies, sum total length of ephemeral gullies, ephemeral gully head location and ephemeral gully classification were compared across operators. To compare the gully head locations, standard distances were computed by means of the ArcGIS® software for the ephemeral gully identified by more than one operator. For a given ephemeral gully, the standard distance corresponds to the mean distance between the gully heads identified by each operator and the center of gravity of the gully head locations. In order to try and explain why some objects were more or less easily identified by the operators, parametric analyses of variance were performed to test for significant effect of the shape of the object (length and sinuosity), the number of parcels traversed by a gully, and the crop types along each segment of the ephemeral gully. Note that it was not possible to estimate the width of the digitized objects because they were digitized as lines. The sinuosity was calculated as the ratio between the actual path length of the ephemeral gully and the shortest path length between the initiation and ending points.

4.2.4 Topographic thresholds

The operator dependence of five topographic thresholding methods was assessed. These methods are: Patton and Schumm (1975) named PS75, Vanwalleghem et al. (2005a) named VW05, Vandekerckhove et al. (1998) named VDK98, Torri and Poesen (2014) named DT14 and the quantile

regression named QR. The PS75 method, the VW05 method, the VDK98 method and the DT14 are presented in Chapter 2 and Figure 2-1. The QR method is based on the recognition that quantiles can be estimated by an optimization function that minimizes the sum of weighted absolute residuals, where the weights are asymmetric functions of the quantile α (Cade and Noon, 2003). This applies to univariate as well as bivariate distributions. For a given quantile α, e.g., α = 10%, quantile regression defines a straight line below which the probability of observing a value is α. For additional information regarding quantile regression, the reader is referred to Koenker and Hallock (2001). In this study, the quantile α used for the regression varied from one dataset to another, because the size of the dataset may affect the topographic threshold parameters if α is fixed. α was determined based on the confidence interval of regression parameters computed from the rank score test method (Koenker, 1994). For each dataset, we used the most extreme quantile (closest to 0) with the 90% confidence interval. In addition, the confidence interval of the exponent b should not include 0. Quantile regressions were performed using the R statistical package Quantreg (Koenker, 2012).

For the 11 operators, only Type 1 ephemeral gullies whose contributing area was not crossed by a road were used for the topographic threshold analysis because the impact of a road on the flow inside a contributing area cannot be predicted on the sole basis of aerial photographs and topography. The roads were identified using the Navstreets inventory of all of the named roads in Wallonia. Type 2 gullies (Figure 3-2B) were not retained because it was not possible to accurately define their contributing area given the current resolution of the DEM. Type 3 gullies (Figure 3-2C) were also excluded from the topographic threshold analysis. Indeed, the soil mechanical properties governing gully formation (e.g., soil cohesion) may differ systematically in wheel tracks, plow furrows or ditches from the soil properties of the plow layer of cultivated fields. This is especially true for ephemeral gullies formed

in spring and summer, whose depth is generally restricted to the plough layer (Nachtergaele et al., 2002). In addition, the true contributing area of Type 3 ephemeral gullies may differ substantially from the topographic contributing area as flow direction may be modified by the anthropogenic features. The 5 thresholding methods were applied to each of the 11 datasets as well as to a compound dataset constructed on the basis of all the Type 1 ephemeral gullies identified by at least 6 operators and whose contributing areas were not crossed by a road. All threshold equations were expressed as Equation 2-1.

4.3 Results

4.3.1 Ephemeral gully characteristics and classification

In the analyzed area, the 11 operators identified between 52 and 139 ephemeral gullies, with a mean of 99 ± 21 (mean ± SD; Figure 4-2). In total, 259 different ephemeral gullies were digitized and most of them were classified as Type 1. All operators identified at least some Type 2 gullies, whereas not all operators identified Type 3 gullies (Figure 4-2). Among the 259 ephemeral gullies, 103 (40%) had been digitized by only one operator and 37 (14%) are shared by only two operators (Table 4-1). Eighty-eight ephemeral gullies (35%) were identified by at least 6 operators, i.e., by more than half of the operators. Only 18 (7%) ephemeral gullies were identified by all 11 operators.

The sum total length of ephemeral gullies (sum of all gullies) also varied strongly across operators (Figure 4-3). The mean total length was 15546 ± 3710 m (range: 8865 - 23724 m). Operators with the longest total length of ephemeral gullies such as operators 1, 2 and 9 were not those which digitized

the greatest number of ephemeral gullies. Therefore, they digitized longer ephemeral gullies on average. Considering all operators, the mean ephemeral gullies length was 179 ± 33 m (range: 151 m – 237 m) for ephemeral gullies classified as Type 1, 100 ± 57 m (range: 51 – 235 m) for Type 2 gullies and 101 ± 22 m (range: 73 – 139 m) for Type 3 gullies.

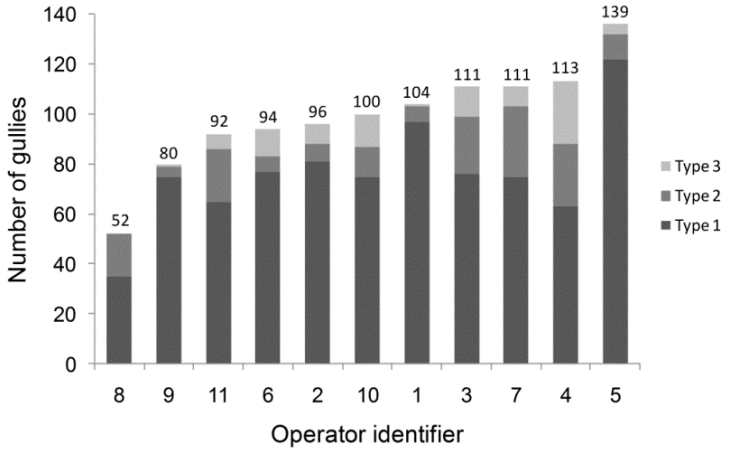

Figure 4-2: Number of gullies per gully type identified by each of the 11 operators.

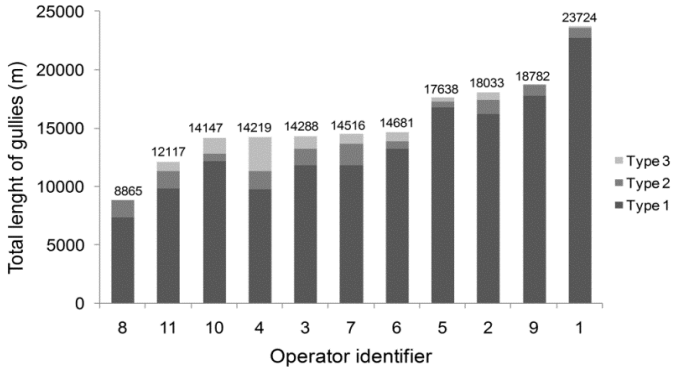

Operator identifier	1	2	3	4	5	6	7	8	9	10	11
Mean length (m)	228	188	129	126	130	156	131	170	235	141	132
Stantard deviation	167	140	115	116	133	128	120	114	151	142	124

Figure 4-3: Sum total length of gullies as a function of the operator and the gully class. The table below the graph reports mean gully length and standard deviation as a function of the operator.

A unique class was attributed to each of the 259 ephemeral gullies (Table 4-1). When a given ephemeral gully was classified differently by different operators, it was classified in the dominant class. If there was no unique dominant class, i.e., when a gully was classified about equally by the operators in two different classes, the attributed class was a mixed class (e.g., [1 or 2], [1 or 3]). Overall, 71 % of the digitized ephemeral gullies were predominantly classified as Type 1, 13% as Type 2 and 10% as Type 3. The remaining 6% could not be associated to a unique dominant class. The majority of Type 2 and Type 3 ephemeral gullies, respectively 58% and 64%, were digitized by only one operator. No single Type 3 ephemeral gully was identified by more than 3 operators. This is in contrast with Type 1 ephemeral gullies, for which 41% were digitized by at least 6 operators. Still, 36 % of Type 1 ephemeral gullies were digitized by only one operator. Table 4-2 shows the distribution of the objects whose dominant class was Type 1 and which were digitized by at least 6 operators (high probability of being gullies). In general, the higher the number of operators who identified a given object, the more the operators agreed on the classification. On average, all operators agreed on the classification for 87% of Type 1 ephemeral gullies, yet some ephemeral gullies were identified as Type 2 (9%) or Type 3 (4%) by some operators.

Analyses of variance showed that the length of the object, the number of parcels crossed and the crop type had a significant effect on the number of operators that identified an object. The objects identified by 11 operators were significantly longer than those identified by 1, 2 or 3 operators ($0.005 < p < 0.030$). The mean length of the objects identified by 11 operators was 235 m (±128 m). When identified by 1, 2 or 3 operators the mean lengths were respectively 129 m (±146 m), 127 m (±88 m) and 84 m (±105 m). The objects identified by 11 operators crossed a significantly larger number of parcels than those identified by 1, 2 or 3 operators ($6 \times 10^{-6} < p < 0.016$). Similarly, objects identified by 10 operators also crossed a significantly larger numbers of

parcels than those identified by 1 or 2 operators ($0.011 < p < 0.016$). The average number of parcels crossed by an object digitized by 11 and 10 operators was 2.2 (±1.2) and 2.0 (±1.2), respectively. When an object was identified by 1, 2 or 3 operators, the average number of parcels crossed were respectively 1.3 (±0.6), 1.2 (±0.5), and 1.4 (±0.6). When an object was located in a sugar beet field, the number of operators who identified it was on average significantly higher (8.8 ± 2.8) than if located in a potato, maize or winter cereal field (respectively $p = 1.2 \times 10^{-5}$, $p = 0.053$, $p = 2.2 \times 10^{-16}$). There were no significant differences when the object was located in potato or maize fields (respectively 7.7 ± 3.6 and 7.6 ± 3.6). However, the number of operators was significantly lower when the object was located in a winter cereal field compared to maize and potato fields (6.3 ± 3.8; $3.3 \times 10^{-6} < p < 0.031$). Sinuosity of the object had no significant effect on the number of operators that identified an object.

Table 4-1: Distribution of the 259 digitized ephemeral gullies per gully class as a function of the number of operators that identified a given gully. [1]: Ephemeral gullies located on a well-defined runoff flow concentration axis (Type 1), [2]: Ephemeral gullies located on planar hillslope sections without apparent flow concentration axis (Type 2), [3]: Ephemeral gullies resulting from linear elements (Type 3), [1 or 2], [2 or 3], [1 or 3]: Ephemeral gullies which were classified about equally by the operators in two different classes (see text).

	Ephemeral gully class							
Number of operators that identified the same gully	*[1]*	*[2]*	*[3]*	*[1 or 2]*	*[2 or 3]*	*[1 or 3]*	Sum	*Percent*
11	24	1	-	-	-	-	25	*10*
10	16	-	-	2	-	-	18	*7*
9	9	3	-	-	-	-	12	*5*
8	11	-	-	1	-	-	12	*5*
7	11	3	-	-	1	-	15	*6*
6	4	2	-	-	-	-	6	*2*
5	5	-	-	-	-	-	5	*2*
4	8	-	-	-	1	-	9	*3*
3	11	4	2		-	-	17	*7*
2	18	2	7	7	1	2	37	*14*
1	66	21	16	-	-	-	103	*40*
Sum	183	36	25	10	3	2	*259*	*100*
Percent	*71*	*13*	*10*	*4*	*1*	*1*	*100*	-

Table 4-2: Distribution among the three ephemeral gully types of the ephemeral gullies dominantly classified as Type 1, as a function of the number of operators that identified a given gully. The distribution reflects the classification of each gully by each individual operator. Only ephemeral gullies digitized by at least six operators are considered

Number of operators that identified the same gully	Number of gullies	Gully classification (percent of operators; mean ± standard deviation)		
		Type 1	Type 2	Type 3
11	24	94 (±10)	3 (±8)	3 (±7)
10	16	91 (±12)	5 (±9)	4 (±10)
9	9	90 (±17)	7 (±10)	3 (±7)
8	11	88 (±15)	8 (±11)	4 (±6)
7	11	82 (±14)	10 (±14)	8 (±11)
6	4	79 (±14)	21 (±14)	0
Mean		87 (±5)	9 (±6)	4 (±2)

4.3.2 Location of the ephemeral gully heads

For the analysis of the ephemeral gully head location, only objects digitized by more than half of the operators (≥6) were retained because they have a great probability to be real gullies. Consequently, only 88 ephemeral gullies were retained. Almost half of these gullies were digitized by 11 or 10 operators, and 85% were classified as Type 1 (Table 4-1). The mean standard distance of the gully head locations was 14.8 ± 18.9 m (mean ± SD). Figure 4-4 shows that the greatest standard distance (16.3 m) pertains to Type 1 ephemeral gullies. Type 2 ephemeral gullies had the shortest standard distance (5.6 m). We investigated the effect of the number of operators on the mean standard distance (Figure 4-5). This was done only for Type 1 ephemeral gullies, considering the low number of Type 2 and mixed ephemeral gullies (Table 4-1). Figure 4-5 shows that the standard distance was lower (between 13 m and 6 m) when only 6 or 7 operators identified the same ephemeral gully. For ephemeral gullies identified by 8 to 11 operators, the standard distance remained fairly constant at 18 m on average.

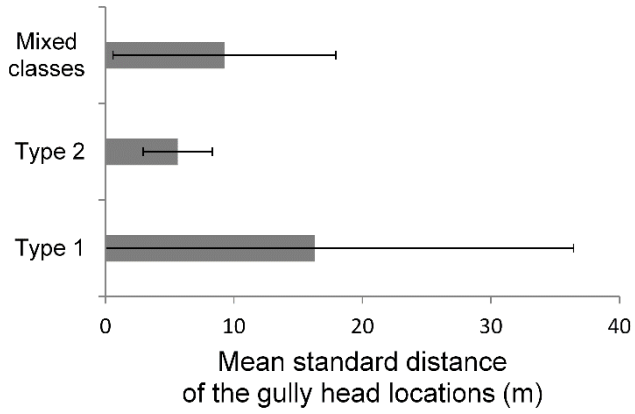

Figure 4-4: Mean standard distance of the gully head locations as a function of the gully type, for gullies identified by at least six operators.

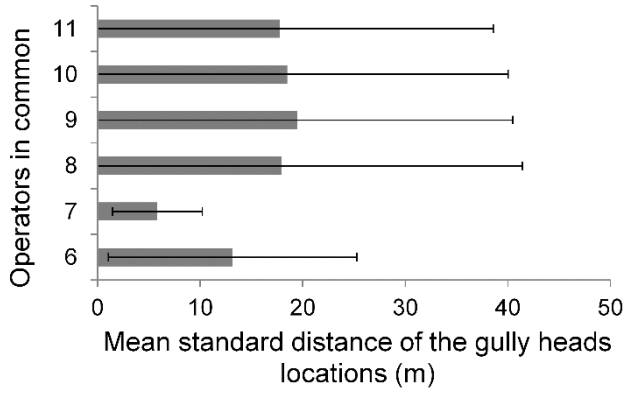

Figure 4-5: Mean standard distance of the gully head locations as a function of the number of operators who identified them.

4.3.3 Topographic threshold analysis

After removing the ephemeral gullies whose contributing area was crossed by a road, the average number of Type 1 ephemeral gullies that could be used to define the topographic threshold for gully initiation was 59 ± 16 (range: 28 to 94). Figure 4-6 shows that the topographic threshold derived by means of the PS75 method was the most sensitive to differences across operators. This was confirmed by the computation of the standard deviation of the *a* (intercept)

and *b* (slope) coefficients (Equation 2-1) of the threshold lines, which were approx. two to four times greater than for the four other methods (Table 4-3). The mean and standard deviations of the *b* values derived by the VW05, VDK98 and the QR methods were very similar. The mean *b* value obtained using these methods were 4 times less important that the *b* value of the DT14 method. The *a* value obtained with the VW05 method and the DT 14 method were similar. They were two times lower than for the QR method on average, while the VDK98 method led to intermediate values. The QR and VDK98 methods had the lowest coefficients of variation of the coefficient *a*.

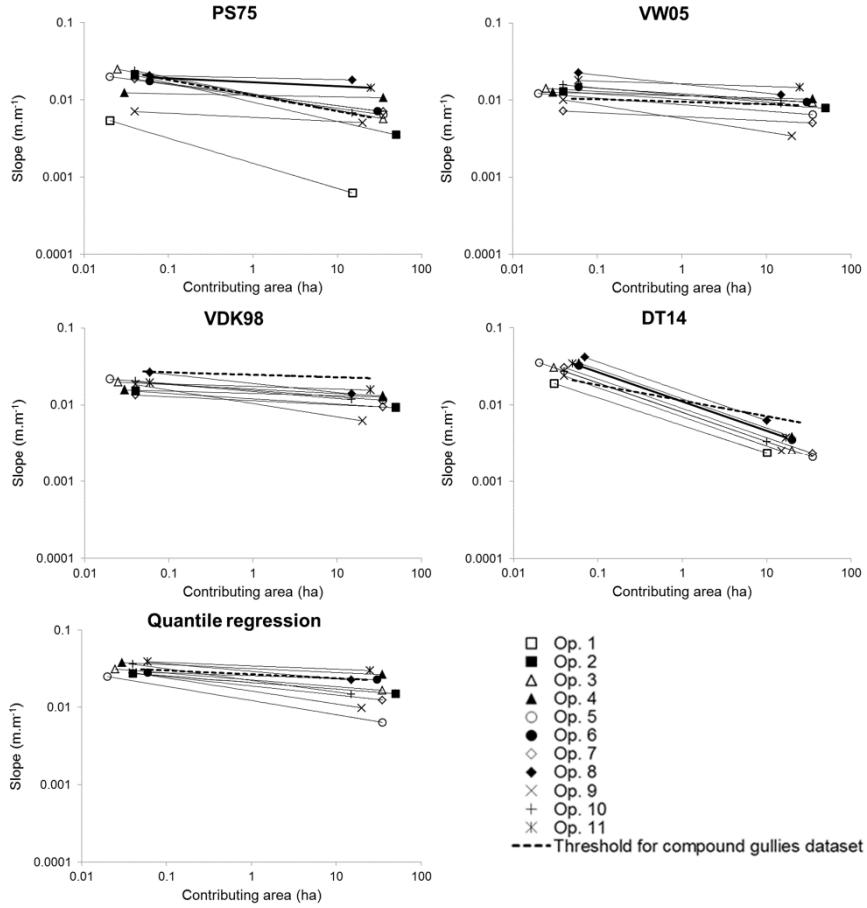

Figure 4-6: Topographic threshold for gully initiation calculated for each of the 11 operators by the five different methods: PS75, VW05, VDK98, DT14 and QR. The bold dashed line represents the threshold calculated for the compound dataset (gullies identified by at least six operators).

Table 4-3: Values of the *a* (intercept) and *b* (slope) coefficients of the topographic threshold lines (Equation 2-1) for each of the 11 operator datasets and five thresholding methods[a]. Only Type 1 ephemeral gullies whose contributing areas are not crossed by roads were considered. The quantile α used for the quantile regression method is also shown. The compound dataset corresponds to all Type 1 gullies identified by six operators or more and whose contributing areas are not crossed by roads.

Operator identifier	PS75		VW05		VDK98		DT14		QR		
	a	*b*	*a*	*b*	*a*	*b*	*a*	*b*	*a*	*b*	α
1	0.002	0.33	0.001	0.19	0.010	0.19	0.005	0.38	0.020	0.10	0.21
2	0.009	0.25	0.010	0.07	0.012	0.07	0.008	0.38	0.021	0.08	0.22
3	0.012	0.20	0.011	0.06	0.016	0.06	0.008	0.38	0.023	0.09	0.16
4	0.040	0.02	0.011	0.03	0.014	0.03	0.012	0.38	0.032	0.05	0.42
5	0.040	0.15	0.009	0.08	0.016	0.08	0.008	0.38	0.012	0.18	0.04
6	0.012	0.14	0.012	0.07	0.016	0.07	0.011	0.38	0.026	0.03	0.17
7	0.012	0.14	0.006	0.05	0.011	0.05	0.009	0.38	0.019	0.12	0.12
8	0.019	0.02	0.016	0.12	0.019	0.12	0.015	0.38	0.029	0.10	0.20
9	0.006	0.05	0.006	0.17	0.010	0.17	0.007	0.38	0.016	0.17	0.14
10	0.012	0.21	0.012	0.09	0.015	0.09	0.008	0.38	0.022	0.15	0.15
11	0.017	0.05	0.016	0.04	0.017	0.04	0.011	0.38	0.034	0.04	0.50
Compound dataset	0.011	0.20	0.009	0.03	0.033	0.03	0.009	0.38	0.027	0.05	0.23
Mean[b]	0.016	0.14	0.010	0.09	0.014	0.09	0.009	0.38	0.023	0.10	
Standard deviation	0.012	0.10	0.004	0.05	0.003	0.05	0.003	0.000	0.006	0.05	
Mean[c]	0.014	0.17	0.009	0.10	0.014	0.10	0.009	0.38	0.021	0.11	
Standard deviation	0.010	0.09	0.004	0.05	0.003	0.05	0.003	0.000	0.005	0.04	

[a] PS75 : Patton and Schumm (1975); VW05 : Vanwalleghem et al. (2005a) ; VDK98 : Vandekerckhove et al. (1998); DT14 : Torri and Poesen (2014) ; QR : quantile regression.

[b] All operators

[c]Without operators 4 and 11

The quantiles that were used to compute the threshold line by means of QR were abnormally high for operators 4 and 11 (0.42 and 0.50) (Table 4-3 and Figure 4-7). When computing the *a* and *b* values without operators 4 and 11, trends remained the same. However, the mean position (intercept) of the QR threshold was lowered and the standard deviation decreased. The mean quantile used for QR was 0.21 ± 0.13, and 0.16 ± 0.05 after excluding operators 4 and 11. Analysis of variance revealed significant differences between the mean *a* value of the QR method compared to the mean *a* value of the VW05 and the DT 14 methods ($p = 0.002$ and $p = 0.001$, respectively) after excluding operators 4 and 11. No significant differences among the thresholding methods for the *b* value were observed between the PS75, VW05, VDK98 and QR methods. However, all these methods resulted in mean *b* values significantly different from the *b* value of the DT14 method ($p < 0.001$).

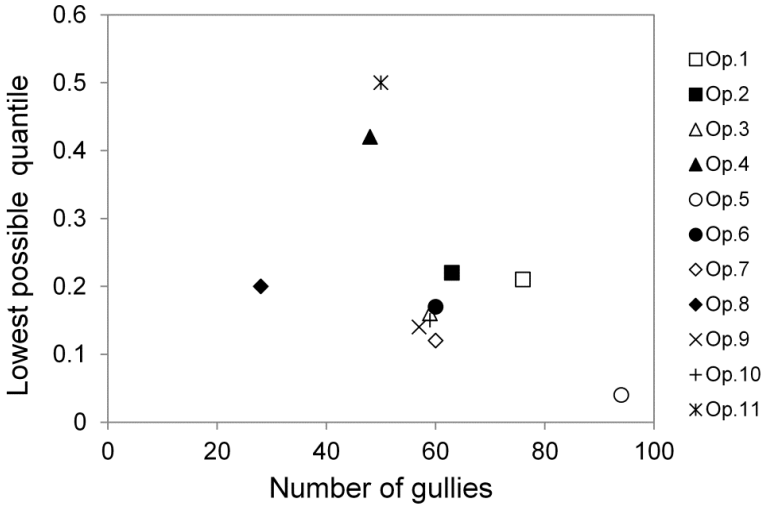

Figure 4-7: Relation between the number of gullies in a given dataset and the lowest quantile that could be used for deriving the topographic threshold line through quantile regression. Each point corresponds to a different operator.

Figure 4-8 shows the value of the slope and contributing areas at the gully heads for all Type 1 ephemeral gullies. For a given ephemeral gully, the mean gully head position was set at the center of gravity of the heads identified by

each operator, after which a 25 m buffer was applied. Data dispersion for the ephemeral gullies identified by 5 operators or less was larger than for the gullies identified by at least 6 operators. Among the 75 ephemeral gullies identified by at least 6 operators (Table 4-1), 61 could be used for the topographic threshold analysis because their contributing areas were not crossed by a road. The topographic thresholds resulting from this compound dataset are shown in Figure 4-6. For the PS75, VW05, DT14 and QR methods, the *a* and *b* coefficient values of the thresholds resulting from the compound dataset were consistent with those defined on the basis of the 11 individual datasets. On the contrary, when applying the VDK98 method to the compound dataset, the position of the resulting threshold was higher than the threshold lines defined with the 11 individual datasets.

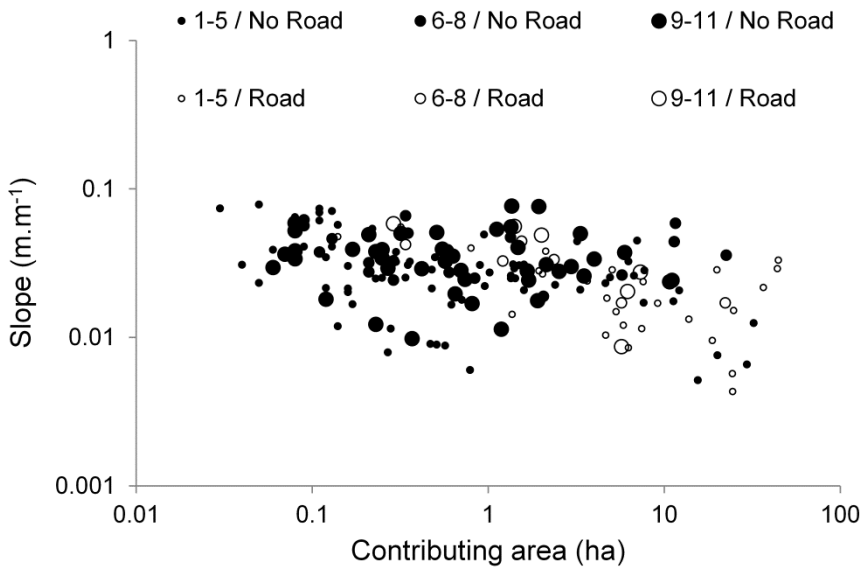

Figure 4-8: Slope and contributing area values at the gully heads of all Type 1 gullies. The size of the symbol is related to the number of operators who identified a given gully. Filled symbols relate to gullies whose contributing areas were not crossed by a road whereas open symbols relate to gullies whose contributing areas were crossed by a road.

4.4 Discussion

4.4.1 Ephemeral gully characteristics and classification

In spite of the decision tree and image catalogue that were made available to the operators, and despite the fact that all operators were familiar with erosion processes, 40% of digitized objects were digitized by only one operator and only 34% of the objects were identified by more than half of the operators (Table 4-1). This large number of gullies identified by only a single operator was not solely caused by operator 5 who identified 139 gullies, i.e., 40 gullies more than the average operator. Indeed, when excluding operator 5 from the analysis, still 36% of gullies were digitized by only one operator and also 36% were identified by more than half of the operators. This demonstrates that ephemeral gully identification on aerial photographs remains particularly subjective. It could be that not all of the operators rigorously followed the decision tree and based their decisions on their own experience.

The statistical analyses revealed that some characteristics may facilitate the detection of ephemeral gullies, such as the object length, the number of parcels crossed by a gully and the crop type along the gully segments. The longer the object, the more likely it will be that the gully will coincide with a runoff flow concentration axis for at least part of its length, and the more certain the operator will feel regarding the identification of the object. At the time the images were taken, vegetation cover of summer crops was highest for sugar beets (sown in April) and lowest for potatoes and maize (sown later in May). Hence the contrast between the vegetation cover and the bare soil of the gully floor was highest for sugar beets and lowest for potatoes and maize, facilitating gully detection in sugar beet fields compared to maize and

potatoes. Even though the vegetation cover was also high for winter wheat (sown in November), the contrast between a gully and the winter cereal vegetation cover was low due to the yellowish dominant color of this crop in summer. Ephemeral gullies formed in winter may also in part have been recolonized by weeds. Hence, this may explain why the detection of ephemeral gullies in winter wheat was the most subjective of all crops. The acquisition date of aerial photographs had therefore an important effect on the identified ephemeral gullies and might induce more uncertainty than the effect due to the operator. The number of parcels crossed by an ephemeral gully also appeared to be an important factor enhancing ephemeral gully detection, because it increases the probability that a gully traverse a field with high gully vs. crop cover contrast. These 3 factors – gully length, crop cover and number of fields crossed – are clearly not independent. Long ephemeral gullies traversing several fields, among which a sugar beet field, therefore have the highest probability to be detected by a large number of operators.

All of the 103 ephemeral gullies detected by only one operator were reinterpreted by author of this thesis. Table 4-4 reveals that these objects appear to correspond mostly to rills or areas of diffuse erosion (Figure 4-9c and d). Other important sources of error were due to linear objects such as wheel tracks, field entrances or heterogeneity in crop planting due to problems with the drilling machines. Sinuous objects without clear signs of erosion but matching flow concentration axes and contrasting with their nearby environment were also problematic (Figure 4-9b). These may for instance correspond to older, filled in gullies, to areas of colluviation in dry valleys or to areas of contrasted crop growth due to differences in water regime, but field validation would be required to be more assertive. The presence of such sinuous objects may explain why sinuosity had no significant effect on the number of operators that identified the same object. Finally, some misidentification errors were due to sediment deposits in furrows when the

latter are oriented perpendicularly to the thalweg, even though these are discontinuous objects and hence should not have been digitized at all (Figure 4-9a).

Table 4-4: Re-interpretation by the lead author of the nature of the 103 objects identified as gullies by a single operator

Reinterpretation of the objects	Number of objects
Linear element (wheel tracks, field entrance, heterogeneous cover due to a problem with the drilling machine)	22
Diffuse erosion	30
Deposition in the furrows crossing a depression	8
Flow concentration axis without erosion signs	16
Rills	27
Total	103

Identification seems to be more subjective for Type 2 and Type 3 ephemeral gullies than for Type 1 ephemeral gullies (Table 4-1). Most Type 2 ephemeral gullies identified by only one operator seemed to be rills rather than gullies. If an ephemeral gully is defined as a channel with a minimal cross section of 929 cm^2 (Hauge, 1977), then rill width will seldom exceed the resolution of the images (0.5 m), making their identification much more difficult and leading to greater discrepancies between the operators. Type 3 gullies were problematic because some operators classified into this group objects such as bare soil areas in wheel tracks or field entrances. Similarly, bare soil areas caused by problems with drilling machines were interpreted by some operators as ephemeral gullies (Table 4-1 and Figure 4-1c). Despite the overall better agreement among operators regarding the identification of Type 1 ephemeral gullies, these gullies were nevertheless also subject to major sources of misidentification since 59% of them were identified by less than 6 operators. As already mentioned above, color contrasts not due to ephemeral gully

erosion (Figure 4-9b), sediment deposition in furrows (Figure 4-9a) or diffuse erosion signs (Figure 4-9c) were interpreted by some operators as being gullies.



Figure 4-9: Four objects digitized as gullies which are not gullies: (a) deposition in the furrows crossing a depression, (b) flow concentration axis without erosion signs, (c) diffuse erosion, (d) rills.

As for ephemeral gully identification, ephemeral gully classification also proved somewhat subjective, although this depended on the gully type. Type 1 ephemeral gullies were classified most consistently by the operators (Table 4-1 and Table 4-2), which can be attributed to their greater length, thereby facilitating their detection but also interpretation. Type 1 ephemeral gullies digitized by at least 10 operators were also the most clearly located on a flow concentration axis or were branched gullies. Confusion was possible with Type 2 gullies when the ephemeral gully did not coincide with a well-defined flow concentration axis. Occasional confusion with Type 3 ephemeral gullies

occurred when a linear element such as a field border or a wheel track coincided with a flow concentration axis, which gave room for interpretation.

4.4.2 Location of the ephemeral gully heads

The standard distance of the ephemeral gully heads was 14.8 m. Besides the operator's subjectivity in deciding where the gully starts, two additional factors affect the standard distance: the number of operators who identified a given ephemeral gully, and the ephemeral gully type. Indeed, Figure 4-5 shows that the mean standard distance increases with the number of operators but stabilizes around 18 m at 8 operators. Type 2 ephemeral gullies have the smallest standard distance and Type 1 gullies the largest one (Figure 4-5). This indicates a greater difficulty in locating the gully head for Type 1 ephemeral gullies. Indeed, Type 2 ephemeral gullies resulted from a unique flow path whereas Type 1 ephemeral gullies resulted from the convergence of multiple flow paths, leaving more room for interpretation regarding the location of the gully head. Note that the observed standard distance of 14.8 m corresponds to a distance of 6 mm on the screen when viewing the aerial photographs at the 1:2,500 scale. So the location of the ephemeral gully heads can be considered fairly consistent across operators. Although the standard distance is somewhat smaller than the buffer distance (25 m) that is used for the topographic threshold analysis, it is still larger than the DEM's resolution (10 m). Hence, the uncertainty in ephemeral gully head location may contribute to additional variations among operators when characterizing the topographic threshold.

4.4.3 Topographic threshold analysis

Figure 4-6 shows that the PS75 method was most sensitive to the operator. This was confirmed by the two to four times higher standard deviations of the *a* and *b* coefficients for this method (Equation 2-1 and Table 4-3) compared

to the four other methods. This is because the method is not statistically based and is very sensitive to outliers. The DT14 method had the highest mean *b* value (slope of the threshold), significantly different from the other methods. This is not in accordance with Torri and Poesen (2014) which suggested that the *b* value of the topographic threshold is essentially constant whatever the study area. The four other thresholding methods resulted in similar *b* values, four times less important than the *b* value of 0.38 proposed by Torri and Poesen (2014).

The positions of the threshold lines (*a* value) varied by a factor 2 across the 5 methods, and differed significantly when comparing the QR method to the VW05 and DT14 methods. Because the threshold position in the VW05 and DT 14 methods are defined by the lowermost points, which makes them sensitive to extreme values, these methods resulted on average in the lowest threshold positions. Although the PS75 method was also sensitive to extreme values, it led to no significant difference with the *a* value of the QR method due to a greater dispersion of the *a* values across the operators than for the VW05 and DT14 methods. The mean *a* value obtained using the DT14 method was in accordance with the mean *a* value reported for topographic threshold for ephemeral gullies formed in cropland compared to the mean *a* values reported for rangeland and forest. Considering all 11 operators, QR resulted in the highest threshold position on average, but this was strongly influenced by the datasets of operators 4 and 11. For these two datasets, it was necessary to use very high quantile values (Table 4-3). Indeed, the lowest acceptable quantile that could be used to carry out QR for operators 4 and 11 was >0.4, whereas it was <0.22 for all other operators (Table 4-3). After excluding operators 4 and 11, there was a tendency for the lowest acceptable quantile to decrease as the number of ephemeral gullies in a given dataset increased (Figure 4-7). However, a larger number of operators with low and high gully numbers would be needed to confirm this. The threshold's position derived by

QR seems to be influenced by both the number of data points and the quality of the dataset (Figure 4-10). For operator 8, the *a* value was relatively high because of the small number of ephemeral gullies. On the other hand, the topographic thresholds for operators 4 and 11 had the highest position, despite a reasonably large number of ephemeral gullies (50). We attribute this to the lower quality of their datasets. Indeed, these operators misclassified some key Type 1 gullies, and misclassified other gullies as being Type 1.

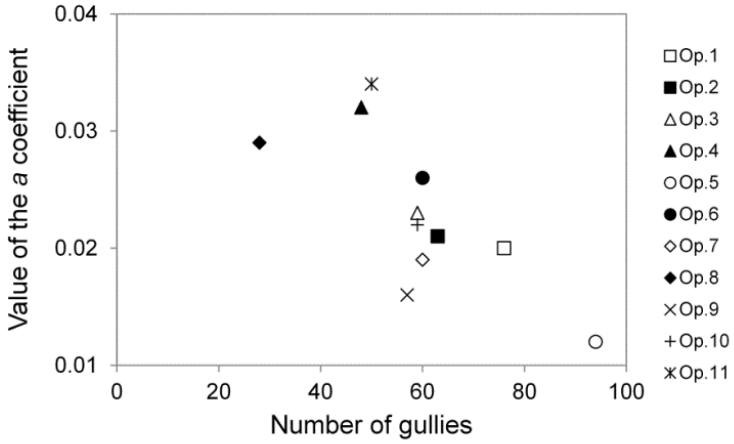

Figure 4-10: Relation between the number of gullies in a dataset and the a value (Equation 2-1) of the topographic threshold line derived by quantile regression. Each point corresponds to a different operator.

Another source of variation across operators was the locations of the ephemeral gully heads. Among Type 1 gullies, only ephemeral gullies whose contributing area was not crossed by roads were used. Accurately locating the gully head is thus important since a difference in the ephemeral gully head location could lead to a change in the size or shape of the contributing area and hence in the probability that the contributing area be crossed by a road. The gully head location may thus determine the acceptance or rejection of the ephemeral gully for topographic threshold analysis. Furthermore, as discussed above, differences in gully head location may affect the slope and contributing areas values, and hence the position of an ephemeral gully on the graphs.

The position of the topographic threshold derived by the VDK98 method was also sensitive to the quality of the dataset. This is clearly revealed through the analysis of the compound dataset. The *a* value of the compound dataset was higher than the *a* value of any of the individual datasets (Figure 4-6 and Figure 4-11). The explanation is that the 95 % confidence interval resulting from the compound dataset was much smaller than the 95 % confidence intervals of the datasets of each individual operator. As opposed to the individual datasets which included objects that had a low probability of being actual ephemeral gullies (identified by few operators), all 61 ephemeral gullies of the compound dataset had a high probability to be 'true' gullies, which resulted in a smaller 95% confidence interval and so a higher position of the threshold. All five thresholding methods appear sensitive to the operator but the impact was least on the topographic thresholds determined through the QR and VDK98 methods considering their coefficients of variation. The slope of the topographic threshold defined using the DT14 method was not sensitive to the operator because the *b* value was a constant but it resulted in a threshold that did not fit well the lower boundary of the scatter plot compared to the QR and VDK. The topographic thresholds defined with QR generally fitted best to the lower boundary of the scatter plot (Figure 4-11). Because the mean positions of the VDK98 and DT14 topographic thresholds were lower compared to the QR method and because they did not always fit well to the lower boundary of the scatter plot, one may expect the VDK98 and DT14 methods to overestimate the range of slope – contributing area conditions that are susceptible to lead to ephemeral gully initiation. On contrary, the topographic threshold defined with the QR method led to the rejection of topographic conditions that would be considered favorable to ephemeral gully initiation based on the other methods. However, the rejection probability is known because it corresponds to the quantile used for the regression. The QR method therefore seems to be the most appropriate method.

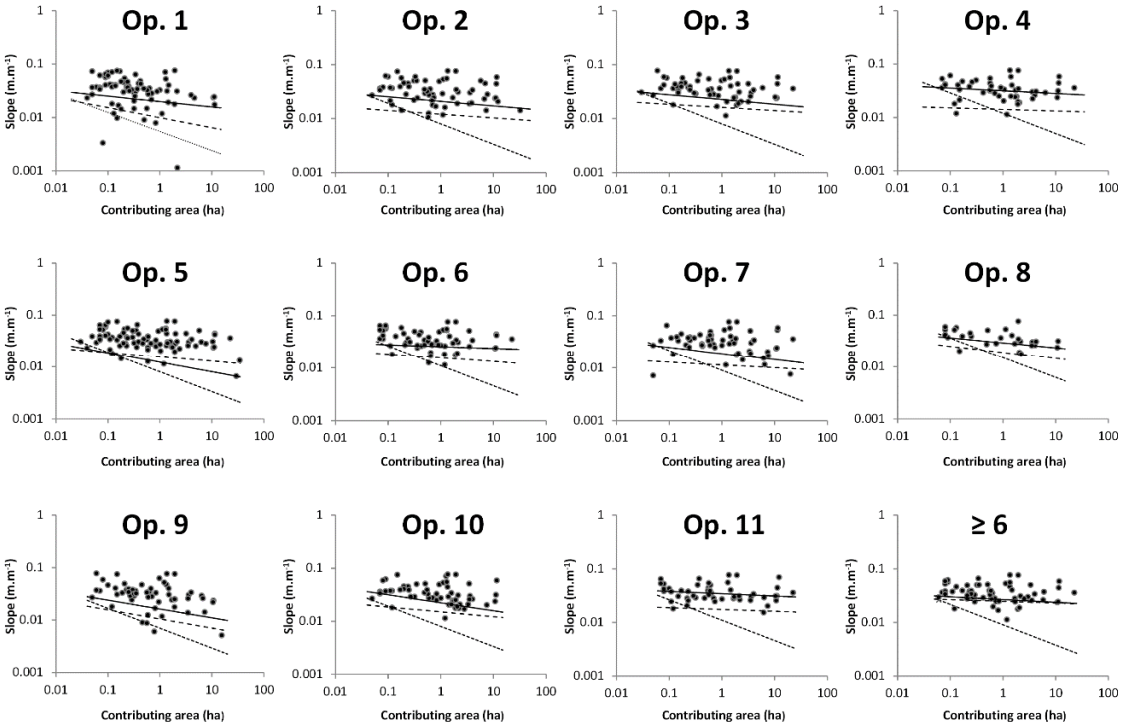

Figure 4-11: Topographic thresholds derived by quantile regression (solid lines), the method of Vandekerckhove et al. (1998) (dashed lines) and the method of Torri and Poesen (2014) (dotted lines) for the 11 operator datasets (Op.) as well as for the compound dataset (≥ 6) consisting of all gullies identified by at least six operators and whose contributing areas are not crossed by a road. Regression coefficients are shown in Table 4-3.

A comparison of the 11 datasets with field data would have been very useful, though impossible in the present case given the date of acquisition of the images (2006) and the short life span of ephemeral gullies. This might have allowed better specifying the actual gully class, the factors facilitating or hampering ephemeral gully detection (e.g., length, width, environmental factors) and the accuracy with which ephemeral gully characteristics can be assessed. Considering the resolution of the photographs, we can expect that narrow yet sometimes deep ephemeral gullies could not be detected reliably, because of their limited width but also because they generally correspond to winter gullies located in winter cereal fields (Vanwalleghem et al., 2005a) and hence offer a poor contrast. Given that the shortest ephemeral gullies were 20 mm long on the screen (= 50 m real length), it can be expected that a width of 2 pixels (1 m; 0.5 mm on the screen) would be sufficient for proper detection given sufficient contrast.

The use of images with a better resolution would most likely decrease the uncertainty in gully detection and delineation, although this will also require viewing at a greater scale (> 1:2500). Another way to decrease operator-dependence would be to resort to automation, as performed in some recent gully mapping studies (see, e.g., Knight et al., 2007; Eustace et al., 2011; Shruthi et al., 2011). However, those studies assumed that no error affected the reference datasets used for training and validation even when they were acquired through manual digitizing. Any discrepancies between the automatically and manually detected gullies are thus solely attributed to deficiencies of the automated system (e.g., Eustace et al., 2011; Shruthi et al., 2011), whereas a substantial part might in fact be explained by observer subjectivity during image interpretation. As emphasized recently by Gardin et al. (2011), human operator performance is rarely questioned in remote sensing studies in general, let alone in automated image analysis schemes. Any proper evaluation of automated schemes should, however, include an analysis of the

uncertainty of the reference datasets, including uncertainty due to the human operator. The present databases could be very useful for this purpose because each gully can be associated with a level of uncertainty. This could be incorporated in the analysis of the automation scheme's accuracy. Sarmento et al. (2009) recently proposed a methodology to integrate the uncertainty in the reference dataset due to human interpretation in the assessment of the overall accuracy of their land cover classification.

Although the present study relied on aerial photographs, the results can be readily extended to satellite imagery with similar resolution whenever manual digitizing is involved. They may also be extended to permanent gullies, although we expect the uncertainty to be lower compared to ephemeral gullies, given that permanent gullies generally have larger dimensions and a clearer incision point.

This study relied on educated operators with several years of working experience in the field of erosion, yet untrained with respect to ephemeral gullies identification on images. Working with trained operators would most likely have reduced the discrepancies between operators. Nevertheless, when results from different studies are being compared, it is safe to assume that the persons who performed the digitizing work in those studies did not go through joint training either. Hence one may expect a similar degree of subjectivity when comparing different studies as was documented in the present study. Admittedly, alternating phases of digitizing and ground truthing would provide the best formal training, but as mentioned earlier, this is rarely feasible in the case of ephemeral gullies when working with commercial imagery.

4.5 Conclusions

For the area under investigation, and for ephemeral gullies in agricultural settings, characteristics such as the number, the sum total length, the gully head location and the classification of ephemeral gullies varied greatly among the operators, despite them having been provided with a standardized methodology. Gullies located on well-defined runoff flow concentrations axes were most easily identified and classified, though still subject to much uncertainty. Long ephemeral gullies crossing several fields, including a sugar beet field, were most easily detected.

Whatever the method used for defining the slope vs. contributing area topographic threshold for ephemeral gully initiation, there was a strong variability in threshold coefficients among operators. This variability resulted from the different number of ephemeral gullies identified by each operator but also from the quality of the datasets. Even the DT14 thresholding method, fixing the slope of the threshold, resulted in non-negligible variations across the operators regarding to the threshold position. Among the thresholding methods compared, the PS75 method appeared most sensitive to differences among operators, whereas the QR method was one of the most robust thresholding methods. The latter is especially recommended when the level of uncertainty on the gully dataset is high.

In future studies or literature reviews, the uncertainties resulting from manual ephemeral gully identification should not be overlooked. Assessing the impact of operator-subjectivity on data quality should therefore be an essential step in any gully image-interpretation scheme whenever it relies, in part (automated approaches) or in full (manual interpretation), on human interpretation.

5 Characteristics and spatio-temporal variability of ephemeral gully erosion in Wallonia[1]

[1] Based on: *Maugnard, A., Van Dyck, S., Bielders, C.L. 2014. Assessing the regional and temporal variability of the topographic threshold for ephemeral gully initiation using quantile regression in Wallonia (Belgium). Geomorphology, **206**, 165-177.*

5.1 Introduction

No study related to ephemeral gully erosion characterization has previously been carried out in Wallonia. However, in view of the results obtained in the Flemish Loess belt (e.g., Nachtergaele et al., 2001, 2002; Nachtergaele and Poesen, 1999, 2002), ephemeral gully erosion is also expected to be a widespread phenomenon in Wallonia. It is expected to vary across Wallonia due to the diversity of topographic contexts, soil conditions and land use but also to vary over the time depending on rainfall and land cover conditions. The aims of this section were therefore to characterize ephemeral gully erosion across different agricultural areas of Wallonia and to assess the recurrence of the phenomenon.

5.2 Material and methods

The gully database #1 (Table 3-1) was used to assess ephemeral gully characteristics in the Loamy area, the Famenne and the Jurassic area (study sites #1 to #3; Figure 3-1). The length of each gully as well as the crop type at the gully head and along the gully were recorded and summarized by gully type (Figure 3-2). The recurrence of ephemeral gully erosion was evaluated for one additional study site (#4; Figure 3-1) by comparing the location of gullies across years (gully database #2; Table 3-1).

5.3 Results and discussion

5.3.1 Characteristics of ephemeral gullies in the study sites

Ephemeral gullies were classified depending on the types defined in Chapter 3 (Figure 3-2). For all study sites the proportion of Type 3 gullies was low (4% to 9%; Table 5-1), indicating that anthropogenic factors play a direct role in gully initiation only in a limited number of cases. The proportions of Type 1 and 2 gullies were similar in the Loamy area. In the Jurassic area, most gullies are Type 2, whereas Type 1 gullies dominate in the Famenne. The mean length of Type 2 gullies was always significantly smaller than for the two other types ($p < 0.001$), which is consistent with its definition. Indeed, the longer the gully, the higher the probability that it will reach a clearly identifiable flow concentration axis and consequently be classified as Type 1. In the Loamy area and the Famenne, the lengths of Type 1 and Type 3 gullies were not significantly different ($p = 0.91$ and 0.08, respectively), whereas in the Jurassic area Type 3 gullies are significantly longer than Type 1. Type 1 gullies were 50 m longer on average in the Loamy area compared to the two other areas ($p = 0.01$). In the Jurassic area, Type 2 gullies were 25 to 30 m shorter than in the two other areas ($p = 0.018$).

The highest number of gullies per ha of agricultural land (gully frequency) was observed in the Loamy area (Table 5-2). A similar gully frequency was observed in the Jurassic area, but it was about three times less in the Famenne. Gully frequency per ha of cropland was the highest for the Jurassic area and about twice as high as in the two other areas. The gully length per ha (gully density) of cropland varied by a factor of almost two across the areas, and was highest in the Jurassic area and lowest in the Famenne (Table 5-2).

Table 5-1: Distribution of the number of gullies by type (Figure 3-2) and their mean length (mean ± SD) for each study site

			All gully types	Type 1	Type 2	Type 3
Loamy area	2006–2007	Number	282	43%	48%	9%
		Mean length [m]	126 (±104)	170 (±119)	80 (±60)	172 (±101)
Famenne	2006–2007	Number	59	56%	36%	8%
		Mean length [m]	107 (±73)	117 (±81)	75 (±37)	177 (±68)
Jurassic area	2006–2007	Number	161	37%	59%	4%
		Mean length [m]	84 (±100)	122 (±101)	50 (±33)	233 (±280)
Condroz / Loamy area	1999	Number	113	70%	23%	7%
		Mean length [m]	145 (±144)	173 (±153)	54 (±36)	159 (±137)
	2006–2007	Number	153	63%	30%	7%
		Mean length [m]	151 (±142)	200 (±149)	60 (±52)	251 (±159)
	2009–2010	Number	102	44%	50%	6%
		Mean length [m]	119 (±149)	193 (±196)	54 (±36)	113 (±63)

Table 5-2: Frequency and density of ephemeral gullies per acreage of agricultural land or cropland for each study site

Agricultural area	Gully frequency per ha agricultural land	Gully frequency per ha cropland	Gully density per ha agricultural land	Gully density per ha cropland
	gullies ha^{-1}	gullies ha^{-1}	m ha^{-1}	m ha^{-1}
Loamy area	0.016	0.020	2.02	2.56
Famenne	0.005	0.016	0.53	1.69
Jurassic area	0.014	0.037	1.14	3.08

These results are quite similar to the gully frequencies and densities for cropland estimated using aerial photographs for four study sites in the Flemish loess belt and reported by Nachtergaele and Poesen (1999). Gully frequencies reported in this study ranged from 0.016 to 0.074 gullies per ha of cropland while gully densities ranged from 2.1 to 13.3 m ha^{-1} depending on the year. Nevertheless, some gully densities and frequencies reported by Nachtergaele and Poesen were two to four times greater than the maximum gully density and frequency observed in the Jurassic area. This could be attributed in part to the areal extent of the study sites and the acreage of cropland which were three to sixteen times smaller in the study of Nachtergaele and Poesen (1999). Gully densities and frequencies reported in the literature are most often related to permanent gullies. Rodzik and Gardziel (2004) reported gully densities up to 90 m ha^{-1} in the area of Lublin in Poland. Voloschuk and Ionita (2006) reported gully densities ranging from 2 to 10 m ha^{-1} in Moldavia. According to Sidorchuk et al. (2006), the mean gully frequencies are 0.003 and 0.001 gullies per ha in European Russia and Byelorus, respectively.

In all the study sites, gully heads and gullies were located mainly on land with summer crops (sugar beet, maize and potatoes; Table 5-3). Gully frequency and density for cereal crops were lower than those for summer crops (Table 5-3). The higher sensitivity to gullying of land with summer crops is consistent

with previous studies in Belgium. Evrard et al. (2007) reported the highest rates of muddy floods in the late spring to early summer, due to the combined effect of convective rainfall and low vegetation cover in fields recently sown with summer crops. Summer crops like potatoes and maize have wide row spacings and a low vegetation cover density for 1–2 months after sowing. For the #1 to #3 study areas, most gullies were restricted to a single parcel, although 16–19% of the gullies crossed two parcels, and 7–10% crossed three parcels or more. It thus appears that field borders, either because of vegetation change or anthropogenic factors, were effective at halting ephemeral gully development.

The largest number and length of gullies in the Loamy area (Table 5-1) can be attributed to the large acreage occupied by cultivated parcels (56% of the total acreage and 80% of the agricultural acreage, Table 3-2), erodible loamy soils (e.g., Vandaele et al., 1996) and the large mean size of fields. Among the summer crops, most gullies in the loamy area were found on land with sugar beet (Table 5-3). This can be explained by the date of sowing, which is about 1.5 months earlier for sugar beet (late March) than for the two other crops (early May) increasing the probability to observe gullies. This could also be attributed to the larger acreage of sugar beet compared to the other summer crops.

The absolute number of gullies in the Famenne was lower than in the Loamy area (Table 5-1) but their frequency for cropland was similar (Table 5-2). The lower total number of gullies can be directly attributed to the lower total acreage of cropland in the Famenne compared to the Loamy area (Table 3-2). The lower mean gully density for cropland in the Famenne may have resulted from the smaller mean field size (Table 3-2). The gully frequency was the highest in sugar beet fields. However, this was not really relevant because sugar beet occupied only 1% of the agricultural land (164 ha).

Table 5-3: Frequency and density of gullies for different crop types

		Maize	Winter cereal	Summer cereal	Potato	Sugar Beet	Other cover type
Loamy area	Cover type acreage (ha)	1414	6346	471	1038	2566	5816
	Number of gully heads per ha	0.031	0.001	0.002	0.030	0.065	0.006
	Length of gully per ha (m/ha)	4.24	0.10	0.14	2.77	8.47	0.75
Famenne	Cover type acreage (ha)	1147	1979	124	3	164	8478
	Number of gully heads per ha	0.031	0.005	0.000	0.000	0.061	0.000
	Length of gully per ha (m/ha)	3.75	0.51	0.00	0.00	4.77	0.03
Jurassic area	Cover type acreage (ha)	1330	2208	421	24	64	7795
	Number of gully heads per ha	0.087	0.014	0.007	0.042	0.047	0.001
	Length of gully per ha (m/ha)	7.63	0.86	0.88	2.72	2.99	7.63

Most gullies in the Famenne were located in maize fields which occupied the largest summer crop acreage. The length of gullies per crop type was similar for maize and sugar beet (Table 5-3). No gullies were observed in potato fields in the Famenne, which may be explained by the low acreage of potatoes (3 ha) in 2006.

As reflected in the high frequency and density of gullies for cropland, the Jurassic area seems to be the most sensitive area to gully erosion (Table 5-2), even though the dates of acquisition of the aerial photographs for the study site were up to three weeks earlier than in the two other study sites, which decreased the probability to observe summer gullies. The gullies were mainly located in maize fields (Table 5-3) even though the photographs were taken on June 10, only about one month after maize sowing. As for the Famenne, maize was the main summer crop in the Jurassic area and the frequency and density of gullies calculated for sugar beet and potato were not really relevant because of their low acreage (64 ha and 24 ha, respectively). The occurrence of two major rainfall events (21 and 25 mm on May 16 and 20, respectively) may partly explain the higher rate of gully erosion in the Jurassic area. Type 2 gullies dominate in the area (Table 5-1), probably because probably because of the steep slopes in the Jurassic area compared to the two other areas (Table 3-2). Furthermore, the mean length of flow concentration axes (with contributing area $\geq$ 1 ha) per ha of cropland was smaller in the study site in the Jurassic area (26 m ha^{-1}) than in the two other study sites (43 m ha^{-1}).

5.3.2 Assessing the recurrence of ephemeral gully erosion

The number of gullies was the highest for the 2006–2007 dataset and the lowest for the 2009–2010 dataset (Table 5-1). The lower number of gullies observed in 2009–2010 may in part result from the fact that the

orthophotographs were taken much earlier (May) than for the two other datasets (July; Table 3-2). It could also explain in part that in 2009-2010 most gullies were Type 2 unlike the 1999 and 2006-2007 datasets where Type 1 gullies dominated. It is indeed expected that some Type 2 gullies could expand due to subsequent rainfall events and reach well defined flow concentration axis, thereby becoming Type 1 gullies.

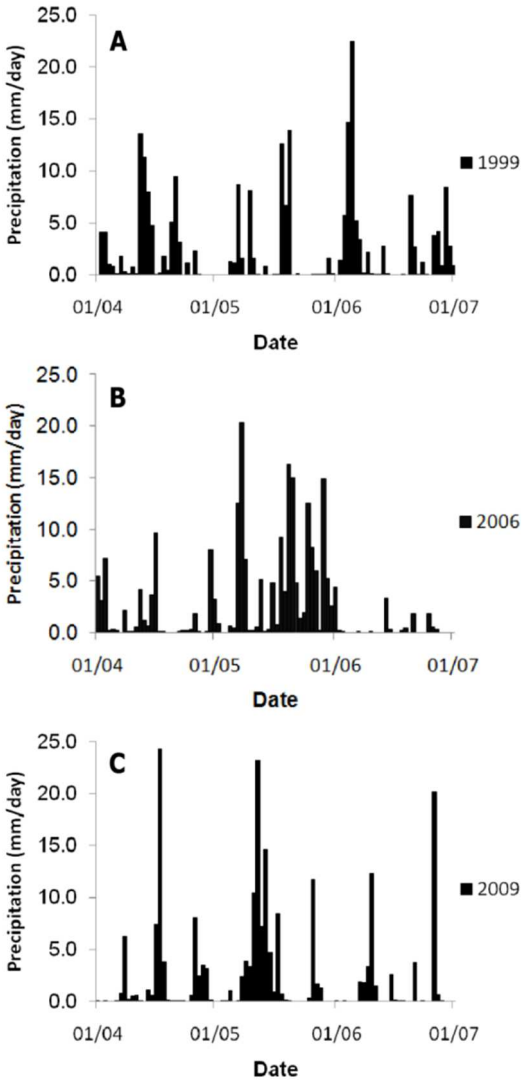

Figure 5-1: Daily precipitation from April to July in (A) 1999, (B) 2006 and (C) 2009 in study site #4.

More numerous events in May 2006 as compared to the two other years may explain the higher number of gullies in 2006–2007 (Figure 5-1). Large rainfall events were also observed in 1999 but these occurred later in the season (June) when the vegetation cover of the summer crops was already higher and hence the soils were less sensitive to erosion. Even if the distribution of the number of gullies by type varied across years, Type 1 gullies always represented the greatest cumulative length (Table 5-1). When comparing the datasets two by two, the percentages of recurrent ephemeral gullies varied from 17% to 38%. Recurrent gullies were mostly of Type 1 (82% to 91%), highlighting the importance of topographic factors on gully initiation and location. However, only between 12% and 18% of the gullies observed in any one dataset was also observed in the two other datasets. Hence, topographic factors alone are clearly not sufficient to explain gully initiation, and other factors such as land use (Table 5-3) and rainfall must play a major role for gully initiation.

5.4 Conclusions

Even though gully characteristics derived from aerial photographs can be affected by substantial uncertainties (cf. Chapter 4), some general trends can nevertheless be observed, consistent with rainfall and land use patterns. First, it was found that ephemeral gullying on cropland was highly variable in terms of type, number and length across different agricultural areas in Wallonia. This appears to result from the combined effects of differences in crop type, mean field size, and characteristics of topography and rainfall. Secondly, in all agricultural areas, the initiation of most gullies was driven by topographic factors, although up to 9% could be directly linked to anthropogenic linear elements such as furrows or fences. Third, summer crops were more sensitive to gullying than other crop types. Finally, the recurrence of ephemeral gully erosion at the same location was limited when comparing three different years, due to changes in crop types and climate.

6 Analysis of the topographic threshold for the initiation of ephemeral gullies[1]

[1] Based on: *Maugnard, A., Van Dyck, S., Bielders, C.L. 2014. Assessing the regional and temporal variability of the topographic threshold for ephemeral gully initiation using quantile regression in Wallonia (Belgium). Geomorphology, **206**, 165-177.*

6.1 Introduction

The topographic threshold has been widely used because it is a simple means to define areas prone to gully initiation (e.g., Montgomery and Dietrich, 1992; Vandaele et al., 1996; Vandekerckhove et al., 1998, 2000; Vanwalleghem et al., 2005a ; Wu and Cheng, 2005, Gomez-Gutierrez et al., 2009). It consists in extracting the land slope and contributing area values at the gully head and to plot those values on a log-log graph. Below the threshold, gully initiation is not observed for the different slope-contributing area combinations, whereas above it gully initiation is possible yet not systematic. It has been shown that the topographic threshold varies depending on the gully types and the environmental conditions (e.g. Vandaele et al., 1996; Torri and Poesen, 2014).

Different approaches have been proposed so far for defining the topographic threshold (Patton and Schumm, 1975; Vandekerckhove et al., 1998 and Vanwalleghem et al. 2005a, Torri and Poesen 2014). These methods, presented in Chapter 2, are questionable. The Patton and Schumm (1975) method may be problematic as multiple thresholds may exist (Figure 6-1A) and no statistical considerations underlie this approach. Furthermore, the threshold line is very sensitive to extreme values (Figure 6-1B) and to the operator when using aerial photographs to identify gullies (see Chapter 4) The thresholds defined by Vandekerckhove et al. (1998) and Vanwalleghem et al. (2005a) reflect the mean statistical weight of all the data points rather than the weight of the points at the lower boundary of the scatter plot because they rely on orthogonal regression (Figure 6-1C). This is not consistent with the concept of 'threshold'. Indeed, the threshold line should reflect the distribution of points in the neighborhood of the threshold line, not the distribution of the entire dataset. The thresholding method of Torri and Poesen (2014) also involves some arbitrary decisions. Indeed, as for the Patton and Schumm

(1975) method, the positioning of the threshold is somewhat subjective and sensitive to the presence of outliers. Furthermore the slope of the topographic threshold is predefined, sometimes resulting in threshold lines that are not well fitted to the lower boundary of the scatter plot (Figure 6-1D and Figure 4-11).

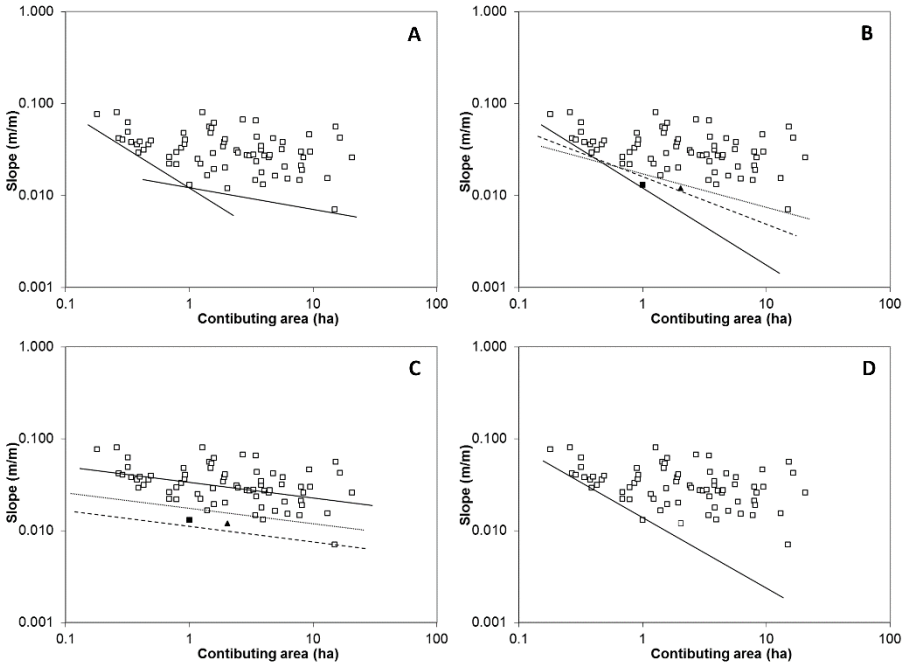

Figure 6-1: Comparison of different thresholding methods for a fictional dataset. A) Patton & Schumm (1975) method: multiple thresholds may exist. B) Patton & Schumm (1975) method: sensitivity to extreme values. The three lines are drawn after excluding 0 (solid line), 1 (dashed line) or 2 (dotted line) extreme data points (closed symbols). C) Methods based on orthogonal regression. Solid line: orthogonal regression. Dashed line: translation of orthogonal regression until the lowermost point while keeping the slope constant (Vanwalleghem et al., 2005a). Dotted line: lower limit of the 95 % confidence interval of the orthogonal regression (Vandekerckhove et al., 1998). D) Torri and Poesen method (2014): constant slope.

Part of the variability of the topographic thresholds published across different studies may result from the use of different thresholding methods. A common methodology is therefore needed to standardize the determination of the topographic threshold. The use of quantile regression, statistically-grounded, robust to outliers (John and Nduka, 2009) and reflecting the mean statistical

weight of the data points near the boundary, appears as a suitable alternative. Furthermore, quantile regression has been found to be more robust when the level of uncertainty on the gully dataset is high (Chapter 4). The aims of this section were to (i) test quantile regression as an alternative method for determining the topographic threshold; (ii) evaluate the regional variability of the topographic threshold across Wallonia; and (iii) assess the temporal stability of the topographic threshold.

6.2 Material and methods

Gully database #1 (Table 3-1) was used to define the topographic thresholds for ephemeral gully initiation across three contrasting agricultural areas: the Loamy area, the Jurassic area and the Famenne (areas #1 to #3; Figure 3-1). Five thresholding methods were compared: the Patton and Schumm (1975) method, the Vandekerckhove et al. (1998) method, the Vanwalleghem et al. (2005a) method, the Torri and Poesen method (2014) and quantile regression (Koenker and Bassett, 1978) (see Chapter 4). The temporal stability of the topographic threshold defined using quantile regression was evaluated on the basis of three datasets of aerial photographs of the Condroz/Loamy area (gully database #2, study site #4; Table 3-1 and Figure 3-1). The values of slope and contributing area at the gully heads that are needed to define the topographic threshold were extracted from the maps of slope and flow accumulation derived from the 10-m DEM. As explained in Chapter 4, only Type 1 ephemeral gullies (Figure 3-2A) were retained for the topographic threshold analysis. Type 1 gullies whose contributing area was crossed by a road were excluded to avoid data with strong interference from human artifacts. The threshold equations were expressed as Equation 2-1.

6.3 Results and discussion

6.3.1 Comparisons of the thresholding methods

The flow accumulation values at gully heads obtained from the DEM were not always consistent with the contributing areas delineated manually using the contour map (Figure 6-2). The former presented a mean bias of 38% against the latter. This could be attributed to the DEM resolution (10m) which does not allow to define properly the contributing area of the gully heads located on small flow concentration axes. The upstream part of the gully did not always fit well the flow concentration axis derived from the DEM whereas the downstream part usually matched them well. The discrepancy between the two methods was high but could be minimized by searching for the maximum value of the flow accumulation within a 15-m radius around the digitized gully head (Figure 6-2).

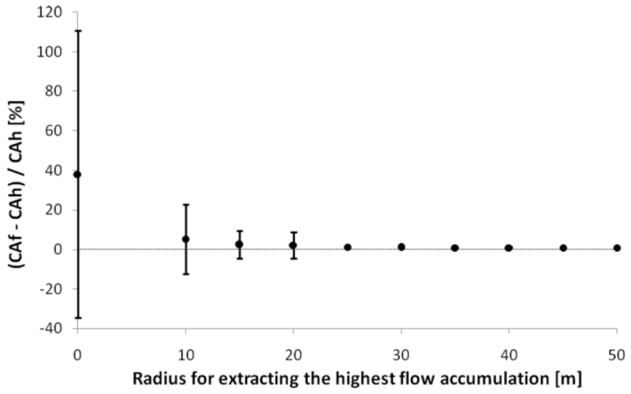

Figure 6-2: Differences between the contributing area values obtained by hand delineation on a contour map (CAh, reference value) and the contributing area obtained from the flow accumulation raster values (CAf). The latter were obtained by searching for the largest flow accumulation value within a given radius around the gully head location.

However, using a 15-m radius may still lead to substantial errors in some cases as can be inferred from the large standard deviation (Figure 6-2). A radius of

25 m allowed minimizing both the bias and the standard deviation. This latter approach was thus used to determine the contributing area for all gully heads. The slope values were also extracted at the location of the corrected contributing areas.

Figure 6-3 shows that the thresholding methods gave thresholds more or less similar depending on the agricultural area. When the correlation between the slope and the contributing area was strong as for the Jurassic area, all the thresholding methods gave similar topographic thresholds (Figure 6-3). On the contrary when the correlation was weak, as for the Famenne, the Torri and Poesen (2014) method resulted in a threshold not well fitted to the lower boundary of the scatter plot. Consequently, this method identifies a wider range of topographic conditions favorable for gully initiation than other more robust methods. Furthermore, given that the Torri and Poesen (2014) and the Patton and Schumm (1975) thresholds rely on just a few data points at the lower boundary of the scatterplot, they are very sensitive to the accuracy with which gully head locations were located. In Figure 6-3 for instance, the threshold will be different after removal of the lowermost points. This is also true for the positioning of the topographic threshold drawn with the Vanwalleghem et al. (2005a) method because the intercept of the threshold line depends on the lowermost point. The position of the threshold when using the Vandekerckhove et al. (1998) method depends on the lower limit of the 95% confidence interval of the orthogonal regression. The position of the intercept tends therefore to be the lower when the dataset size is small and when the correlation between the slope and the contributing area is weak as for the Famenne (Figure 6-3). This resulted in a topographic threshold not well fitted to the lower boundary of the scatter plot. Furthermore, the Vandekerckhove et al. (1998) and Vanwalleghem et al. (2005a) methods reflect the mean behavior of all the datasets rather than the distribution of points at the threshold.

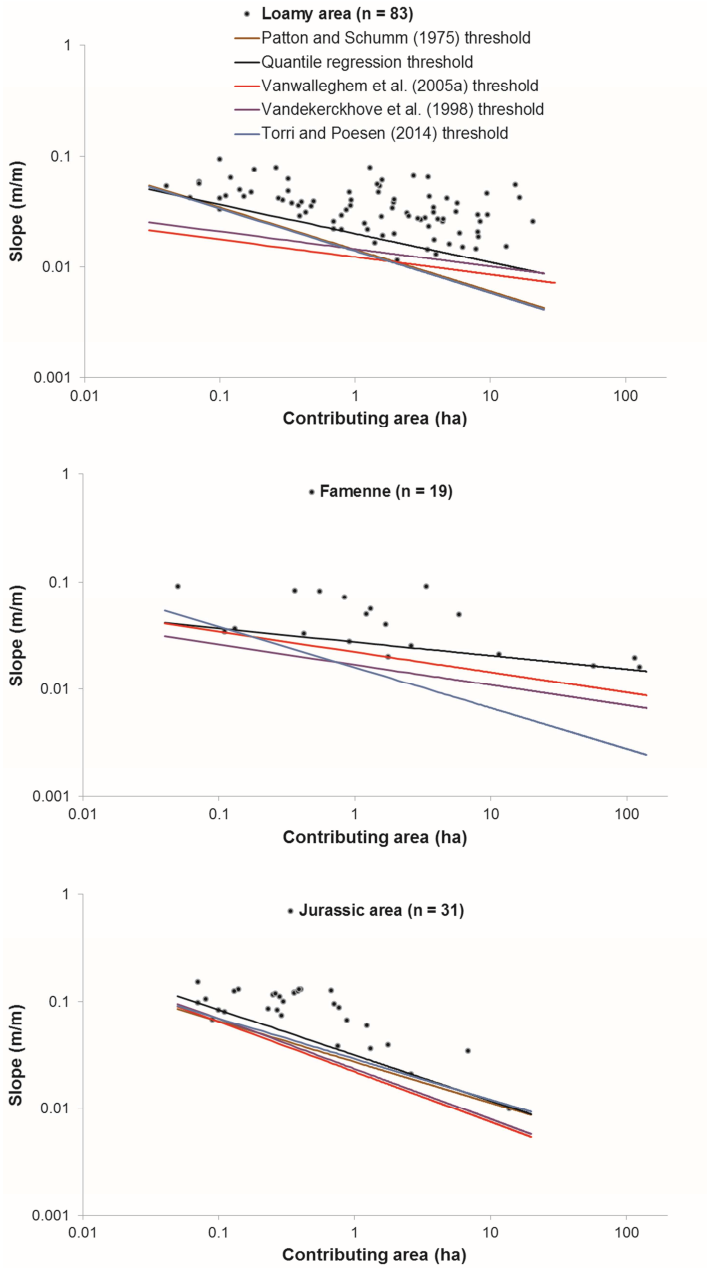

Figure 6-3: Five thresholding methods applied to the gully head datasets from (A) the Loamy area, (B) the Famenne and (C) the Jurassic area. The quantile regression is calculated for α = 0.06, 0.17, and 0.13 for the three areas, respectively. These values correspond to the most extreme quantiles for which the regression parameters can be estimated with acceptable precision. Note that for the Loamy area, the Patton and Schumm (1975) threshold and the Torri and Poesen (2014) threshold overlap. For the Famenne, the Patton and Schumm (1975) threshold and the Vanwalleghem et al. (2005a) threshold overlap.

By essence, the threshold derived through quantile regression reflects the behavior of the dataset at the threshold. However, rather than using a fixed quantile for all datasets, α differed depending on the data distribution and the size of the dataset. Calculating the confidence intervals of *a* and *b* (Equation 2-1) for a range of quantiles allows defining the most extreme quantile for which the regression parameters can be estimated with acceptable precision (Cade and Noon, 2003). The parameters *a* and *b* and their confidence intervals were calculated for the quantiles 0.01 to 0.50 with a 0.01 increment (Figure 6-4) The most extreme quantile (α as close as possible to 0) with acceptable confidence intervals for both a and b are 0.06 for the Loamy area, 0.17 for the Famenne and 0.13 for the Jurassic area (Figure 6-4).

The thresholds defined through quantile regression generally fit best to the lower boundary of the scatter plot. However, the dataset characteristics affect the quantile value that can be used for regression and hence the position of the threshold. In particular, the number of data points appears to affect the quantile that can be used for defining the threshold. The lower the number of data points, the higher the quantile needed to define the threshold (Figure 6-5), and the narrower the range of topographic conditions favorable to gully initiation. Although this does not allow for a comparison of regression parameters across the three areas for the same quantile, the use of a fixed quantile (e.g., 0.1) may result in regression parameters with very large uncertainty, as for the Famenne or Jurassic area. The proposed quantile regression method with data-dependent α therefore appears to be the most robust and to best reflect the topographic boundary conditions for gully initiation. Nevertheless, for best performance and reliable comparison of datasets, each dataset seems to need at least 50 data points. This may not always be achievable as this may require a wide study area with more heterogeneity.

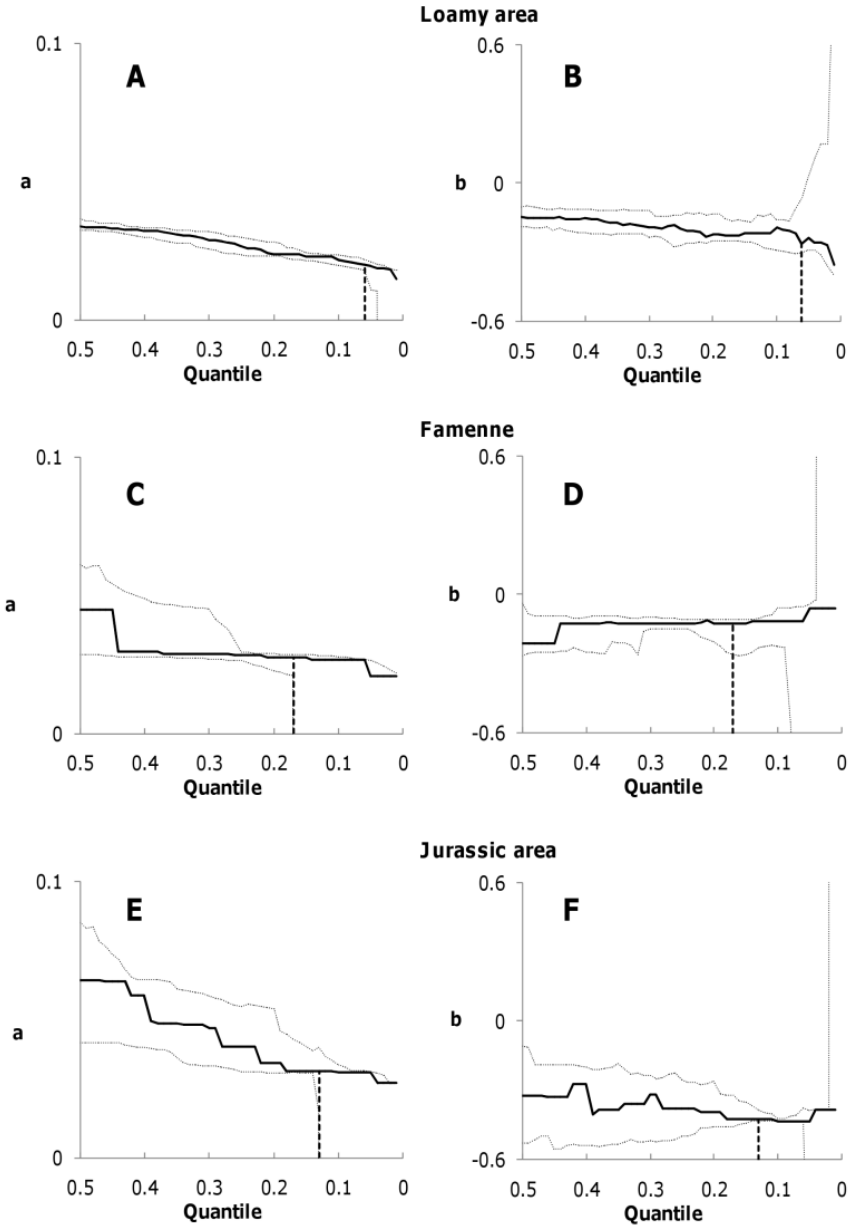

Figure 6-4: Estimates of *a* and *b* parameters of the topographic threshold (Eq. 2-1) using quantile regression, for quantiles comprised between 0.01 and 0.5 (solid lines) for the Loamy area (A and B), the Famenne (C and D) and the Jurassic area (E and F). Dotted lines are the 90% confidence intervals. The dashed vertical lines mark the most extreme quantile for which the confidence intervals of both regression parameters can be estimated with acceptable precision.

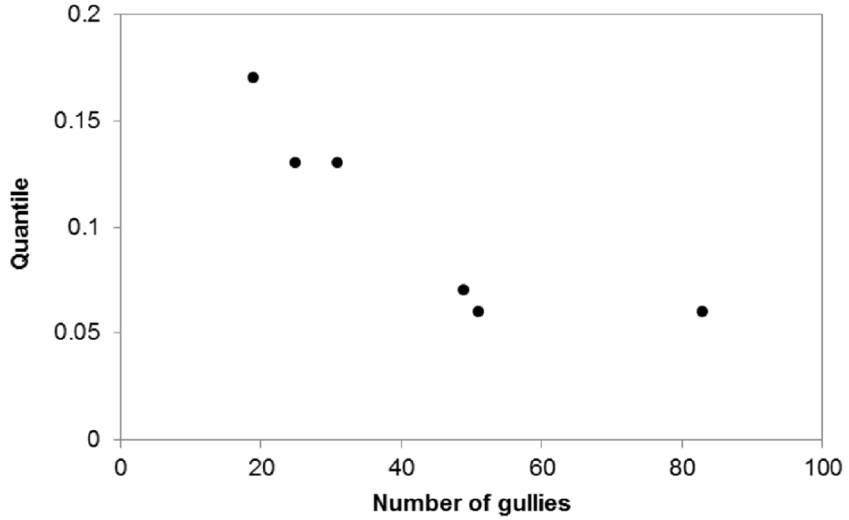

Figure 6-5: Relation between the highest quantile which can be used with acceptable precision for quantile regression and the number of gullies in each dataset, for the six datasets used in this study.

6.3.2 Regional differences in the topographic thresholds

Figure 6-6 shows the 90% confidence intervals for the *a* and *b* parameters of the topographic thresholds determined using quantile regression. The *a* value is the lowest for the Loamy area and is similar for the Famenne and Jurassic area. There is an overlap between the 90% confidence intervals of the *a* and *b* parameters of the Loamy area and those for the Famenne. Hence, we conclude that there was no significant difference between the topographic thresholds of the latter two areas, in spite of differences in the absolute number of gullies (Table 5-1). This indicates that topographic contexts favoring gully initiation were very similar for the Loamy area and the Famenne.

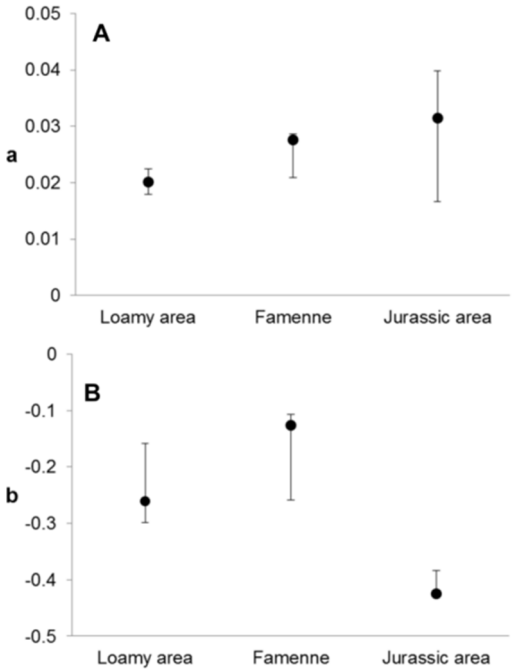

Figure 6-6: Comparison of the best values of (A) *a* (intercept) and (B) *b* (slope) parameters of the topographic threshold (Eq. 2-1) for the study sites #1 to #3 (Figure 3-1). The best values were obtained by quantile regression for the highest possible quantile for which the 90% confidence interval can be extracted with acceptable precision estimated. Vertical bars correspond to the 90% confidence intervals computed with the rank-score test method.

However, Type 1 gullies in the Famenne had, on average, larger contributing areas than in the Loamy area. The mean contributing area was 17.3±37.1 ha (mean ± SD) in the Famenne and only 3.1±3.9 ha in the Loamy area. The largest contributing area in the Famenne was 123.6 ha in contrast to 20.7 ha in the Loamy area. This may be due to the important proportion of stony soils in the Famenne are (Table 3-3). According to Vandaele et al. (1996), the contributing area for a given slope is systematically larger for valleys with a high rock fragment cover because the stony soils are less erodible and have a higher flow resistance than non-stony soils, thereby reducing the detaching and transport capacity of runoff (Govers et al., 1990). Furthermore, land use in the three largest gully contributing areas in the Famenne was mainly forest.

As forests tend to generate less runoff than cropland, a larger area is needed to generate a runoff volume sufficient to initiate gullying in forested terrain. However, in some cases, it might be that the contributing areas were overestimated and that the effective contributing area were not the entire catchment, as suggested by Torri and Poesen (2014).

The Jurassic area differed from the Loamy area and the Famenne in terms of the *b* exponent of the topographic threshold (Figure 6-6). The slope of the threshold was higher than for the two other areas. This is because the gully heads with the smallest contributing areas had higher slope values than in the two other areas (Figure 6-3). The Jurassic area is characterized by a more pronounced relief with steeper slopes, whereas the relief of the Loamy area and Famenne is characterized by vast undulating terrain. In cultivated parcels, for pixels whose contributing area values were between 0.05 and 0.2 ha, the median slope values were 3.3%, 4.2% and 6.2% for the Loamy area, Famenne and Jurassic area, respectively. The 10th percentiles were, respectively, 1.5%, 1.6% and 2.9 %, and the 90th percentiles were 6.7%, 9.2% and 13%. This implies that, for the same contributing area, gullying was more likely to be initiated on steep slopes in the Jurassic area compared to the two other areas.

When analyzing the regional variability on the basis of the other four methods, the conclusions differ significantly (Table 6-1). Regarding the Patton and Schumm (1975) method, the Loamy area and Jurassic area thresholds presented similar *b* values and differed only by their *a* value. The *b* value for the Famenne was two times lower than for the two other areas. This could be attributed to an overestimation of the “effective” contributing area, which causes a bias by decreasing the value of the *b* exponent (Torri and Poesen, 2014). The Torri and Poesen (2014) method gave almost similar results as the Patton and Schumm (1975) method in the Loamy area and the Jurassic area. The *a* value of the Jurassic area was almost two times greater than for the

Loamy area and the Famenne when using the Torri and Poesen (2014) method. The regional trends for the Vanwalleghem et al. (2005a) and the Vandekerckhove et al. (1998) methods are fairly similar to the quantile regression method, though large differences in absolute value of the parameters are apparent. The *b* values were very similar for the Loamy area and the Famenne (-0.16 and -0.19) yet 2.5 to 3 times smaller than for the Jurassic area (-0.47) when applying the Vandekerckhove et al. (1998) method. For the Vanwalleghem et al. (2005a) method, the *a* values of the Famenne and the Jurassic area were the same (0.022) but almost two times larger than for the Loamy area (0.012). Regional differences were smaller when considering the Vandekerckhove et al. (1998) method.

Table 6-1: *a* and *b* parameters of the topographic thresholds (Equation 2-1) obtained by the Patton and Schumm (1975) method, the Torri and Poesen (2014) method, the orthogonal regression method as implemented by Vandekerckhove et al. (1998) or Vanwalleghem et al. (2005a), and the quantile regression method.

	Patton and Schumm method (1975)		Torri and Poesen (2014) method		Orthogonal regression method (Vandekerckho-ve et al., 1998)		Orthogonal regression method (Vanwalleghem et al., 2005a)		Quantile regression method	
	a	*b*	*a*	*b*	*a*	*b*	*a*	*b*	*a*	*b*
Loamy Area	0.014	-0.38	0.014	-0.38	0.015	-0.16	0.012	-0.16	0.020	-0.26
Famenne	0.022	-0.19	0.016	-0.38	0.017	-0.19	0.022	-0.19	0.028	-0.13
Jurassic Area	0.027	-0.38	0.029	-0.38	0.023	-0.47	0.022	-0.47	0.032	-0.43

6.3.3 Comparison with topographic thresholds from other areas

Results of the estimation of *a* and *b* in some previous studies have been compiled in Table 6-2. Vandaele et al. (1996) used the Patton and Schumm (1975) method and interpreted the *a* value in terms of erosion process. All other conditions being similar, low *a* values (i.e., a = 0.0035 for central Belgium) can be linked to rilling whereas high values would be indicative of gullies initiated by small land sliding (i.e., *a* = 0.35; Montgomery and Dietrich, 1988). Intermediate *a* values, as found in the present study (0.014 to 0.027; Table 6-1), correspond to gullying. According to Patton and Schumm (1975), a higher critical shear stress needed to initiate gullying would be reflected in a higher value of the coefficient *a*. Hence, besides being sensitive to the erosion form, the coefficient *a* is also expected to depend on geology, soil, climate and vegetation. Based on theoretical considerations, Patton and Schumm (1979) suggested that *b* should range between −0.20 and −0.40. According to the review of Vandaele et al. (1996), *b* values reported in the literature ranged between −0.30 and −0.40 and were reasonably independent of site-specific conditions across a number of sites in Europe and the USA. The *b* values obtained by the method of Patton and Schumm (1975) in the present study ranged between −0.19 for the Famenne and −0.38 for the Loamy and Jurassic areas (Table 6-2). This is consistent with the theoretical prediction of Patton and Schumm (1975). Although the *b* values fall outside the range of values reported by Vandaele et al. (1996), other studies also reported *b* values > −0.3 (Table 6-2). In particular, Boardman et al. (1992) reported a relatively low value for the UK South Downs (−0.25), which is not very different from the value of *b* for the Famenne (−0.19).

The *a* values obtained for Mediterranean contexts in the study of Vandekerckhove et al. (2000) are higher compared to our *a* values, but the

range of the *b* values is similar. The *a* and *b* parameters reported by Vanwalleghem et al. (2005a) for central Belgium are also similar to the parameters obtained for the Loamy area and Famenne. Torri and Poesen (2014) extracted the topographic thresholds from datasets collected in various parts of the world based on their method (constant *b*). They showed that the *a* value increases from tilled soils exposed to runoff (i.e. on cropland) to soils protected from erosion by a permanent vegetation cover (i.e. rangeland, pasture, forest, grassland). They calculated a mean *a* value of 0.043 ± 0.029 (mean ± SD) for cropland, 0.154 ± 0.139 for rangeland and pasture and 0.628 ± 0.318 for forest and grassland. Whatever the thresholding method used, the *a* value calculated in the Loamy area, the Famenne and the Jurassic area were close to the mean *a* value for cropland according to Torri and Poesen (2014). The *a* values obtained based on the method of Torri and Poesen (2014) for the three agricultural areas were consistent with the *a* value of 0.03 obtained by Torri and Poesen (2014) when using the dataset of Vandaele et al. (1996) in the Flemish loess belt. Topographic thresholds values for ephemeral gully initiation similar to those found for the Loamy area, the Famenne and the Jurassic were also reported for gully datasets from Africa, Americas, Asia and Europe in the study of Torri and Poesen (2014).

Even though the range of *a* and *b* values appears reasonably consistent between the present study and previous studies, a large variability is apparent, which seems to reflect large differences in environmental conditions leading to gullying. However, it is very difficult to interpret the parameters in terms of processes, as suggested by Vandaele et al. (1996), because this interpretation requires that one of the two threshold parameters remain constant. In practice, except when using the Torri and Poesen (2014) method, both parameters vary from one dataset to another and threshold lines may even cross, implying that conditions for gully initiation do not have a fixed correlation with the contributing area.

Table 6-2: Parameters *a* and *b* of the topographic thresholds (Eq. 2-1) for ephemeral gullies reported by various studies. The parameters were obtained by the method of Patton and Schumm (1975) (PS) or the orthogonal regression method (OR, Vandekerckhove et al., 1998 or Vanwalleghem et al., 2005a).

Reference	*a*	*b*	Method	Observation method	Region
Vandaele et al. (1995)[1]	0.025	-0.40 to -0.35	PS	Aerial photographs	Central Belgium
Poesen et al. (1995)[1]	0.080	-0.40 to -0.30	PS	Field survey	Central Belgium
Govers (1991)[1]	0.004	-0.400	PS	Field survey	Central Belgium
IGN (1983)[1]	0.060	-0.400	PS	Aerial photographs	France
Boardman (1992)[1]	0.090	-0.250	PS	Field survey	UK-South Downs
Vandaele et al. (1995)[1]	0.020	-0.350	PS	Aerial photographs	Portugal
Vandekerckhove et al. (2000)	0.157	-0.133	OR	Field survey	Southestaern Spain
	0.146	-0.142		Field survey	Southestaern Spain
	0.227	-0.104		Field survey	Southestaern Spain
	0.101	-0.267		Field survey	Southwestern Spain
	0.102	0.226		Field survey	North Portugal
	0.083	0.303		Field survey	South Portugal
	0.077	0.414		Field survey	South Portugal
	0.285	0.139		Field survey	Greece
Vanwalleghem et al. (2005a)	0.020	0.141	OR	Field survey	Central Belgium

[1]in Vandaele et al. (1996)

6.3.4 Temporal stability of the topographic threshold

Fourty-nine, 51 and 25 data points were available for drawing the threshold lines for the 1999 (PPNC), 2006–2007 and 2009–2010 aerial photograph datasets, respectively. As previously, the most extreme quantile used was the quantile which allowed estimating the parameters with acceptable precision. The quantiles of 0.07, 0.06 and 0.13 were used for the 1999 (PPNC), 2006–2007 and 2009–2010 datasets, respectively (Figure 6-7). The corresponding topographic thresholds are shown in Figure 6-8. Given that the topographic factors and the soil conditions may be assumed constant within a given region, differences in the threshold should reflect differences in non-topographic factors across years. The *b* values for the three datasets were similar because the 90% confidence intervals overlapped. This was also true for the *a* coefficient of the 1999 (PPNC) and 2009–2010 datasets (Figure 6-9). There was nearly no overlap between the 2006–2007 and 2009−2010 datasets. This may have been caused by the large difference in number of gullies between the two datasets, which has a strong impact on the quantile used for the regression (Figure 6-5).

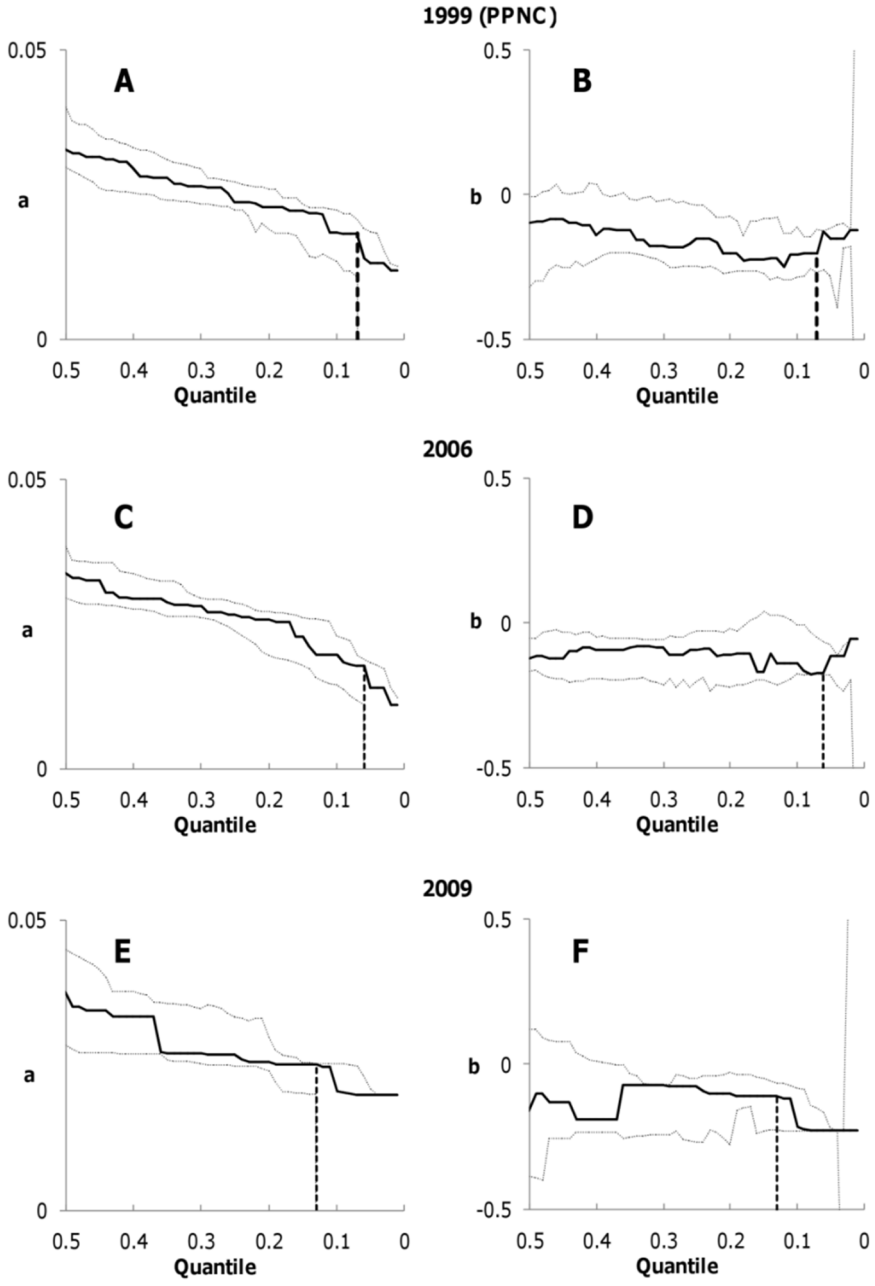

Figure 6-7: Estimates of *a* and *b* parameters of the topographic threshold (Eq. 2-1) using quantile regression, for quantiles comprised between 0.01 and 0.5 (solid lines) for area #4 (Figure 3-1) for 1999 (A and B), 2006 (C and D) and 2009 (E and F). Dotted lines are the 90% confidence intervals. The dashed vertical lines mark the most extreme quantile for which the confidence intervals of both regression parameters can be estimated with acceptable precision.

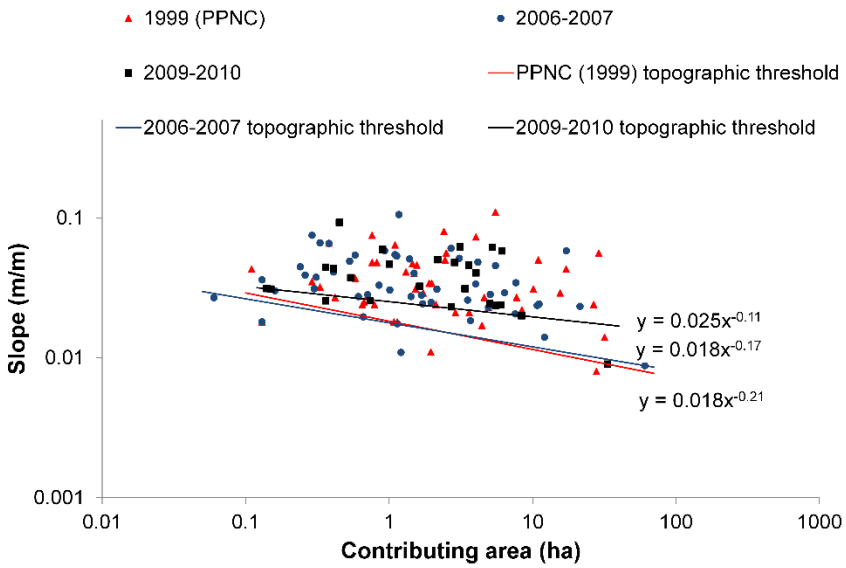

Figure 6-8: Topographic threshold determined with the quantile regression method for area #4 (Figure 3-1) for three different years. Quantile α = 0.07 for 1999 (PPNC), 0.06 for 2006–2007 and 0.13 for 2009–2010).

Since most gullies were different from one year to another, but the threshold parameters were basically similar, it appears that changes in crop types and precipitation did not significantly affect the topographic threshold parameters. So for a specific area, the topographic threshold provided consistent information about the relationship between the slope and the contributing area for gully initiation whatever the year. No gully will be formed whatever the crop type and rainfall event, for rainfall intensities within the range explored in the present study, if the combination of slope and contributing area is unsuitable for gullying (i.e., below the threshold line). However, suitable topographic conditions for gully initiation do not systematically lead to gullying. A specific combination of crop types and precipitation is required to initiate a sufficient runoff volume for gully initiation. This explains why gullies were not systematically formed at the same location from one year to another. Crop types and weather conditions explain the probability of observing a gully above the topographic threshold and their density.

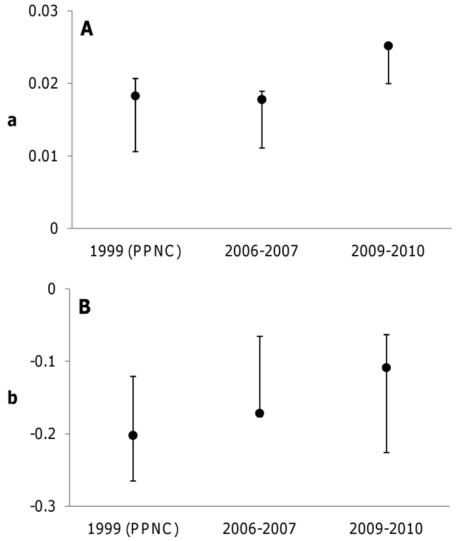

Figure 6-9: Comparison of the best values of *a* (A) and *b* (B) parameters of the topographic threshold (Eq. 2-1) for area #4 (Figure 3-1) for three different years. The best values were obtained by quantile regression for the highest possible quantile for which the 90% confidence interval could be estimated with acceptable precision. Vertical bars correspond to the 90% confidence.

6.4 Conclusions

Gullies located in hollows where overland flow concentrates were used to define the topographic threshold. Among the available thresholding methods, quantile regression appears to be the most appropriate. Indeed, this method is robust to outliers and allows to better evaluate the mean statistical weight of the data at the threshold. It was successfully applied to highlight regional differences in the topographic contexts favoring gully initiation. The resulting topographic thresholds appear stable over time and unaffected by changes in type of crop and precipitation. However, dataset-dependent differences in the quantile used for defining the topographic threshold may introduce a bias in the interpretation when small datasets are compared. Hence, sufficiently large datasets should be used whenever possible. Quantile regression should be recommended as a reference method for establishing topographic thresholds because it is statistically-based and robust to outliers.

7 What factors cause ephemeral gullies to end?

7.1 Introduction

Because of their strong negative environmental impact, there is a great need to understand the factors that drive the initiation, trajectory, expansion and stoppage of ephemeral gullies. Whereas factors controlling gully initiation, trajectory and expansion have received widespread attention (e.g., Desmet et al., 1999; Istanbulluoglu et al., 2002; Jetten et al., 2006; Momm et al., 2012), much less attention has been paid to the factors causing gullies to end and the relative importance of such factors. Such knowledge is of crucial importance to predict their length and the amount of sediment exported (e.g., Nachtergaele et al., 2001a). Information about the factors causing gullies to end would also improve our understanding of the role of gullies in overland flow connectivity and may prove useful to promote land use patterns or practices that limit gully length. Takken et al. (1999), Beuselinck et al. (2001) and Poesen et al. (2002) specifically addressed the factors controlling where gullies end. They demonstrated that ephemeral gully end was mainly controlled by topography, changes in vegetation at field borders or linear elements such as roads. As mentioned in Chapter 2, critical slope thresholds and topographic thresholds have been proposed to characterize locations prone to gully deposition controlled by topography (e.g., Poesen et al., 1998; Vandekerckhove et al., 2000). A major drawback of both concepts is that they assume that gullies end when slope or topographic conditions fall below a certain threshold, whereas deposition may in fact be more dependent on a change in topographic conditions (i.e., a change in transport capacity) rather than on the absolute values. In addition, the threshold values say nothing about the likelihood of occurrence of deposition when the threshold values are reached. Indeed, threshold conditions for deposition may have been met at different positions along the gully, yet without actually halting gully development.

Studies on gully ending points in Belgium have so far focused exclusively on the Flemish loess belt which is characterized by fairly homogeneous soil and land use conditions. It has been shown in Chapter 5 that the extent of gullying and gully characteristics vary significantly across Wallonia due to differences in local conditions such as topography, soil, cropping system and its spatial organization or the density of linear elements. Accordingly, one may also expect the factors triggering the end of ephemeral gullies to vary, thereby providing better insight into how region-specific factors influence gully ending.

The aim of this chapter was therefore to quantify the main factors controlling where ephemeral gullies end in four contrasting agro-pedological regions of Wallonia. In particular, the relevance of both topographic thresholds and simple slope thresholds for characterizing ephemeral gully ending points will be tested. To reach these objectives, 837 gullies identified on aerial were used.

7.2 Materials and methods

7.2.1 Databases used

The database #1 (Table 3-1) related to the Loamy area, the Famenne and the Jurassic area (zones #1 to #3, Figure 3-1) was used to characterize the spatial variability of the main factors controlling ephemeral gully end. The database #2, though resulting from the identification of ephemeral gullies across two regions (Condroz/Loamy area; zone #4; Figure 3-1), was included because a rich gully dataset was available for a 3-year period.

7.2.2 Characterization of the main factors controlling ephemeral gully ending points

At the downstream end of each ephemeral gully, the following factors were recorded: land use, crop type, slope, contributing area, presence of linear features such as roads, banks or hedges. When gully ending points coincided with a field border, land use and crop type on both sides of the field border were recorded. Land use and crop type were extracted from the numerical land cover map updated annually by the SPW. Slope and contributing area values were extracted from the 10-m DEM. The contributing area was determined using the flow accumulation raster, derived from the flow direction raster based on the D8 method. The presence of linear elements and their nature were determined on the basis of the aerial photographs aided by the topographic map which highlights most of them. In case of discontinuous ephemeral gullies along a flow concentration axis, the end of each gully section was considered as an ephemeral gully ending point. Parametric analyses of variance were performed to test for a significant effect of the agricultural area but also of the vegetation type on the local slope at the gully ending point.

7.2.3 Critical slope and topographic thresholds

The critical slope for gully ending was defined as the value of the slope such that 90 % of the observed ephemeral gully ending points occur at slopes smaller than the critical value (Nachtergaele et al., 2001a). The topographic thresholds were determined for the gully ending points in each study site based on Equation 2-1. They were defined using quantile regression (Chapters 4 and 6). Unlike gully initiation points, no correction was needed to extract the contributing area because flow axes were well defined for large contributing areas. The slope and the contributing area values were therefore extracted at the gully ending point location.

Based on the critical slope thresholds, each gully grid cell was classified as gully ending point or not. The classified grid cells were then compared to observed grid cells using confusion matrices to assess the relevance of the critical slope threshold for gully ending point prediction. The same methodology was used to assess the performance of the topographic thresholds.

7.2.4 Probabilistic approach to predict gully ending points controlled by topography

In each agricultural area, topographic characteristics were extracted for each 10-m grid cell along observed ephemeral gullies and at the ending point. Slope of grid cell *i*, contributing area of grid cell *i* and slope variations before and after grid cell *i* were recorded. The slope variations were calculated before and after each grid cell on a 20 m distance ($slope_{i, i-2}$ and $slope_{i, i+2}$). The total slope variation ($slope_{i+2, i-2}$) was also considered. The slope variations were used to highlight the breaks of slopes and their intensities in the proximity the ending points. Then multivariate logistic regressions were performed using the R software to create a prediction model of ephemeral gully ending points. The best model was selected based on stepwise regressions and backward eliminations. First, all parameters and interactions between the factors were integrated. Then only parameters significant at p-level = 0.05 were retained.

7.3 Results

7.3.1 Regional variability of the main factors controlling ephemeral gully ending points

A total of 837 gully ending points were analyzed. Gully ending points could be classified according to one of four situations (Figure 7-1 and Table 7-1): (1) the gully ended when it hit a linear element such as a bank, road, ditch or hedge. These elements were located at field borders. These will be referred to as 'linear element-controlled ending points'; (2) the gully ended at a field border but this was not caused by linear elements. In most cases, this coincided with a change in vegetation cover from one parcel to another. These ending points will hereafter be referred to as 'vegetation-controlled ending point'; (3) the gully ended as a result of a change in tillage direction in the headland. These cases will be referred to as 'headland-controlled ending points'; (4) the gully ending was located well inside the parcel boundaries but was not caused by a change in tillage direction. It was assumed that in such cases the gully ended as a result of changes in topographic conditions. Hence, these situations are referred to as 'topography-controlled ending points'. In some cases, for gullies ending at the field borders, it was not possible to determine reliably whether the ending was controlled by a change in vegetation or by a linear element. Such cases represented 1.3% of all gully ending points and were classified in a separate class.

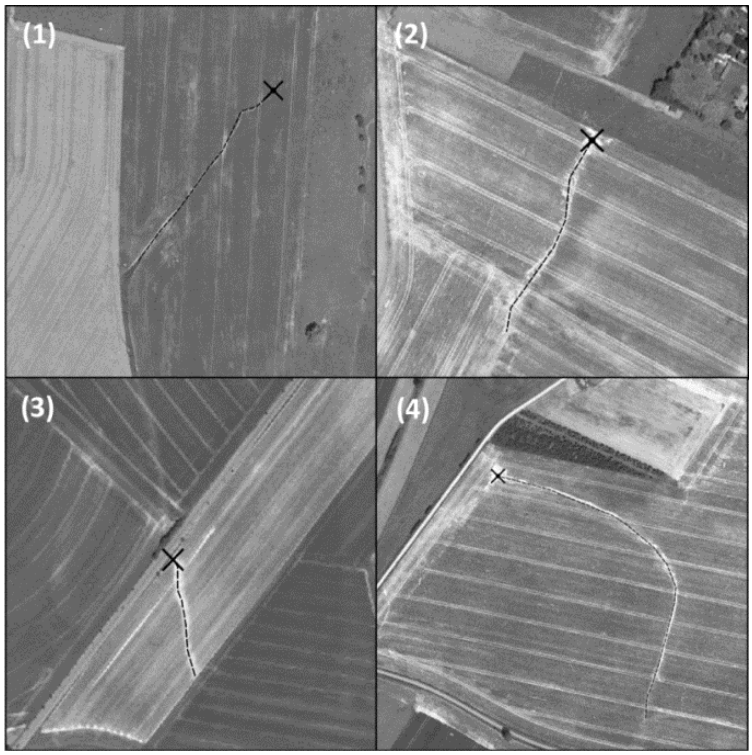

Figure 7-1: Examples of gully ending points controlled by (1) topography, (2) change in vegetation cover (in this case, from sugar beet to grassland), (3) linear element (here, road associated with a bank) and (4) headland. Dashed lines indicate ephemeral gullies and crosses indicate their ending points.

Table 7-1: Total number and proportion of the different factors causing gullies to end in the 4 study areas.

Agricultural area	Total number of ending points	Vegetation	Linear element	Headland	Topography	Vegetation or linear element
Loamy area	256	115 (45%)	37 (15%)	16 (6%)	80 (31%)	8 (3%)
Famenne	41	24 (55%)	4 (10%)	1 (2%)	15 (33%)	0 (0%)
Jurassic area	146	51 (35%)	65 (45%)	5 (3%)	22 (15%)	3 (2%)
Condroz / Loamy area	394	174 (44%)	37 (10%)	9 (2%)	174 (44%)	0 (0%)

In the Loamy area and the Famenne, ephemeral gullies ended mainly because of changes in vegetation and to a lesser extent for topographical reasons (Table 7-1). In the Condroz/Loamy area zone, the gully ending points were controlled by vegetation and topography to an equal extent. As opposed to the other three regions, the location of the ending points in the Jurassic area was mainly controlled by linear elements. The proportion of ending points controlled by linear elements was 3 to 4 times higher in the Jurassic area than in the other agricultural areas. Whatever the region, the proportion of headland-controlled ending points was small (<6%). An inverse relationship between the proportion of ending points controlled by vegetation or linear elements and the mean size of cultivated parcels was observed (Table 3-2 and Table 7-1; Figure 7-2). There was also a positive correlation between the percentage of linear element-controlled ending points and the density of linear elements present alongside cropland (Figure 7-2).

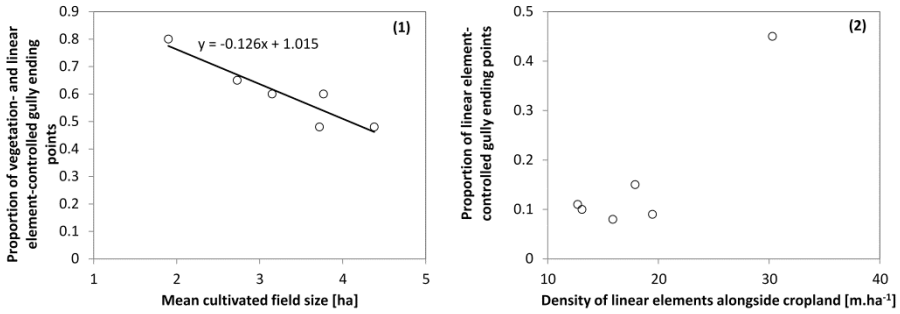

Figure 7-2: Relations between (1) the proportion of vegetation- and linear element-controlled gully ending points and the mean size of cultivated fields; (2) the proportion of linear element-controlled gully ending points and the density of linear elements present alongside cropland. Each symbol corresponds to an agricultural area. Data from the Condroz/Loamy area are split by year.

7.3.2 Topography-controlled ephemeral gully ending points

For topography-controlled gully ending points, the mean local slope at the gully ending point varied widely across regions. The mean local slope in the Loamy area was significantly lower than in the Jurassic area and the Famenne (Table 7-2; respectively $p < 0.001$ and $p = 0.023$). The Jurassic area had the steepest mean local slope for gully ending points, which was significantly different from the Condroz /Loamy area ($p < 0.001$). There was a strong correlation between the mean local slope at the gully ending points and the mean slope of cultivated parcels ($r = 0.99$; not shown).There was an important overlap between the distributions of the slope values of gully grid cells or gully ending point grid cells, whatever the agricultural area (Figure 7-3).

The critical slope thresholds ranged from 5.4% to 12.8% depending on the agricultural areas (Table 7-2). It was not possible to determine the topographic threshold for the Famenne using quantile regression because of an insufficient number of ephemeral gullies ($n = 15$, Table 7-1). Figure 7-4 shows the topographic threshold at the gully ending points for the Loamy area, the Condroz/Loamy area and the Jurassic area. The slopes of the topographic thresholds relative to gully ending points in the Loamy area and the Condroz/Loamy areas were quite similar. However, the position of the threshold was higher in the Condroz/Loamy area than in the Loamy area. The slope of the topographic threshold for gully ending points was two times higher in the Jurassic area than in the Loamy and Condroz/Loamy areas.

Table 7-2: Mean local slope (± standard deviation; SD) and critical slope threshold of topography-controlled gully ending points as a function of the agricultural area

Agricultural area	Topography	Critical slope threshold
	Mean local slope [%] (±SD)	[%]
Loamy area	3.2 (±1.5)[a]	5.4
Famenne	5.2 (±2.1)[b]	7.3
Jurassic area	7.0 (±4.5)[b]	12.8
Condroz/Loamy area	4.1 (±2.5)[c]	7.6

means followed by the same letter are not significantly different at p = 0.05

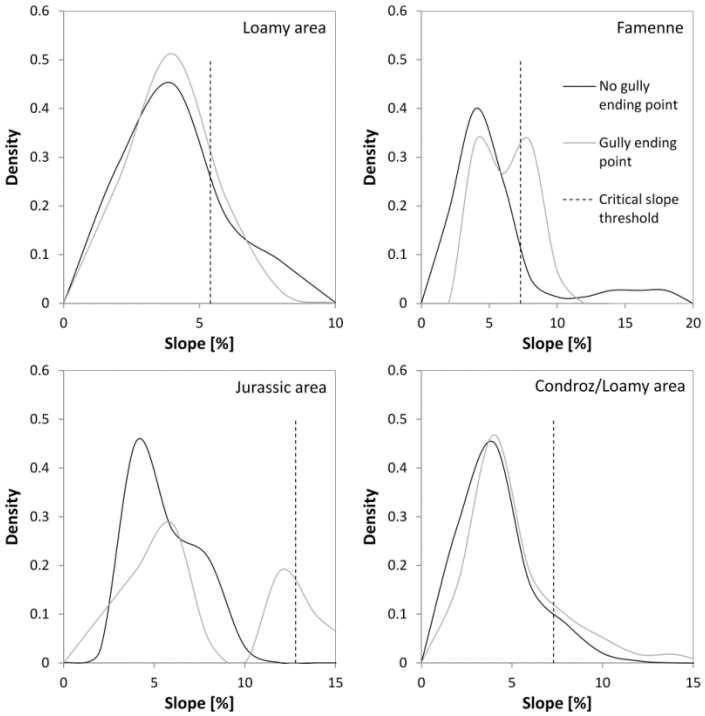

Figure 7-3: Distributions of slope values for gully ending point grid cells (grey line) and gully grid cells (black line) in the four study regions. Vertical dashed lines correspond to the critical slope thresholds.

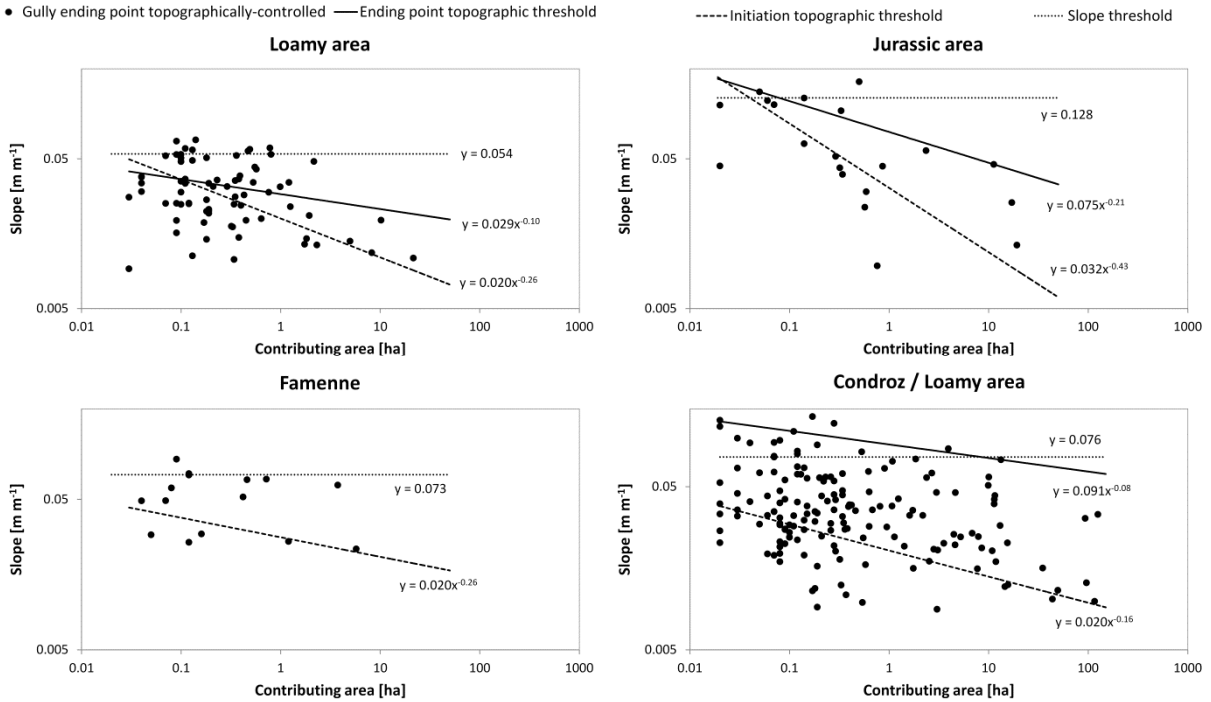

Figure 7-4: Topographic thresholds for topography-controlled ending points (continuous lines) and for gully initiation (dashed lines; Chapter 6) and critical slope thresholds for topography-controlled ending points. The quantiles α = 0.95, 0.76 and 0.97 were used for the topographic thresholds of the Loamy area, the Jurassic area and the Condroz/Loamy area, respectively. For initiation topographic thresholds, quantiles α = 0.06, 0.17, 0.13 and 0.05 of the Loamy area, the Famenne, the Jurassic area and the Condroz/Loamy area.

Using the critical slope threshold in each agricultural area to predict gully ending points caused most gully grid cells to be classified as gully ending points (85% to 100%). Only 8% to 13% corresponded in fact to observed gully ending points (Table 7-3). The use of the topographic thresholds also resulted in classifying most gully grid cells as gully ending points (88% to 99%) but only 3% to 9% corresponded to observed gully ending points (Table 7-3).

Table 7-3: Confusion matrices when classifying observed gully or gully ending point grid cells using the critical slope threshold or the topographic threshold for each agricultural area. NO E = gully grid cell excluding ending points, E = gully ending point.

			Predicted class			
			Classifiation criterion			
			Critical slope threshold		*Topographic threshold*	
			NO E	E	NO E	E
Observed class	Loamy area	NO E	12%	1%	6%	6%
		E	79%	8%	85%	3%
	Famenne	NO E	13%	3%	-	-
		E	72%	13%	-	-
	Jurassic area	NO E	2%	0%	1%	0%
		E	92%	6%	91%	8%
	Condroz / Loamy area	NO E	3%	1%	1%	0%
		E	88%	8%	90%	9%

Given the low number of topography-controlled ephemeral gullies in the Jurassic area and Famenne (Table 7-1), it was not possible to perform relevant logistic regressions based on the topographic factors in these areas. The results of logistic regression relating the probability of occurrence of gully ending to various topographic indices are shown below for the Loamy and Condroz/Loamy areas (Eq. 7-1 and 7-2; Figure 7-5).

$$p(1|X) = \frac{e^{(-2.26+0.27*\Delta S_{i-2,i+2}*\Delta S_{i,i+2}+0.18*\Delta S_{i,i+2}*S_i)}}{1+e^{(-2.26+0.27*\Delta S_{i-2,i+2}*\Delta S_{i,i+2}+0.18*\Delta S_{i,i+2}*S_i)}} \quad (7\text{-}1)$$

$$p(1|X) = \frac{e^{(-2.36+0.28*\Delta S_{i-2,i+2}*\Delta S_{i,i+2}+0.19*\Delta S_{i,i+2}*S_i)}}{1+e^{(-2.36+0.28*\Delta S_{i-2,i+2}*\Delta S_{i,i+2}+0.19*\Delta S_{i,i+2}*S_i)}} \quad (7\text{-}2)$$

where S*i* is the slope of the grid cell *i* [%], $\Delta S_{i,i+2}$ is the change in slope from cell *i* to cell *i+2* [%], $\Delta S_{i-2,i+2}$ is the change in slope from cell *i-2* to cell *i+2* [%].

The logistic regressions performed in the Loamy area and Condroz/Loamy area show that the interaction between the slope variation after a given grid cell ($\Delta S_{i,i+2}$) and the total slope variation ($\Delta S_{i-2,i+2}$) as well as the interaction between the slope variation after a given grid cell and its local slope (S_i) were the most significant factors. However, the logistic regressions are not very useful because they do not allow predicting with a high level of probability the occurrence of gully ending points (max < 17% and max < 53% for the Loamy and Condroz/Loamy areas respectively; Figure 7-5). Figure 7-6 shows that the distributions of the topographic factors for gully grid cells or gully ending point grid cells were quite similar in the Loamy area. The same trend was observed in the Condroz/Loamy area (data not shown).

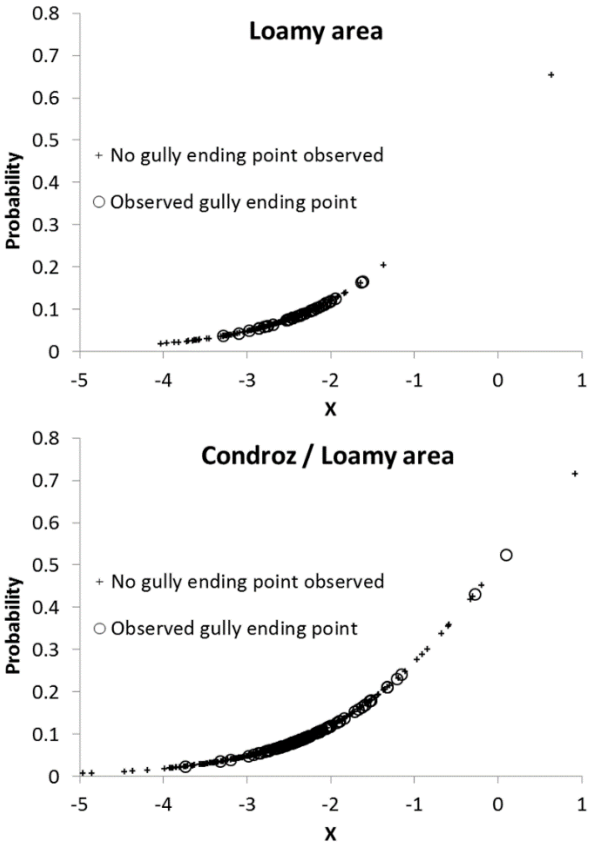

Figure 7-5: Logistic regressions applied to the datasets of the Loamy (Eq. 7-1) and Condroz/Loamy areas (Eq. 7-2). Dot symbols are gully grid cells whereas round symbols correspond to observed topography-controlled gully ending points.

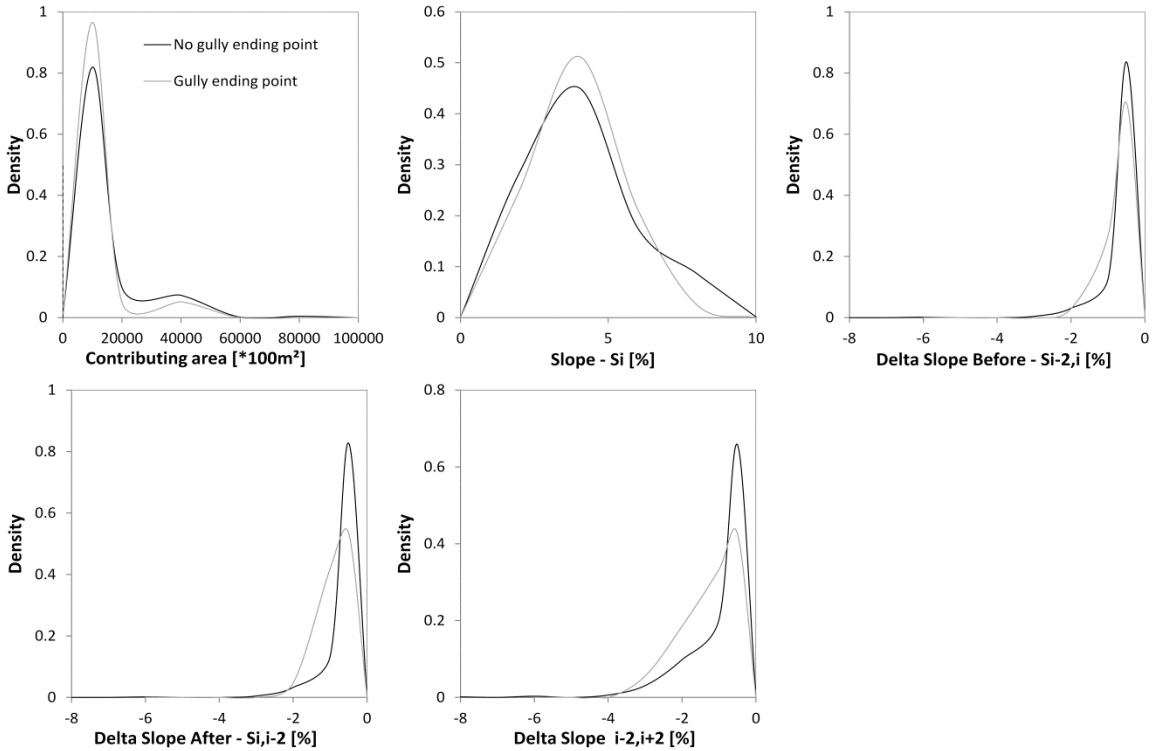

Figure 7-6: Distributions of the topographic parameters used for the logistic regression in the Loamy area

7.3.3 Vegetation-controlled ephemeral gully ending points

For vegetation-controlled gully ending points, the vegetation type at the downstream end of the parcel border was mainly vegetation with a high vegetation cover such as winter crops, grassland or grass strips (78% to 92%, Table 7-4). Only 8% to 16% of vegetation-controlled ephemeral gully ending points were due to summer crops. In the Loamy area and Condroz/Loamy area ephemeral gullies stopped by winter crops, grassland or grass strips occurred at significantly steeper slopes than when stopped by summer crops (respectively $p = 0.008$ and $p = 0.014$; Figure 7-7). At parcel borders, ephemeral gullies were stopped on slopes up to 8% in the Loamy area and up to 15% in the Condroz/Loamy area. In the Jurassic area and the Famenne no significant differences in slope were found depending on the vegetation type, but the number of ephemeral gullies stopped by summer crops was very small (respectively $n = 6$ and $n = 2$). Ending points were observed on slopes up to 15% in the Jurassic area and up to 9% in the Famenne in the presence of winter crops or grassland

Table 7-4: Distribution of vegetation types observed at the downstream end of the parcel border for vegetation-controlled gully ending points

Agricultural area	Vegetation type at the downstream end of parcel border controlling gully end			
	Summer crop	Winter crop	Grass land or Grass strip	Other (Wood, Vegetable crop…)
Loamy area	15.7%	38.3%	41.7%	4.3%
Famenne	8.0%	46.0%	46.0%	0.0%
Jurassic area	11.8%	9.8%	70.6%	7.8%
Condroz/Loamy area	13.2%	24.1%	54.0%	8.6%

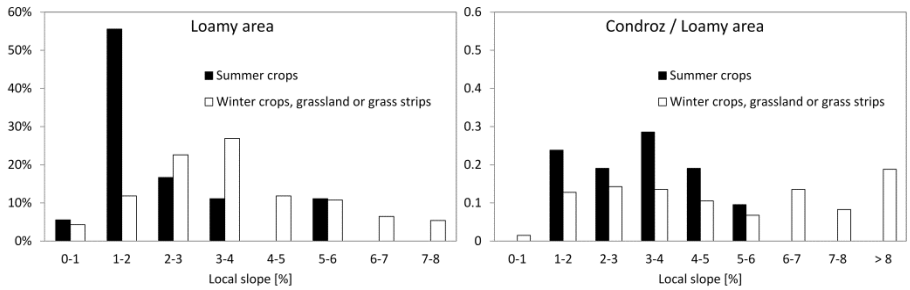

Figure 7-7: Distribution of slope values at gully ending points controlled by vegetation as a function the vegetation type in the Loamy and Condroz/Loamy areas.

Across all sites, 124 gullies (i.e., 15%) were observed to cross several fields and not to be affected when passing from one parcel to another. Table 7-5 shows that the probability of an ephemeral gully to pass from one parcel to another is clearly dependent on the crop transition type. Whatever the upstream crop, the probability that grassland causes gullies stop was more than 90%. Grass strips were also effective at stopping ephemeral gullies coming from summer crops (88%). When coming from winter crops, grass strips were able to stop 50% of the ephemeral gullies. However, the number of winter crop – grass strip transitions observed was small (n=10; Table 7-5). The probability of an ephemeral gully coming from a summer crop to be stopped by a winter crop was 83%. On the contrary, an ephemeral gully coming from a summer crop had an 81% probability to continue if the downstream parcel was also occupied by a summer crop. Fifty-one percent of the transitions between two winter crops caused gullies to end. Note that, although only cropland was considered to digitize gullies, some transitions where the upstream field was grassland or grass strip were also observed. These corresponded to gullies initiated in cropland, crossing grassland or a grass strip and then continuing in another cultivated parcel.

Table 7-5: Effect of vegetation transitions on the end of ephemeral gullies

Vegetation transitions	Number of transitions observed along gully trajectories	% of gully stopped
Summer crop - Summer crop	132	19%
Summer crop - Winter crop	87	83%
Summer crop - Grassland	119	98%
Summer crop - Grass strip	64	88%
Summer crop – Wood	22	100%
Summer crop - Vegetable crop	2	0%
Winter crop - Winter crop	37	51%
Winter crop - Summer crop	23	57%
Winter crop – Grassland	10	90%
Winter crop - Grass strip	10	50%
Winter crop – Wood	1	100%
Grassland - Grassland	1	100%
Grassland- Winter crop	3	33%
Grass strip - Summer crop	3	33%
Grass strip - Winter crop	8	33%
Grass strip- Grassland	1	100%

7.3.4 Linear element- and headland-controlled ephemeral gully ending points

Linear features controlling gully ending were mainly banks, roads or hedges (Table 7-6). Some other elements such as streams or urban areas could occasionally also trigger deposition. Only few data were available in the Famenne because of the small size of the dataset. The proportion of gully ending points due to hedges was higher in the Jurassic area than in the Loamy and Condroz/Loamy areas.

Table 7-6: Types of linear elements controlling gully ending in the four study areas

Agricultural area	Bank	Road	Hedge	Other (Stream, Urban area...)
Loamy area	62.2%	24.3%	8.1%	5.4%
Famenne	25.0%	50.0%	25.0%	0.0%
Jurassic area	43.1%	32.3%	23.1%	1.5%
Condroz/Loamy area	30.6%	50.0%	11.1%	8.3%

Table 7-7 shows that banks were the most frequent linear landscape elements except in the Famenne. Roads in the Jurassic area were also frequent. The density of hedges in the Jurassic area was eight times more important than in the Loamy area and four times more important than in the Condroz/Loamy area. Densities of hedges were comparable in the Famenne and the Jurassic area. Out of the 166 gullies that had a linear element crossing their trajectory, only 3 were able to pass through. Gullies were therefore systematically stopped by linear landscape elements. On the contrary, headlands were little effective at stopping ephemeral gullies. Only 24% of the 128 gullies reaching a headland were stopped. No relation was found between the type of crop in headlands and the probability to stop gullies.

Table 7-7: Density of different linear landscape elements present alongside cropland in the four study areas

Agricultural area	All linear elements	Banks	Roads	Hedges	Other
	Density of linear elements [m ha^{-1}]				
Loamy area	17.9	11.7	3.9	1.0	1.3
Famenne	13.1	3.8	3.0	5.2	1.0
Jurassic area	30.3	10.5	10.3	7.5	1.9
Condroz/Loamy area	16.0	9.0	4.1	2.1	0.9

7.4 Discussion

7.4.1 Topography-controlled ephemeral gully ending points

The mean local slope at gully ending points controlled by topography in the Walloon Loamy area (3.2%±1.15%; Table 7-2) was consistent with previously reported data for the Flemish Loamy area. Indeed, Poesen et al. (1998), Beuselinck et al. (2000) and Nachtergaele et al. (2001a) showed that most ephemeral gully ending points were located on slopes < 4%. Nevertheless, the mean local slope at gully ending points varied strongly across regions, with significantly higher values in the three other regions compared to the loamy area (Table 7-2). Across the four regions, the mean local slope at the ending points was well correlated with the mean slope of cultivated parcels (Table 3-2 and Table 7-2). This may indicate that deposition was controlled more by changes in slope (i.e., a change in sediment transport capacity) rather than by absolute slope values. Other factors such as changes in soil properties (clay content, stoniness…) could also affect gully deposition. According to Vandekerckhove et al. (2000), a positive relationship exists between the rock fragment content at the apex of the sedimentation fan of the ephemeral gullies and the slope angle at this location for Mediterranean contexts. Stoniness may thus in part explain the higher mean local slopes of topography-controlled gully ending points in the Famenne, Jurassic area and Condroz/Loamy area where rock fragment content is higher than in Loamy area (Table 3-3). However, it was not really the case, because whatever the agricultural area, only few gullies were stopped on soils with rock fragment content > 5% because of the restricted number of gullies located on such soils.

Just as the mean local slope, the critical slope threshold for gully ending points varied widely across regions. For the Loamy area, the critical slope threshold was higher than those reported by Poesen et al. (1998), Beuselinck et al. (2000) and Nachtergaele et al. (2001a) for the Flemish Loess belt (2 to 4%). The critical slope threshold was particularly high in the Jurassic area (12.8%, Table 7-2) but plausible given that the 90th percentile of the slope at the gully initiation points was more than 15% in that area. Furthermore, Table 5-1 shows that gullies in the Jurassic area were relatively short. The calculated critical slope threshold for the Jurassic area was therefore not irrelevant and highlights that gully deposition was probably more controlled by changes in slope gradient rather than by absolute slope gradients. Furthermore, 40% of the gully ending points controlled by topography in the Jurassic area occurred on clay loam to clayey soils. Such soil textures are much more resistant to soil detachment than loamy soils and can therefore induce gully deposition on steeper slope. In the other agricultural areas no gully ending points were located on such soils. They mainly occurred on loamy soils. Nevertheless, more data are needed to define more accurately the critical slope threshold in the Jurassic area because it was defined based on the 90th percentile of a distribution of only 22 gully ending points (Table 7-1). This was also the case for the Famenne. In all agricultural areas, the critical slope threshold was always larger than the mean slope of cultivated parcels, but also larger than the slope of most gully grid cells (Figure 7-3). Consequently, most gully grid cells were classified as gully ending points when using the critical slope threshold to predict ephemeral gully ending points (Table 7-3). This demonstrates that the critical slope threshold was not sufficiently restrictive to identify accurately conditions prone to deposition. More generally, the strong overlap between the distributions for the slope of gully grid cells and gully ending point grid cells indicates that a slope criterion alone would be insufficient to discriminate between erosion and deposition (Figure 7-3). This could be in part due to the quality of the DEM, affecting the extracted slope

values at the gully ending point. Another possible reason for this lack of discrimination capacity of slope alone may be the interaction between slope and contributing area. As the contributing area increases, the slope required to induce deposition decreases (Figure 7-4). However, the use of the topographic threshold rather than a critical slope also did not allow for a good discrimination between eroding or depositing gully grid cells (Table 7-3). This can be attributed to the fact that the topographic thresholds related to gully ending points always had a higher position than the topographic thresholds for gully initiation derived in Chapter 6, except for contributing area less than 0.1 ha in the Loamy area (Figure 7-4). The same can be observed when analyzing the topographic thresholds for gully initiation and deposition reported by Nachtergaele et al. (2001a) and Vandekerckhove et al. (2000). This implies that a fairly wide range of slope-contributing area combinations are prone to either ephemeral gully initiation or deposition. When a grid cell equals these topographic conditions, it becomes impossible to discriminate between gullying and deposition. However, the relative positions of the topographic thresholds for gully initiation and gully end are difficult to compare because they are in part dependent on the number of data used for quantile regression. Indeed, the smaller the dataset, the higher (lower) the gully initiation (ending) threshold line (Chapter 6).

The probabilistic approach to predict topography-controlled gully ending points also gave poor results (Equations 7-1 and 7-2). This is because there were no significant differences in the distributions of the topographic factors of gully ending point grid cells vs. gully grid cells (Figure 7-6). This indicates that factors other than topography may have contributed to ending the gullies. The tillage direction might be one of these factors. Indeed, it is expected that when tillage occurs perpendicular to the gully direction, the increased hydraulic roughness could facilitate sediment deposition, as opposed to tillage occurring roughly parallel to the gully direction.

7.4.2 Vegetation-controlled ephemeral gully ending points

Table 7-5 shows that crop transitions towards winter crops, grassland or grass strips generally stop gullies at field borders. This is in accordance with Beuselinck et al. (2000), who reported that this kind of vegetation acts as strong vegetation barriers and can trigger deposition on steep slopes due to an increase of both topsoil resistance and hydraulic roughness. On the contrary, successive summer crops along the gully trajectory allow gully propagation if the transport capacity is not affected by changes in topography such as a lowering of slope gradient or the widening of the flow cross section. This can be explained by the low vegetation density of most summer crops during the late spring-early summer when most ephemeral gullies are formed (Verstraeten et al., 2006). Such crops (e.g. maize, potato) are also characterized by wide row spacing which offers favorable conditions for gullying. For these reasons, only few vegetation-controlled ending points were due to summer crops (Table 7-4) even though almost half of the cultivated fields in areas #1 to #3 were planted with summer crops and more than 34% in the Condroz/Loamy area (Table 3-2). Last, there is an uncertainty for the few gullies stopped by woods because it could be that the gullies continued but were no longer visible on the images. In this case some of these gully ending points were maybe controlled by topography.

7.4.3 Ephemeral gully ending points controlled by linear landscape elements and headlands

In the Jurassic area, about 15% of all gully ending points coincided with roads whereas it was less than 5% in the other regions (Tables 7-1 and 7-6). This is attributable to the higher density of the road network in the Jurassic area

(Table 7-7). Substantial damage to roads from gully sediment deposition is therefore to be expected in this latter region. In the Jurassic area, the proportion of ephemeral gully ending points caused by hedges was almost two and three times higher than in the Condroz/Loamy and Loamy areas, respectively (Table 7-6). This can be attributed to the much larger density of hedges in the Jurassic area (Table 7-7) and is directly related to the landscape structure of these areas (bocage in the Jurassic area vs. open-field in the Loamy and Condroz/Loamy areas).

In the Loamy area, the high density of banks present alongside cropland (Table 7-7) explains the higher proportion of ephemeral gullies stopped by this feature (Table 7-6). In general, linear landscape elements were highly effective at stopping gullies, since less than 2% of all gullies crossing a linear landscape element were able to cross them. This demonstrates that banks and hedges are effective at stopping gullies and, wherever they exist, they should be preserved in watershed management schemes to protect downstream vulnerable sites such as roads or urban areas from muddy floods caused by gullies. On the contrary headlands were found to be little effective to halt gullies despite often being perpendicular to gully direction.

7.4.4 Regional variability of the main factors controlling ephemeral gully ending points

Gully ending points were much more often controlled by a change in vegetation or by linear landscape elements present alongside field borders than by topography (Table 7-1). This was particularly true in the presence of small fields because a smaller field size increases the probability that a gully will cross a field border before meeting the conditions for a topographic control of deposition (Figure 7-2). This explains why fewer gully ending points were topography-controlled in the Jurassic area compared to the three other study

sites (Table 7-1). The proportion of ending points controlled by linear elements was 3 to 4 times higher in the Jurassic area than in the other agricultural areas due to a higher density of linear elements alongside cropland (Table 7-7). Those differences between the Jurassic area and the other areas are due to differences in the spatial organization of land use. The Jurassic area is characterized by a bocage-type landscape, that is to say small fields frequently delineated by hedges. Because of the smaller fields sizes, there are also more secondary roads for accessing fields. Furthermore, fields are mainly grassland, effective at stopping ephemeral gullies (Table 7-5). Ephemeral gullies in this landscape are shorter than in open-field landscapes such as the Loamy area (Chapter 5). In the latter one, agricultural intensification has resulted in field enlargement, the near-complete disappearance of hedges and a larger proportion of summer crops compared to grassland. This kind of landscape favors gullying and also decreases the probability for an ephemeral gully to be stopped by linear features. It therefore results in longer ephemeral gullies, crossing several parcels, transporting more sediment and water, and which have a higher probability to reach a vulnerable site. Consequently, the impact of ephemeral gullying on the hydrological connectivity is expected to be higher in open-field landscapes than in bocage-type landscapes.

7.5 Conclusions

Four main factors controlling the ending of ephemeral gullies were identified: topography, vegetation, linear landscape elements and headlands. For topography-controlled ending points, the slope at the deposition point varied widely across regions. This could result from differences in slope steepness distributions between the agricultural areas. Local differences in topsoil rock fragment content may also have affected the slope value at the deposition point, but only few gullies were located on stony soils. Clayey soils seem to allow gully to end on steeper slopes compared to loamy soils. However, more

data are needed to confirm these results. Both critical slope and topographic thresholds were not sufficiently restrictive to identify accurately the topographic conditions causing gullies to stop. The probabilistic approach including slope gradient variation did not lead to satisfactory results either. Other factors such as tillage direction may have interfered with the characterization of topographic conditions leading to the ending of gullies.

Winter crops, grassland and grass strips were particularly effective at halting ephemeral gullies, whereas parcel transitions to summer crops allowed most gullies to continue. Given that most ephemeral gullies are formed in parcels cultivated with summer crops, the spatial distribution of crop types within agricultural catchments plays a key role in ending gully extension. Whatever their nature, linear landscape elements were highly effective at halting gully development. Linear elements halting ephemeral gullies were mainly roads or banks. In bocage-type landscape characterized by high hedge density, hedges also play a significant role in gully ending. Headlands were found not to be real obstacle to the downstream extension of ephemeral gullies.

Overall, large differences were found across regions in terms of the factor causing gullies to end. These regional differences were mainly due to differences in the spatial organization of land use (mean field size, grassland acreage, density of linear landscape elements). Banks and hedges should be preserved in the bocage landscapes structure in order to limit the length of ephemeral gullies, reduce the hydrological connectivity and the risk of damage by muddy floods to roads and infrastructures. However, it does not seem really realistic to promote new banks and hedges in open-field landscapes. In such cases, other mitigation techniques such as grass strips, brushwood dams or grassed waterways where runoff concentrates have to be promoted.

8 How effective are hydraulic and topographic indicators at predicting the occurrence of ephemeral gullies in agricultural settings?

8.1 Introduction

In view of the extensive on- and off-site damage caused by ephemeral gully erosion, mitigation techniques should be implemented in areas sensitive to gullying. Existing ephemeral gully erosion mitigation techniques rely on decreasing the runoff production (land cover change, improved soil structure …), slowing down concentrated runoff flow or increasing the soil's resistance to particle detachment (e.g., through grassed waterways, sowing cereals at double density, brushwood check dams …). However, in order to target such measures to the most critical areas and to maximize the returns from investments by land managers in the prevention or remediation of gully erosion, it is necessary to develop tools capable of predicting the risk of gully initiation as well as the trajectory of gullies in the landscape (e.g., Desmet et al., 1999; Eustace et al., 2011).

As mentioned in Chapter 2, gullies form along water flow pathways when the threshold tractive force for particle entrainment and transport is exceeded (Horton, 1945). Several methods have been used to assess whether the critical threshold leading to gullying is exceeded. They include simple topographical indices, physically-based modeling of gully erosion processes or empirical multivariate approaches. The main drawback of empirical statistical approaches (e.g. Gutierrez et al., 2009; Eustace et al., 2011; see Chapter 2) is that they provide little insight into the processes at play and are inherently site-specific. Topographical indices typically combine local slope, upstream drainage area and sometimes local planform curvature. They are assumed to be proportional to the stream power of the flow (e.g. Thorne et al., 1986). Satisfactory results for predicting gully location using topographical indices were obtained for small catchments ranging from 7.5 ha to 252 ha (Moore et al., 1988; Desmet et al., 1999; Jetten et al., 2006, Momm et al., 2012). Using

topographic indices for predicting gully locations is very attractive given the low computation requirements. However, such indices omit to take into account several factors which are known to impact ephemeral gully formation such as rainfall or land use (e.g. Poesen et al., 2011).

Physically-based models constitute an attractive alternative for predicting ephemeral gully location because they provide insight into the actual processes at play but mostly because they may be more easily transposable from one context to another. According to Bryan (2000) and Knapen et al. (2007b), many simple hydraulic indices are related directly to the critical tractive force causing soil detachment such as water depth, peak discharge, flow velocity, flow shear stress, effective shear stress, shear velocity, stream power, unit stream power or effective stream power. Knapen et al. (2007b) recommended the use of simple hydraulic parameters for practical applications because of their straightforwardness, and recommended stream power, shear stress and peak discharge as relevant indicators to predict soil detachment by concentrated overland flow. Bryan (2000) showed that flow velocity and unit stream power were also consistently useful hydraulic indicators.

Given the wide range of indicator types used hitherto for predicting large concentrated flow erosion, the aim of this chapter was to test commonly used hydraulic and topographic indicators for their ability to predict ephemeral gully occurrence in agricultural settings.

8.2 Materials and methods

8.2.1 Study area and gully database

The gully database #3 (Table 3-1) was used. The related study site was located in the Loamy agricultural area of Wallonia (#5; Figure 3-1). The total area of the selected study zone was 5235 ha with a large acreage of agriculture land (4703 ha), mostly cropland (3875 ha) (Table 3-2). The main crops were summer crops (sugar beet, potato, maize…). Among the gullies identified independently by 11 operators only gullies identified by at least 6 operators located on a well-defined runoff flow concentration axis, i.e., dry valley, were retained (Figure 3-2). Gullies resulting from strong interference with human artifacts (roads, banks, ditches, wheel tracks…) were excluded. This is why gullies located on a well-defined runoff flow concentration axis but whose contributing area crossed a road were excluded. The roads were identified using the Navstreets inventory of all of the named roads in Wallonia. Finally, because the topographic and hydraulic indicators were expected not to apply to winter gullies, gullies located in winter crops were also excluded. Indeed, gullies formed at the end of the winter are usually the result of a slow, gradual erosion process resulting from successive rainfall events with moderate rainfall depths and intensities on wet sealed soils (Nachtergaele et al., 2001). On the contrary, gullies formed in the early spring usually result from a single, high intensity event on soil with low vegetation cover. A total of 68 gullies were therefore available to test the different indicators. For these gullies, a unique gully was defined as the center of gravity of the digitizing lines of the different operators.

8.2.2 Baseline data

Data about topography, soil, land use and rainfall were needed to compute the topographic and hydraulic indicators. Maps of slope and flow accumulation (i.e., contributing area) were derived from the Walloon, 10-m resolution digital elevation model (DEM) by Demarcin et al. (2009). The map of agricultural land, updated yearly by the Walloon administration, was used to determine crop type in each field. For non-agricultural parcels, the land use map provided by the Walloon administration was used. Rainfall data from the weather radar located at Wideumont (100 km from the study area) was provided by the Royal Meteorological Institute (IRM). Several radar-gauge merging method were used by Goudenhoofdt and Delobbe (2009) to correct the radar data. Those resulting from the kriging with external drift method were used because they were the more accurate regarding to the root mean square error and the mean absolute error (3.498 mm and 1.485 mm, respectively). The rainfall data grid had a spatial resolution of 600 x 600 m² and a temporal resolution of 5 minutes.

8.2.3 Calculation of the topographic and hydraulic indicators

Two topographic indicators (topographic index and contributing area) and six hydraulic indicators (runoff volume, peak discharge, flow velocity, stream power, unit stream power and flow shear stress) were calculated for each 10-m grid cell located in summer crops whose contributing area was not crossed by a road. Two variants of flow velocity, unit stream power and flow shear stress were calculated depending on the assumptions related to the geometry of the flow cross section and the flow width. The main parameters required to compute the eleven gully erosion indicators are summarized in Table 8-1.

Table 8-1: List of gully erosion indicators and required parameters

	Rainfall in the CA[1]	Slope	Geometry of the cross section	Crop stage	Soil crusting stage / roughness	Surface of the CA[1]	Crop(s) stage(s) in the CA[1]	Soil type in the CA[1]	Soil crusting stage / roughness in the CA[1]
Contributing area	-	-	-	-	-	X	-	-	-
Topographic index	-	X	-	-	-	X	-	-	-
Runoff volume	X	-	-	-	-	X	X	X	X
Peak discharge	X	-	-	-	-	X	X	X	X
Stream power	X	X	-	-	-	X	X	X	X
Flow velocity 1	X	-	X	X	X	X	X	X	X
Flow velocity 2	X	-	-	-	-	X	X	X	X
Unit stream power 1	X	X	X	X	X	X	X	X	X
Unit stream power 2	X	-	-	-	-	X	X	X	X
Flow shear stress 1	X	X	X	X	X	X	X	X	X
Flow shear stress 2	X	X	X	X	X	X	X	X	X

[1]CA : Contributing Area

The indicators were not calculated on grid cells with a contributing area less than 0.1 ha because it had been demonstrated earlier that gullies almost never form under those conditions (Chapter 5). A detailed description of each indicator is provided below. For the hydraulic indicators, it was assumed that gullying was the result of a single rainfall event that led to the maximum value of the gully erosion indicator. The latter one depended on the rainfall but also on other parameters such as crop cover or soil roughness which change over time. Because the date of gully formation was not known, it was necessary to determine for each grid cell the rainfall events which caused the hydraulic indicators to be maximum between the date of sowing, which is crop-dependent, and the date of acquisition of the aerial photographs. The rainfall events were extracted assuming that six successive hours without rain was necessary to distinguish two different rainfall events. Only rainfall events ≥ 10 mm were retained, which is a bit less restrictive than the critical rainfall of 15 mm reported by Poesen et al. (2003) for gully initiation among different studies in Europe. Therefore, for each grid cell, the hydraulic indicators were calculated for each rainfall event and the maximum values were extracted. For a given grid cell, the rainfall event used was potentially different depending on the hydraulic indicator. Similarly, for a given hydraulic indicator, the rainfall event used was potentially different from one to another grid cell.

Depending on the method used to compute the flow velocity, the unit stream power and the flow shear stress, the geometry of the flow cross section and the flow width were needed. Two hypotheses were considered. In the first hypothesis, the flow was assumed to pass through the entire width of the cross section of the concentrated flow axis (Figure 8-1). The wetted cross section of the concentrated flow axis A_{m1} [m²] was assumed to be semi-circular and was defined using Equation 8-1:

$$A_{m1} = \frac{r^2 * (\theta - \sin\theta)}{2} \quad (8\text{-}1)$$

where the radius *r* [m] (Figure 8-1) was given by the inverse of the cross sectional curvature determined on the basis of the DEM (10-m resolution) using DEM Surface Tools ®[1]. The angle θ ([rad], Figure 8-1) corresponds to the intersection of the lines from the center of the flow cross section to each extremity of the water surface depending on the water depth (H_1, [m]). It was calculated using Equation 8-2:

$$\theta = 2 * a\cos\left(\frac{r - H_1}{r}\right) \quad (8\text{-}2)$$

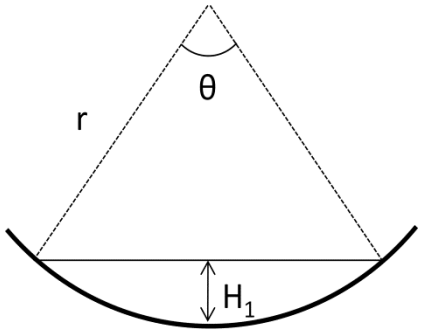

Figure 8-1: Semi-circular cross-section of a concentrated flow axis and associated parameters.

In the second hypothesis, it was assumed that the flow was not passing through the entire width of the cross section but that the flow width was close to the width of the expected ephemeral gully. In this case, the flow cross section was assumed to be rectangular.

[1] http://www.jennessent.com/arcgis/surface_area.htm

8.2.4 Performance assessment of the topographic and hydraulic indicators to predict ephemeral gully occurrence

The study area was divided into 14 zones corresponding to the extent of the aerial photographs. Three zones were used to compare the performance of the topographic and hydraulic indicators (Zones #3, #8 and #12; Figure 8-2). Twenty-two gullies were available. Slight discrepancies were observed between the digitized gully lines and the runoff flow concentration axes derived from by the DEM. This may be due both to the quality of the digitizing and the DEM resolution but also to errors in the relative positioning of the DEM and the aerial photographs. For each gullied grid cell, the highest value of each indicator was therefore extracted from one of the eight neighborhood grid cells. For the ungullied grid cells, the indicator values were extracted at the grid cell location if not already attributed to a gullied grid cell. Otherwise, the initial indicator value of the gullied grid cell was attributed to the ungullied grid cell. The values of the topographic and hydraulic indicators were therefore known for each gullied and ungullied grid cell. It was assumed that the probability of ephemeral gully occurrence increased when the indicator value increased. In a perfect situation, a threshold value should allow to perfectly discriminate gullied and ungullied grid cells. However, the distribution in indicator values of the gullied and ungullied grid cells were expected to overlap. In this case, defining a threshold value to discriminate between gullied and ungullied grid cells results in the misclassification of ungullied grid cells as gullied grid cells and vice-versa. To determine the number of grid cells correctly predicted or not for a given indicator threshold value, a confusion matrix can be created (Table 8-2).

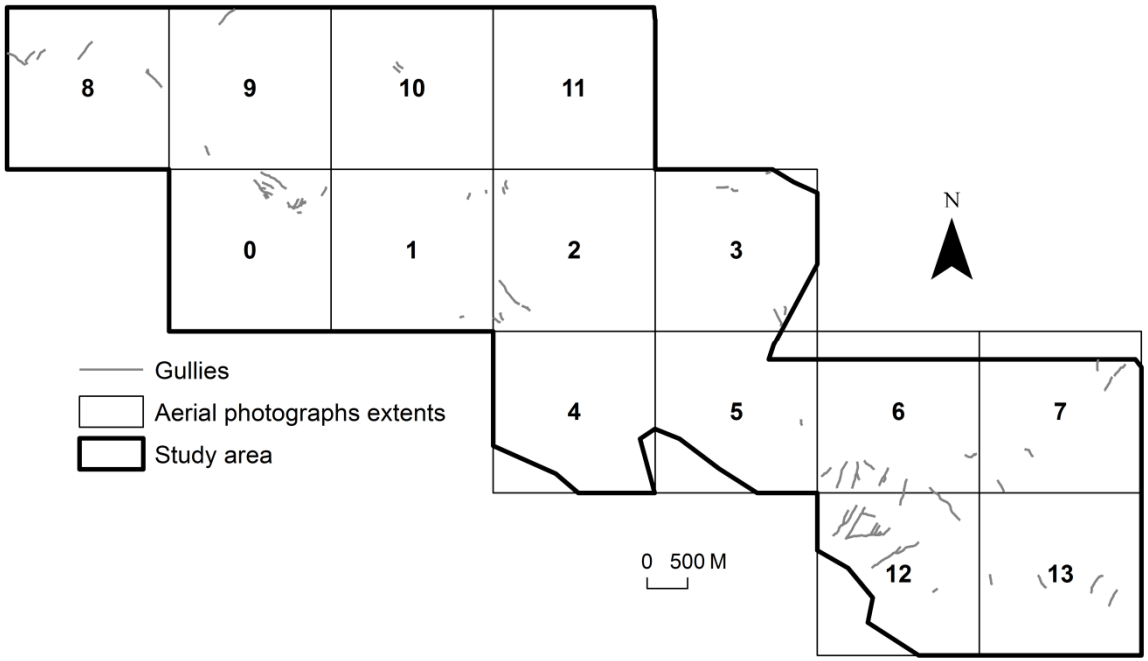

Figure 8-2: The study area divided into the 14 zones. Zones #3, #8 and #12 were used to compare the topographic and hydraulic indicators. The remaining zones were then used for validation of the most relevant indicator.

Table 8-2: Confusion matrix to compare the predicted ungullied and gullied grid cells to the "true" ungullied and gullied grid cells when defining a threshold value above which gullying is expected. c, d, e and f can be expressed either in terms of number of grid cells, or as a percentage of the total number of grid cells.

	True "Gulllied"	True "Ungullied"
Predicted "Gullied"	*c*	*d*
Predicted "Ungullied"	*e*	*f*

Such a confusion matrix can be characterized by its sensitivity and its specificity. The sensitivity is the true positive rate, that is to say the proportion of gullied grid cells correctly predicted (Equation 8-3).

$$Sensitivity = \frac{c}{c+e} \tag{8-3}$$

where *c* and *e* are the number of true positives and false negatives, respectively (Table 8-2). The specificity is the true negative rate, that is to say the proportion of ungullied grid cells correctly predicted (Equation 8-4).

$$Specificity = \frac{f}{d+f} \tag{8-4}$$

where *f* and *d* are the number of true negatives and false positives, respectively (Table 8-2).

By plotting the true positive rate (sensitivity) vs. the false negative rate (1-specificity) for each threshold value ranging from the minimum to the maximum values of the indicator, a Receiving Operating Characteristics (ROC) curve can be drawn (Figure.8-3; Spitalnic, 2004). Such a curve allows determining the performance of the indicator by computing the Area Under

the Curve (AUC) ranging from 0.5 to 1. If AUC = 0.5, the indicator is not able to discriminate between ungullied and gullied grid cells. If AUC ≥ 0.9 the indicator is excellent because it is able to discriminate almost all the grid cells between ungullied and gullied. Between those two situations, the indicator can be qualified as good, fair, poor and bad for respectively 0.8 ≤ AUC < 0.9, 0.7 ≤ AUC < 0.8, 0.6 ≤ AUC < 0.7 and 0.5 ≤ AUC < 0.6. The AUCs of the ROC curves were calculated using the R Verification package (Gilleland, 2012), which also allowed determining if the AUCs were significantly different from 0.5 at p-level = 0.05. Two by two comparisons were performed using the R pROC package (Robin et al., 2014) to test for significant differences between the AUCs of the 11 indicators at p-level = 0.05.

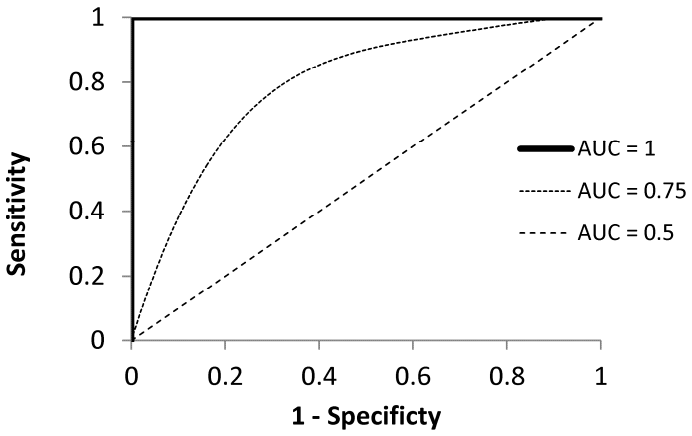

Figure 8-3: Examples of ROC Curves. Bold line: perfect ROC curve (AUC = 1), all the positives can be separated from the negatives. Dashed line: No discrimination between positives and negative (AUC = 0.5). ROC curves can vary between those two extreme situations such as the dotted line (AUC = 0.75).

8.2.5 Calibration and validation of the best indicator to predict ephemeral gully occurrence

The best indicator was identified based on a comparison of the ROC curves. For the best indicator, calibration consisted in identifying the threshold value which allowed to best discriminate between ungullied and gullied grid cells.

This threshold value can be defined as the indicator value maximizing simultaneously the sensitivity and the specificity (Equation 8-3 and Equation 8-4; e.g., Riddle and Stratford, 1999; Gallop et al. 2003). It corresponds to the indicator value which excludes the most ungullied grid cells without missing an acceptable number of gullied grid cells. After plotting the sensitivity and the specificity for each value of the indicator, the threshold value is given by the intersection of the two curves (Figure 8-4). The probability for gully occurrence can then be defined as the ratio between the number of observed gullied grid cells and the total number of grid cells above the threshold. It is possible to refine the discrimination between ungullied and gullied grid cells by defining a second threshold value maximizing simultaneously the sensitivity and the specificity for the values of the indicator ranging from the first threshold value to the maximum value.

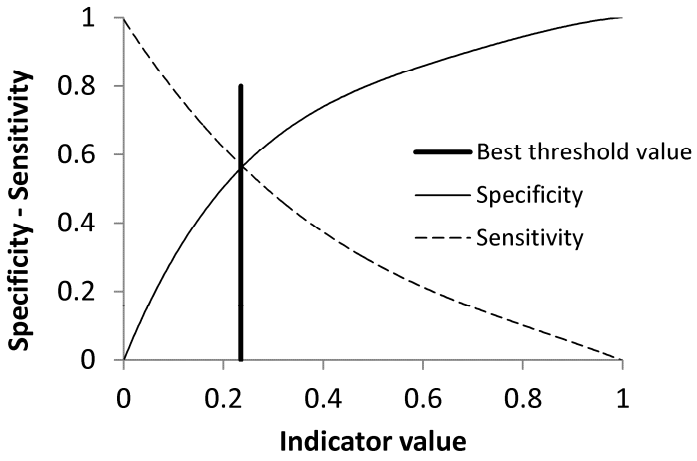

Figure 8-4: Best threshold value of the indicator to discriminate between gullied and ungullied grid cells.

The second threshold is relevant if the probability of gully occurrence above it is higher than when using the first threshold value. This procedure was repeated until a threshold value above which the probability of gully occurrence did not increase was reached. This led to define several classes of indicator values whose limits corresponded to the threshold values. Each class

of indicator values was associated with a specific probability of gully occurrence. These classes were then validated using the forty-six gullies in the 11 remaining zones of the study area (Figure 8-2). In this validation area, the best gully erosion indicator was computed for each gullied and ungullied grid cell. The probability of gully occurrence was then calculated for each class of indicator values defined during the calibration step.

8.3 Ephemeral gully erosion indicators tested

8.3.1 Topographic indicators

Two topographic indicators were tested: the contributing area whose values were extracted from the flow accumulation raster, and the topographic index I [m^b] based on the combination of the local slope and contributing area (Equation 8-5; e.g. Moore et al., 1988; Desmet et al., 1999):

$$I = S * A^b \qquad (8\text{-}5)$$

where S is the local slope gradient [m m^{-1}], A is the upslope contributing area [ha], b is an exponent [dimensionless]. Desmet et al. (1997) showed that the prediction of ephemeral gully location in Central Belgium did not vary significantly when changing the b exponent and recommended using b =1. In Equation 8-5 the upslope contributing area A have been replaced by the unit contributing area As [m^2 m^{-1}], that is to say the upslope contributing area per unit length of contour (Moore et al, 1988) which is theoretically independent of the resolution of the DEM.

8.3.2 Runoff volume

The runoff volume (*Vr*, [m³]; Equation 8-6) reaching a grid cell was calculated as the product of the runoff depth (*Hr*, [mm]) and the acreage of the contributing area (*A*, [m²]). The runoff depth was calculated using the NRCS Runoff Curve Number method (Equation 8-7).

$$V_r = A * H_r \tag{8-6}$$

$$H_r = \frac{(Pl - \lambda * S_{CN})^2}{(Pl + (1-\lambda) * S_{CN})} \tag{8-7}$$

where *Pl* is the rainfall depth [mm], S_{CN} is the potential retention [mm] and λ is the fraction of S_{CN} which represents the initial abstraction. The potential retention is a storage index estimated using Equation 8-8:

$$S_{CN} = \left(\frac{1000}{CN_w} - 10 \right) * 25.4 \tag{8-8}$$

where CN_w is the weighted Curve Number of the drainage area. It is estimated based on the adjusted Curve Number (*CN*) of each grid cell of the drainage area as a function of the crop stage and the soil crusting stage (Equation 8-9; Van Oost, 2003).

$$CN = CN_{\max} - (\frac{C_c}{100} * c_1) + (\frac{C_r}{4} * c_2) \tag{8-9}$$

where CN_{max} is the maximum *CN* derived from the USDA SCS handbook for a combination of cover type and hydrological soil group for the agricultural

practices observed in Wallonia (Table 8-3). The cover types were defined based on the agricultural map and land use map. The hydrological soil groups were extracted from the 10-m resolution digital map of hydrological soil groups, which was derived from the digital soil map by Demarcin et al. (2011). In Equation 8-9, C_c is the crop cover percentage, C_r is the crusting stage (Le Bissonnais et al., 2005) and c_1 and c_2 are coefficients. Crop cover percentages were estimated based on field monitoring of the main crops in Wallonia every ten days (Maugnard et al., 2013) while monthly crusting stage data were available in Wallonia for the main crops (Evrard et al., 2008). Four crusting stages were identified (initial fragmentary structure C_r = 1, altered fragmentary state with structural crusts C_r = 2, local appearance of depositional crusts C_r = 3, continuous state with depositional crusts C_r = 4). The value for c_1 was set as the difference between CN_{max} and CN_{min} defined as the minimum *CN* value for the crop-soil combination used to determine the maximum *CN* value (Table 8-3). The value for c_2 was set so that *CN* in Equation 8-9 equals the value for a fallow soil surface when the crop cover equals 0% (CN_{bare}; Table 8-3).

Equation 8-7 was first derived for $\lambda = 0.2$ but Hawkins and Khojeini (2000) showed that median λ values ranged from 0 to 0.0966 for 97 small watersheds in the USA. Cazier and Hawkins (1984) computed a mean value of 0.0006 for 109 small watersheds in US. Hawkins et al. (2009) recommended a value of 0.05. Because λ seemed to be dependent on local conditions it was necessary to calibrate it. For this purpose, rainfall-runoff data from 3 small watersheds located in the Loamy area of Belgium were used (Ganspoel, GISER I and GISER II; Table 8-4). Only rainfall events $\geq$ 10 mm were used for the calibration (n = 17) and the optimal value of λ was calculated for each event by inverting Equation 8-7. A linear regression between the optimal λ values, the rainfall depth (*Pl*; Equation 8-7), the weighted Curve Number (CN_w; Equation 8-8) and their interaction was performed. Only significant factors at

a p level = 0.05 were retained. Even though the CN method was originally designed for daily rainfall, it has been applied here using event-based rainfall. Rainfall events initiating ephemeral gullies during spring and summer are generally heavy storms, which can be considered as quite similar to the daily rainfall.

Table 8-3: Parameters used to adjust the CN value for each grid cells (Equation 8-9) depending on the crop type and the hydrological soil group

Crop type		Hydrological soil group				Cover description treatments
		A	B	C	D	
Row crops (Sugar beet, Maize Potato…)	CN_{max}	72	81	88	91	Straight row and straight row + crop residue
	CN_{min}	64	75	82	85	
	CN_{bare}	77	86	91	94	
	c_1	8	6	6	6	
	c_2	5	5	3	3	
Small grain (Wheat, Barley…)	CN_{max}	65	76	84	88	Straight row and straight row + crop residue
	CN_{min}	60	72	80	84	
	CN_{bare}	77	86	91	94	
	c_1	5	4	4	4	
	c_2	12	10	7	6	
Vegetable crops	CN_{max}	72	81	88	91	Straight row and crop residue
	CN_{min}	64	75	82	85	
	CN_{bare}	77	86	91	94	
	c_1	8	6	6	6	
	c_2	5	5	3	3	

Table 8-4: Watersheds and rainfall-runoff volume data used for the calibration of the λ parameter of the NRCS Runoff Curve Number method

Name	Outlet coordinates	Area [ha]	Dominant soil type	Number of rainfall-runoff volume data	Rainfall range [mm]	Runoff volume range [m³]
Ganspoel (Steegen et al., 2001; Van Oost et al., 2005)	50°48'N, 4°35'E	110.0	Loamy soil	9	11 - 61	164 - 6154
GISER I	50°79'N, 4°27'E	4.0	Loamy soil	2	18 - 18	4 - 14
GISER II	50°80'N, 4°28'E	84.3	Loamy soil	5	9 -20	40 - 386

8.3.3 Peak discharge

Peak discharge (Q_p, [m³ s^{-1}]) was calculated using Equation 8-10 based the unit hydrograph procedure (Rossi, 2014).

$$Q_p = \frac{9}{8} * \frac{V_r}{t_c} \tag{8-10}$$

where t_c is the time of concentration [s] of the drainage area computed using Equation 8-11.

$$t_c = \frac{\left(\frac{l}{0.305}\right)^{0.8} * (S_{CN} + 1)^{0.7}}{1.140 * Y^{0.5}} \tag{8-11}$$

where l is the flow length [m] of the drainage area and Y is the average land slope of the drainage area [%].

8.3.4 Stream power

The stream power Ω [W m^{-2}] was computed using Equation 8-12:

$$\Omega = \gamma * Q_p * S \quad (8\text{-}12)$$

where γ is the specific weight of water [N m^{-3}].

8.3.5 Flow velocity

When using the first hypothesis on the flow cross section and flow width (see 8.2.3), the flow velocity (V_1; [m s^{-1}]) was calculated based on Equation 8-13 as the ratio between the peak discharge and the wetted cross section of the concentrated flow axis assumed to be semi-circular.

$$V_1 = \frac{Q_p}{A_{m1}} \quad (8\text{-}13)$$

The computation of A_{m1} (Equation 8-1) requires knowledge of the water depth in the semi-circular cross section (H_1; Figure 8-1 and Equation 8-2). By inverting the Manning's formula (Equation 8-14):

$$Q_p = \frac{1}{n} * \frac{A_{m1}^{5/3}}{P^{2/3}} * S^{1/2} \quad (8\text{-}14)$$

where n is the Gauckler-Manning coefficient and P [m] is the wetted perimeter defined by Equation 8-15 for a semi-circular section:

$$P = r * \theta \quad (8\text{-}15)$$

an empirical relationship (Equation 8-16 and Appendix) was derived to estimate the water depth (H_1 [m]) based on peak discharge, slope and soil roughness:

$$Log(H_1) = (0.46 + 10^{-Log(r)-2.18}) \cdot Log(\frac{Q_p \cdot (n_b + n_a)}{S^{0.5}}) - 0.10 \cdot Ln(r) - 0.07 \quad (8\text{-}16)$$

In Equation 8-16, S is the slope gradient [m m^{-1}] and the Gauckler-Manning coefficient is assumed to be the sum of the effects of soil roughness due to grain size (n_b) and roughness due to vegetation, obstructions and surface irregularities (n_a; Arcement and Schneider, 2008). The part of the roughness due to grain size was determined using Equation 8-17 (Yen, 1992), where d_{50} is the median sediment diameter [m]

$$n_b = k * d_{50}^p \quad (8\text{-}17)$$

For a loamy soil, p = 1/6, k =0.0474, and d_{50} = 26 µm, giving approximately n_b = 0.01. n_a is the sum of the soil roughness coefficient (n_s) and roughness coefficient due to crop (n_v). The maximal value of n_s (0.01) was set as the difference between the Gauckler-Manning coefficients under normal conditions for a bare soil (n = 0.02; Te Chow, 1959) and n_b. n_s was allowed to vary gradually between 0 and the maximal value (0.01) depending on the crusting stage (C_r; Equation 8-9) using Equation 8-18.

$$n_s = 0.01 * \frac{4 - C_r}{3} \quad (8\text{-}18)$$

The maximal value of n_v was set as the difference between the Gauckler-Manning coefficient under normal conditions depending on the crop type and

the Gauckler-Manning coefficient for a bare soil. It was assumed that the development of roots or stems which can affect roughness due to vegetation was proportional to the crop cover percentage (C_c; Equation 8-9). n_v was therefore allowed to vary gradually between 0 and the maximal value (n_{max} = 0.015 for row crops and n_{max} = 0.020 for small grains) depending on the crop cover percentage using Equation 8-19.

$$n_v = n_{\max} * \frac{C_c}{100} \qquad (8\text{-}19)$$

When using the second hypothesis on the flow cross section and flow width (see 8.2.3), the flow velocity (V_2 [m s^{-1}]) was computed on the basis of peak discharge (Equation 8-10) using Equation 8-20 proposed by Govers (1992). This equation allowed to predict the flow velocity in rills in loose on homogeneous soils from discharge alone.

$$V_2 = 3.52 * Q_p^{0.294} \qquad (8\text{-}20)$$

8.3.6 Unit stream power

The unit stream power U [m s^{-1}] was calculated according Yang (1977) as the product of the flow velocity and the slope gradient. The unit stream power was therefore different depending on the hypothesis regarding the geometry of the flow cross section and the flow width (Equation 8-21 and Equation 8-22).

$$U_1 = V_1 * S \qquad (8\text{-}21)$$

where V_1 is the flow velocity defined for a semi-circular cross section and for a flow passing through the entire width of the cross section (Equation 8-13).

$$U_2 = V_2 * S \quad (8\text{-}22)$$

where V_2 is the flow velocity calculated using Equation (8-20).

8.3.7 Flow shear stress

The total flow shear stress is partitioned between the shear stress acting on the soil on the one hand, and acting on the vegetation and other surface irregularities on the other hand (Flanagan and Nearing, 1995). Only the shear stress acting on the soil was considered. Depending on the hypothesis on the geometry of the flow cross section and the flow width, the flow shear stresses acting on the soil τs ([N m^{-2}]) were approximated using Equation 8-23 or Equation 8-24 (e.g. Tiscareno-Lopez et al., 1994).

$$\tau_{s1} = \gamma * H_1 * \sin(S) * \left(\frac{n_b}{n_b + n_a} \right)^{1.5} \quad (8\text{-}23)$$

where H_1 is the water depth for a semi-circular cross section and a flow passing through the entire width of the cross-section (Equation 8-16 and Figure 8-1).

$$\tau_{s2} = \gamma * H_2 * \sin(S) * \left(\frac{n_b}{n_b + n_a} \right)^{1.5} \quad (8\text{-}24)$$

H_2 was calculated using Equation 8-25:

$$H_2 = \frac{A_{m2}}{W} \quad (8\text{-}25)$$

where *W* is the flow width [m] estimated using Equation 8-26 proposed by Nachtergaele et al. (2002) for ephemeral gullies in Central Belgium.

$$W = 2.51 * Q_p^{0.412} \qquad (8\text{-}26)$$

A_{m2} [m²] is the rectangular wetted flow cross section defined by Equation 8-27 as the ratio between the peak discharge (Equation 8-10) and the flow velocity V_2 (Equation 8-20).

$$A_{m2} = \frac{Q_p}{V_2} \qquad (8\text{-}27)$$

8.4 Results

8.4.1 Calibration of the λ parameter of the NRCS Curve Number method

Linear regression analysis showed a significant correlation between the optimal λ value (Equation 8-7), the rainfall depth and the weighted Curve Number of the contributing area expressed by Equation 8-28 ($R^2 = 0.76$, Nash-Sutcliffe coefficient = 0.77, RMSE= 0.025, n=17). Figure 8-5 shows the relation between the observed runoff volumes at the outlet of the 3 small watersheds for rainfall event of 10 mm at least and those simulated based on the λ estimation using Equation 8-28. The correlation and Nash-Sutcliffe coefficients were respectively 0.93 and 0.94, and the RMSE was 570 m³.

$$\lambda = -0.01527 - 0.04806 * Pl + 0.0007609 * Pl * CN_w \qquad (8\text{-}28)$$

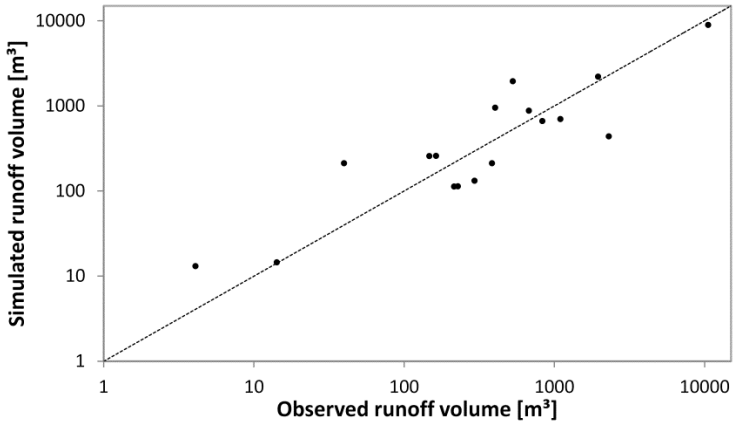

Figure 8-5: Relation between the observed runoff volumes and those simulated using the NRCS Curve Number method with λ estimated using Equation 8-28. The dashed line corresponds to the 1:1 line.

8.4.2 *Performance assessment of the topographic and hydraulic indicators to predict ephemeral gully occurrence*

Topographic and hydraulic indicators were rescaled from 0 to 1 to facilitate their comparison (Figure 8-6 and 8-7). The general pattern of the spatial distributions of the highest and lowest values of the rescaled topographic and hydraulic indicators was different for the unit stream power U_1, the flow velocity V_1 and the flow shear stress Ts_1 compared to the other indicators, because it was not possible to calculate the former for about 30% of the grid cells (Figure 8-7A, C and E). It corresponded to grid cells whose curvature was assessed as slightly convex when using DEM Surface Tool ®. Except for the unit stream power U_1 and U_2 as well as for the flow shear stress Ts_2 (Figure 8-7C, 8-D and 8-F), the highest values of the topographic and hydraulic indicators matched the main flow concentration axes.



Figure 8-6: Rescaled topographic indicators and runoff volume, peak discharge and unit stream power in zone #12 (Figure 8-2).

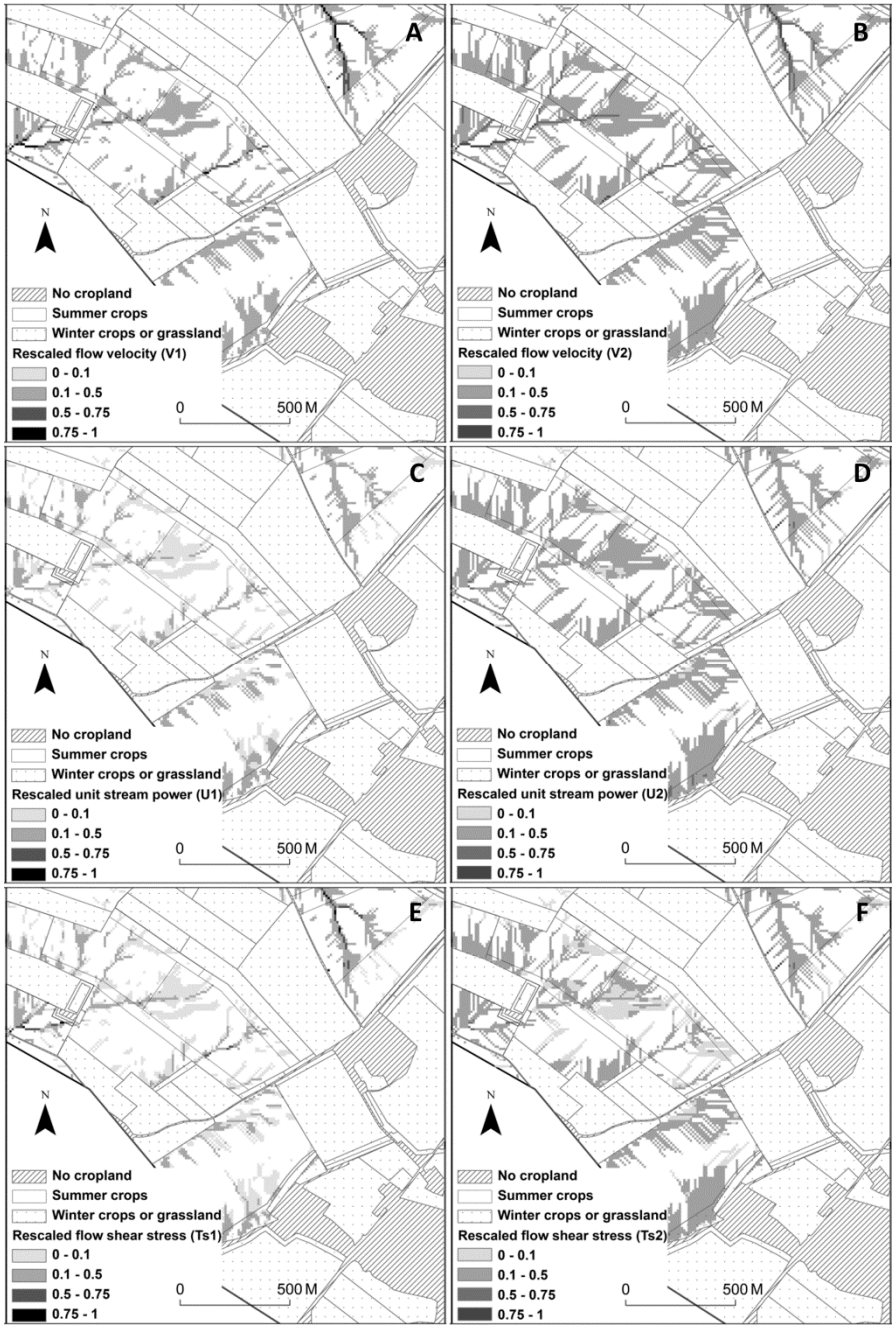

Figure 8-7: Rescaled flow velocity indicators (V_1 and V_2, respectively A and B; Equations 8-13 and 8-20), rescaled unit stream power indicators (U_1 and U_2, respectively C and D; Equations 8-21 and 8-22) and rescaled flow shear stress indicators (Ts_1 and Ts_2, respectively C and D; Equations 8-23 and 8-24), in zone #12 (Figure 8-2).

The ROC analysis showed that all the computed AUC were significantly different from 0.5 (Table 8-5). The flow shear stress Ts_1 and the unit stream power U_1 and U_2 were not good predictors because their ROC curves were close to the 1:1 line (respectively AUC = 0.538; AUC = 0.569 and AUC = 0.601; Table 8-5 and Figure 8-8). There were no significant differences between the AUCs of the unit stream power U_1 and the flow shear stress Ts_2 (Table 8-6). The AUC of unit stream power U_2 was significantly different from the AUC of the flow shear stress Ts_2, but was similar to the AUC of the unit stream power U_1 (Table 8-6). Overall, using those indicators as predictors was almost equivalent to randomly classifying the grid cells as gullied or ungullied.

Table 8-5: AUC values and associated p-value of the test AUC < > 0.5

Gully erosion indicator	AUC	p-value	Ranking
Runoff volume	0.813	5.03E-85	1
Contributing area	0.808	5.89E-83	2
Peak discharge	0.790	2.00E-73	3
Flow velocity - V2	0.790	2.00E-73	4
Topographic index	0.782	1.21E-69	5
Stream power	0.756	8.50E-58	6
Flow velocity - V1	0.698	2.13E-34	7
Flow shear stress - Ts1	0.674	4.26E-27	8
Unit stream power - U2	0.601	1.44E-10	9
Unit stream power - U1	0.569	9.36E-06	10
Flow shear stress - Ts2	0.538	8.20E-03	11

The flow shear stress Ts_1 and the flow velocity V_1 resulted in similar AUCs indicating a poor discrimination between gullied and ungullied grid cells (AUC < 0.7). Their AUCs were significantly different and were also different from the AUCs of the other indicators (Table 8-6). The stream power and the topographic index gave similar AUCs leading to acceptable results when classifying grid cells as gullied or ungullied (AUC = 0.756 and 0.782,

respectively). The AUC related to the stream power was significantly different from those of the other indicators while the AUC related to the topographic index was similar to those of the flow velocity V_2, the peak discharge and the runoff volume (Table 8-6). The flow velocity V_2 and the peak discharge gave exactly the same ROC curves (Figure 8-8) and their AUC indicated that they were good predictor (Table 8-5). The AUC related to the contributing area and the runoff volume were the highest (AUC = 0.808 and AUC = 0.813, respectively; Table 8-5 and Figure 8-8). Even though there were no significant differences between the AUCs of the runoff volume, the contributing area, the peak discharge and the flow velocity V_2, the runoff volume was retained for the calibration and validation steps because of its highest absolute AUC value and the lowest p-value when comparing its ROC curve to the 1:1 line (Table 8-5).

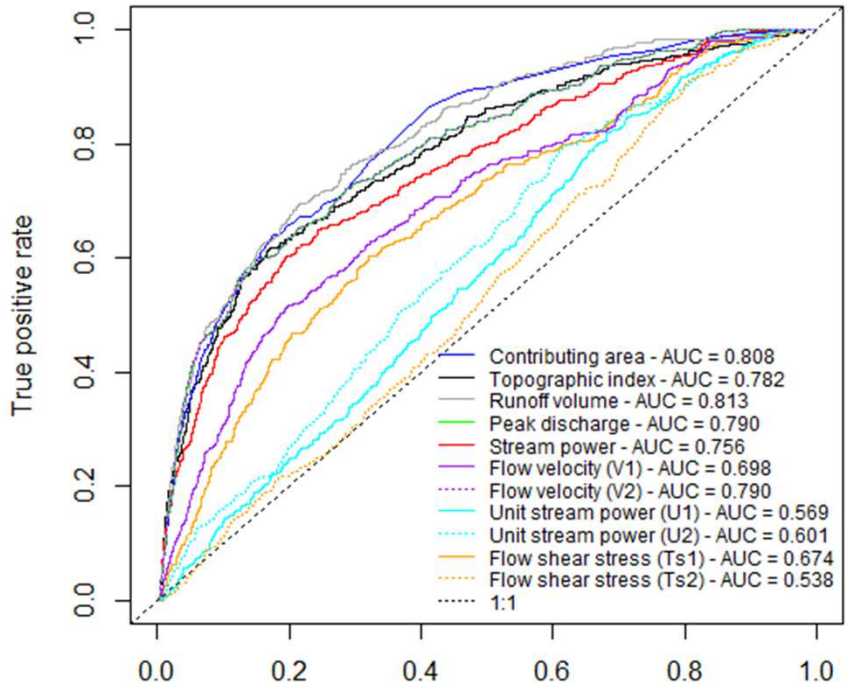

Figure 8-8: ROC curves for the various topographic and hydraulic indicators and their relative AUC. Note that the curves related to the peak discharge and the flow velocity (V_2) perfectly overlap

Table 8-6: P-values resulting from to the two by two comparison tests for significant differences of the AUC values

	Runoff volume	Contributing area	Peak discharge	Flow velocity - V_2	Topographic index	Stream power	Flow velocity - V_1	Flow shear stress - Ts_1	Unit stream power – U_2	Unit stream power – U_1	Flow shear stress - Ts_2
Runoff volume	-	8.00E-01	2.01E-01	2.01E-01	9.19E-02	2.31E-03	3.18E-09	7.46E-13	< 2.2E-16	< 2.2E-16	< 2.2E-16
Contributing area		-	2.99E-01	2.99E-01	1.89E-04	4.86E-03	1.19E-08	3.69E-12	< 2.2E-16	< 2.2E-16	< 2.2E-16
Peak discharge			-	3.17E-01	6.80E-01	5.18E-07	4.78E-06	7.84E-09	< 2.2E-16	< 2.2E-16	< 2.2E-16
Flow velocity - V2				-	6.80E-01	5.18E-07	4.78E-06	7.84E-09	< 2.2E-16	< 2.2E-16	< 2.2E-16
Topographic index					-	1.86E-01	3.73E-05	1.15E-07	< 2.2E-16	< 2.2E-16	< 2.2E-16
Stream power						-	5.06E-03	7.63E-05	< 2.2E-16	< 2.2E-16	< 2.2E-16
Flow velocity - V_1							-	< 2.2E-16	4.15E-06	< 2.2E-16	4.99E-14
Flow shear stress - Ts_1								-	4.84E-04	< 2.2E-16	1.23E-10
Unit stream power – U_2									-	1.26E-01	< 2.2E-16
Unit stream power – U_1										-	1.33E-01
Flow shear stress - Ts_2											-

8.4.3 Calibration and validation of the best indicator to predict ephemeral gully occurrence

The highest runoff volume values in the calibration area did not always match gullied grid cells and vice-versa (Figure 8-9). There was an important overlap between the distribution of the runoff volume values for ungullied and gullied grid cells (Figure 8-10). However, from approximately 500 m³ to 2500 m³ the relative density of gullied grid cells was higher than for ungullied grid cells. For runoff volumes > 4000 m³, no gullied grid cells were observed, and the associated probability of ephemeral occurrence was therefore set to 0.

The step by step thresholding method based on the maximization of the sensitivity and the specificity resulted in the identification of 4 thresholds values (Table 8-7). These thresholds allowed defining 5 classes of runoff volume with specific probabilities of ephemeral gully occurrence (Table 8-8). As from 291 m³, the probability of gully occurrence was greater than 25%. The AUC of the ROC curve associated with runoff volumes ranging from 291 m³ to 4000 m³ was 0.679. The highest probability of ephemeral gully occurrence was 34% and was associated with runoff volumes ranging from 561 m³ to 4000 m³. Less than 20% of the total number of gullied grid cells was associated with this range of runoff volumes. The AUC of the corresponding ROC curve was 0.571. The locations with runoff volumes ranging from 0 to 124 m³ had a low probability to be gullied (≤ 5.1%). However, 58% of the gullied grid cells were associated with runoff volumes < 124 m³. The AUC of the related ROC curves ranged from 0.741 to 0.815.

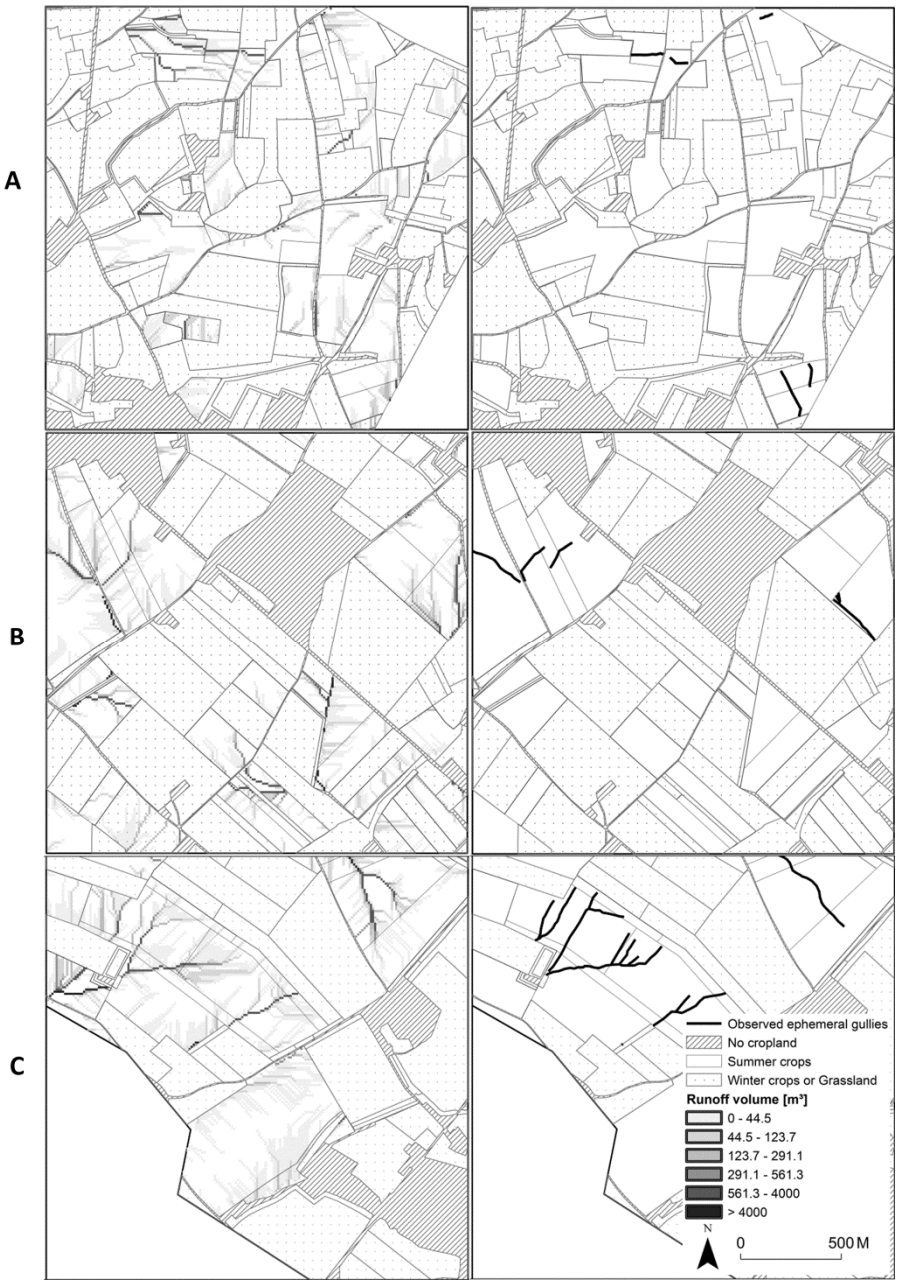

Figure 8-9: Runoff volumes and observed ephemeral gullies in the calibration area (zones A) #3,B) #8 and C) #12; Figure 8-2).

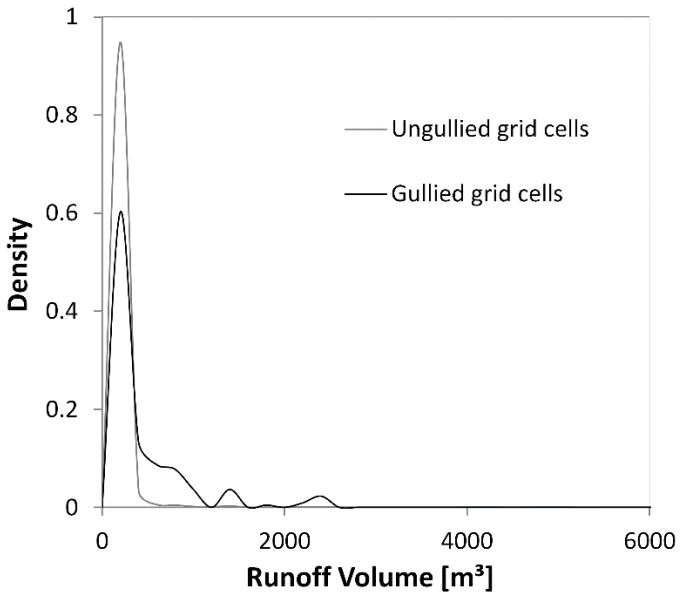

Figure 8-10: Distributions of the runoff volume for ungullied and gullied grid cells in the calibration area (zones #3, #8 and #12; Figure 8-2).

Table 8-7: Threshold values and AUC of the related ROC curves.

Runoff volume [m³]	AUC	Threshold value
0 - 4000	0.815	44.5
45 - 4000	0.741	123.7
124 - 4000	0.679	291.1
291 - 4000	0.571	561.3

As for the calibration area, the highest runoff volume values in the validation area did not always match gullied grid cells and vice-versa (Figure 8-11). Likewise, no gullied grid cell was observed in the validation area for runoff volumes > 4000 m³ (Table 8-9). For the runoff volume classes < 4000 m³, the probabilities of gully occurrence in the validation area were divided by a factor of almost 1.5 compared to the calibration area. The highest probability of ephemeral gully occurrence was 22.6% and pertained to 16% of the gullied grid cells.

Table 8-8: Probability of gully occurrence depending on the runoff volume in the calibration area.

Runoff volume [m³]	Observed grid cells	Gullied grid cells	Probability of gully occurrence [%]
0 - 45	5848	92	1.6%
45 - 124	1537	79	5.1%
124 - 291	499	61	12.2%
291 - 561	185	48	25.9%
561 - 4000	171	58	33.9%
> 4000	25	0	0.0%
Total	*8265*	*338*	

Table 8-9: Probability of gully occurrence in the validation area based on the runoff volumes classes defined in Table 8-7.

Runoff volume [m³]	Observed grid cells	Gullied grid cells	Probability of gully occurrence [%]
0 - 45	12677	145	1.1%
45 - 124	3427	112	3.3%
124 - 291	951	70	7.4%
291 - 561	348	57	16.4%
561 - 4000	323	72	22.3%
> 4000	0	0	0.0%
Total	*17726*	*456*	

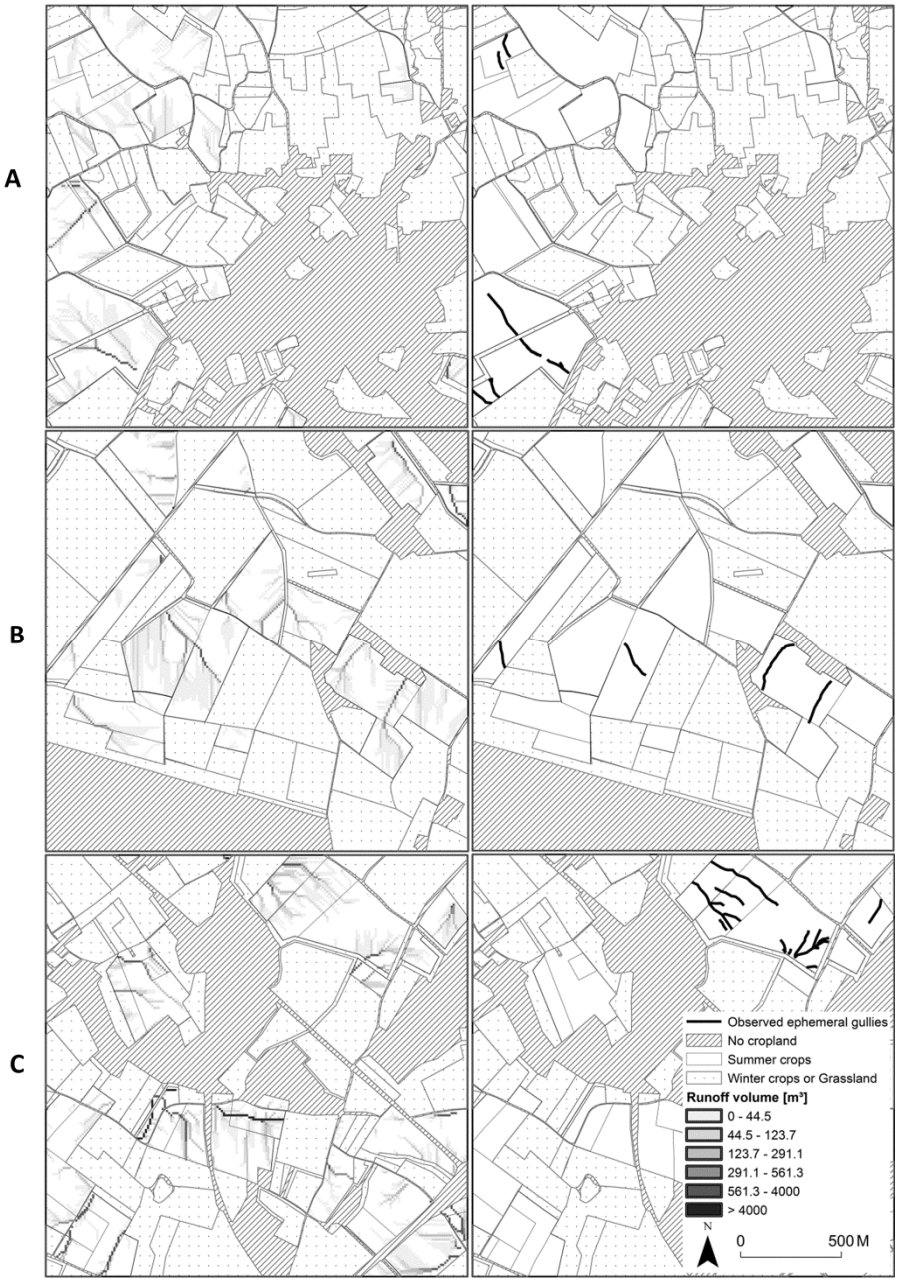

Figure 8-11: Runoff volumes and observed ephemeral gullies in three zones of the validation area (zones A) #2,B) #13 and C) #0; Figure 8-2).

8.5 Discussion

8.5.1 Performance assessment of the topographic and hydraulic indicators to predict ephemeral gully occurrence

Overall, the more the indicator was complex, the less it was effective at predicting ephemeral gully occurrence (Table 8-1, Figure 8-6 and Figure 8-7). The poor results related to the unit stream power U_1, the flow velocity V_1 and the flow shear stress Ts_1 may partly be due to the accuracy of the DEM which is characterized by a standard deviation of the elevation of 0.2 m. This introduced errors when assessing the cross sectional curvature and hence water depth (Equation 8-16). In addition, 30% of the grid cells presented a convex curvature despite being located in the flow pathway, such that water depth could not be calculated. Furthermore, it was assumed that the flow was passing through the entire width of the semi-circular cross section of the flow concentration axes. In reality, in many cases, the width of the flow may be less than the width of the cross section. The simulated water depths have therefore probably been underestimated. However, assessing the flow width using Equation 8-26 led to worse results. Unlike the flow shear stress Ts_1, the flow shear stress Ts_2 did not match the main flow concentration axes (Figure 8-7E and F). The highest values of Ts_1 are observed for the main flow concentration axes because of the assumption of the geometry of the flow cross section. For a given value of peak discharge, the highest values of water depth are observed for the highest values of cross section curvature that is to say for the main flow concentration axes (Equation 8-16). Furthermore, the values of peak discharge were the highest on the main flow concentration axes (Figure 8-7D). Equation 8-25 can be expressed as Equation 8-29 when combining Equations 8-20, 8-26 and 8-27. It shows that an increase in peak discharge on the flow

concentration axes leads to a smaller increase of the water depth and hence flow shear stress than when using Equation 8-16.

$$H_2 = 0.11 * Q_p^{0.296} \quad (8\text{-}29)$$

Overall, including the slope of the terrain in the calculations appeared to decrease the efficiency of the indicators. The best gully erosion indicators were those which did not take into account the local slope gradient (runoff volume, contributing area, peak discharge, flow velocity V_2). The contributing area was significantly better than the topographic index combining contributing area and local slope gradient (Tables 8-5 and 8-6). The peak discharge was also significantly better than the stream power combining discharge and local slope gradient. This agrees with Desmet et al. (1999), who showed that when using the topographic index to predict the location of a gully, the local slope gradient mostly controls incipient gully incision whereas the location of the gully trajectories is mainly controlled by contributing area.

Overall, taking into account land use and rainfall did not improve significantly the prediction of gully location when comparing hydraulic indicators to topographic indicators. Results from the best hydrological indicators (runoff volume and peak discharge) were close to those calculated using the topographic indicators (contributing area or topographic index) (Figures 8-6 and 8-8, Table 8-5). This was maybe in some cases due to the fact that we did not identify the correct rainfall event. This may also in part be due to the large standard error affecting the predicted runoff volume (i.e., 530 m³; Figure 8-5), and the limited dataset that was available to calibrate the method. Currently, results using Equation 8-28 are promising because it allowed a decrease of 20% and 400% of the runoff volume RMSE as compared to the use of λ =0.20 and λ =0.05, as proposed by Hawkins et al. (2009), respectively. This indicates

that there is scope for improvement of the NRCS curve number method. Integrating additional parameters such as soil moisture status or rainfall characteristics (intensity and distribution) may also improve predictions (Hawkins et al., 2009). The prediction could also be improved by combining the hydraulic indicators with the related critical soil parameters (e.g., flow shear stress vs. critical shear stress…) into "excess models" as proposed by Foster (1982; Equation 2-2). However, this would require reliable critical shear stress data for applications at regional scale. The transport capacity of the flow could also be taken into account for more realistic results.

8.5.2 Calibration and validation of the best indicator to predict ephemeral gully occurrence

The discrimination between gullied and ungullied grid cells based on runoff volume was difficult in view of the large overlap in the distributions (Figure 8-10). The runoff volume performed better for identifying areas where ephemeral gully occurrence was unusual rather than usual (Table 8-8 and Table 8-9). However, such areas concerned most of the gullied grid cells (> 50%). This resulted from the imbalance between the number of ungullied and gullied grid cells for small runoff volumes (Figure 8-10, Table 8-8 and Table 8-9). The runoff volume was not able to identify reliably areas prone to ephemeral gully occurrence. Indeed, the highest probabilities of ephemeral gully occurrence, obtained for the largest runoff volumes (< 4000 m^3) did not exceed 34% (Table 8-8 and Table 8-9). Furthermore, the AUC value of the ROC curves for runoff volumes ranging from 291 to 4000 m^3 revealed that the discrimination was inefficient (Table 8-7). Results showed that no grid cells were gullied in the calibration and validation areas for runoff volume > 4000 m^3. The correlation between the runoff volume and the contributing area was strong (r = 0.81), and the grid cells associated to runoff volumes > 4000 m^3 were also characterized by the largest contributing areas (at least 20 ha). In

practice, there is a high probability for the concentrated water runoff not to reach those grid cells located at the downstream end of the flow concentration axes. This is due to flow interception by linear features which was not observable on the DEM because of its resolution, causing the flow to stop or flow rerouting upstream. Such linear elements could be secondary roads, small banks or ditches. Furthermore, the concentrated erosion following long flow concentration axes crossing several fields also has a large probability to be stopped due to changes in vegetation cover that may increase soil erosion resistance. Beuselinck et al. (2000) pointed out that, in the spring, up to 28% of ephemeral gully deposits in the Belgian Loam Belt were triggered at field borders due to grassland or winter wheat acting as a vegetation barrier.

Recent studies have stressed the importance of the effect of linear features such as roads when predicting gully occurrence or susceptibility (i.e. Conoscenti et al., 2014; Dube et al., 2014, Makanzu Imwangana et al., 2014). In the present study, only the grid cells whose contributing area was crossed by a named road (NavStreets) were excluded. Grid cells whose contributing area was crossed by small roads without name were integrated. In practice, flow rerouting by these small roads has probably led to predict ephemeral gullies on flow concentration axes where they cannot occur and to miss some ephemeral gullies formed due to rerouting. Finally, there were discrepancies between the location of the digitized gullies and the location of the flow concentration axes due to the DEM resolution. A higher resolution DEM may improve the positioning of flow concentration axes and may allow taking into account the linear landscape elements. Such a DEM will be available for Wallonia in the near future.

8.6 Conclusions

Among the tested topographic and hydraulic indicators, those excluding local slope gradient were the best to predict ephemeral gully occurrence. Results related to flow velocity V_1, flow shear stress Ts_1 and unit stream power U_1 were affected by errors due to the assessment of the cross section curvature because of the DEM resolution. However, the flow shear stress Ts_1 gave better results than the flow shear stress Ts_2, indicating that it was better to consider the flow cross section as semi-circular with flow passing through the entire width of the cross section rather than rectangular with a flow width proportional to peak discharge.

Based on a ROC analysis, the runoff volume, the contributing area, the flow velocity V_2 and the peak discharge gave statistically similar performances when classifying grid cells as gullied or ungullied. Because it had the best overall performance, the runoff volume was retained to be calibrated and was then validated to predict ephemeral gully erosion occurrence. The results showed that this ephemeral gully erosion indicator was not reliable because 1) most of the gullied grid cells were not predicted and 2) it did not allow predicting gully occurrence with a probability level > 34%. Two factors explaining the poor results were pointed out. First, the standard error on the runoff volume provided by the hydrological model based on the NRCS Curve Number method. Secondly, the DEM resolution that did not allow taking into account the linear elements playing a crucial role in the trajectory of gullies by rerouting or stopping flow. The combination of an improved hydrological model and a high resolution DEM may allow improving the prediction of ephemeral gully location using a simple indicator.

9 Conclusions

9.1 Main findings of the thesis

For the purpose of characterizing and predicting ephemeral gully erosion across Wallonia, five specific questions have been addressed in the different chapters of the thesis. The main findings are summarized in the present section.

1) What is the uncertainty associated with ephemeral gully characteristics when using aerial photographs and what is the impact of this uncertainty on the topographic threshold for ephemeral gully initiation?

It has been shown that manual photo-interpretation can lead to a great variability related to ephemeral gully characterization (number, length, classification,…) depending on the operator. This caused a great variability in the resulting topographic thresholds for gully initiation. The quantile regression method was found to be one of the most robust thresholding methods. It is especially recommended when the level of uncertainty on the gully dataset is high.

2) What are the extent and characteristics of ephemeral gullies in Wallonia? What is the spatial and temporal variability of ephemeral gully erosion?

The spatial density of ephemeral gully erosion in cropland ranged from 0.17 to 0.31 km km^{-2} across the study areas. This is within the range of ephemeral gully densities reported by Nachtergaele and Poesen (1999) for the Flemish loess belt (0.21 to 1.33 km km^{-2}). In other parts of the world such as in Australia for instance, Hughes et al., (2011) reported smaller ephemeral gully densities ranging from 0.05 to 0.20 km km^{-2} whereas in Poland gully densities may reach up to 9 km km^{-2} (Rodzik and Gardziel, 2004). Besides differences

in density, the total length and dominant gully type were also found to vary across the agricultural areas. The main factor explaining differences in the dominant gully type was the general relief characterizing each agricultural area. In agricultural areas with rugged relief and steep slopes, gullies that developed on slopes without awell-defined flow concentration axes (Type 2) dominated. In areas with gentle relief and large valleys, gullies developed mainly on well-defined flow concentration axes such as thalwegs (Type 1). Gullies driven by anthropogenic factors (Type 3) were the least common whatever the study area. Type 2 gullies were on average significantly smaller than Type 1 and Type 3 gullies, Types 1 and 3 having similar mean lengths. The total number of gullies and gully length were much more important in the Loamy area due to the important acreage of cropland, the large mean field size and the limited presence of obstacles to halt ephemeral gullies. Whatever the agricultural area, gullies mainly developed on summer crops due to the combined effects of erosive rainfall and low vegetation cover in the late spring to early summer. The recurrence of gullies at the same location over time was shown to be low, most likely because of changes in crop type and climate variability from one year to another.

3) *What is the variability of the topographic threshold for ephemeral gully initiation across various agricultural areas in Wallonia and over the years?*

Among the tested thresholding methods, it was shown that quantile regression was the most appropriate for two main reasons. First, the quantile regression method is statistically-based and robust to outliers. Secondly, it allows defining a straight line consistent with the threshold concept because, unlike to the other thresholding methods, it is based on the distribution of the points at the boundary of the scatter plot. However, sufficiently large datasets should be used whenever possible because reliable estimates of the regression

parameters cannot be obtained for small datasets. A minimum of 50 data points seems to be needed to define reliable topographic thresholds when using quantile regression. The topographic thresholds defined using quantile regression highlighted the spatial variability of the topographic contexts leading to gullying across Wallonia. The observed differences appear to stem mostly from differences in the general relief of the study sites but could also be attributed in part to differences in topsoil rock fragment content. The topographic threshold defined using quantile regression appeared stable over time. This means that it was not affected by temporally variable factors such as crop type and climate.

4) What are the main factors controlling where ephemeral gullies end?

Gully end was mainly controlled by topography, changes in vegetation at field borders and linear landscape elements. It was not possible to identify accurately the topographic conditions leading to gully deposition using a critical slope threshold, a topographic threshold and a probabilistic approach based on slope variations. Crops with dense vegetation cover such as winter crops, grassland or grass strips were particularly effective at halting ephemeral gullies even on steep slopes. On the contrary, when a gully crossed a summer crop the probability to continue was high. Linear landscape elements were found to stop almost all ephemeral gullies. They were mainly roads or banks. However, hedges also played a non-negligible role in stopping gullies when their density was important such as in a bocage landscape structure. Large differences were found across regions in the distribution of the main factors causing gullies to end. They were attributed to differences in slope distributions and topsoil rock fragment contents but also to differences in the spatial organization of land use. Indeed, differences were marked between bocage and open-field type landscapes due to differences in mean field size, grassland acreage and density of linear landscape elements.

5) What is the best indicator for predicting ephemeral gully location based on the data readily available at Walloon scale?

Except for the unit stream power, all the tested topographic and hydraulic indicators identified the runoff flow concentration axes as being prone to ephemeral gully erosion. However, they did not allow discriminating between runoff flow concentration axes where the risk was high and those where the risk was low. Among the ephemeral gully erosion indicators, runoff volume was found to be the best but it did not allow predicting gully occurrence with a probability level > 34%. Furthermore, it was not able to identify most of the observed gullied locations. The poor results may result from the hydrological model used, which led to substantial error when predicting the runoff volume, but also from the resolution of the DEM as well as the non-inclusion of the main linear landscape elements.

9.2 Main recommendations for policy

With the current data and the tested models, gullying remains difficult to predict. However, the thesis provides relevant information regarding where and why ephemeral gullies form or stop. This information is useful to prevent on-site damages but also to protect downstream vulnerable sites such as roads and other infrastructures. It was shown that the topographic contexts favorable to gully initiation require a minimal runoff volume resulting from a combination of land use and rainfall. Because land managers cannot control topographic conditions and rainfall, they have to manage land use to avoid or limit gullying. For instance, it has been shown that that summer crops are much more sensitive to gully erosion than winter crops. Large fields were also found to enhance ephemeral gully erosion by increasing the hydrological connectivity in watersheds.

The contexts sensitive to gullying have to be managed taking into account the importance of the risk and the technical and economic constraints for farmers. First, agricultural practices affecting soil protection or soil structure and allowing a decreasing of runoff such as the maintaining of crop residue on soil surface, intercropping, no-tillage or reduced tillage have to be promoted. Land managers have also to find a compromise with famers by adapting the spatial distribution of land use, the acreage of summer crops and the field sizes. A balance has to be found between the factors affecting gully initiation by increasing or decreasing runoff volumes and those controlling gully expansion by creating favorable conditions or not to stop gullying. In most cases, an optimal solution might probably be to divide the watershed sensitive to gullying into a mosaic of small summer crop parcels alternating with winter crops or grassland. Furthermore, when possible, summer crops have not to be located where flow concentrates. However, such solutions are not always feasible or realistic. Therefore, changes in land use or landscape structures that could lead to an increase of ephemeral gully erosion have to be avoided. For example, the increase of maize acreage at the expense of grassland in the Ardenne and Région Herbagère is an important issue which should be addressed by land managers. The existing banks and hedges should also be maintained in bocage landscapes such as in the Jurassic area where they have been shown to significantly limit the expansion of gully erosion by decreasing the hydrological connectivity of the watersheds. Such measures could be supplemented with small hydraulic measures such as grass strips or brushwood dams to force gullies to stop, or ditches and grassed waterways to conduct concentrated flow in a secure and controlled manner. Finally, another key point to avoid damages to downstream sites caused by gully erosion is also to take into account the risk of gullying when installing a new house, road or other infrastructure.

9.3 Perspectives for future research

Two main issues related to the prediction of ephemeral gully occurrence and the uncertainty of gully identification when using aerial photographs have to be addressed in the future research.

1) How to reduce the uncertainty on gully identification when using aerial images?

It has been shown that gully characteristics and topographic thresholds for gully initiation are operator-dependent when extracting manually information from aerial photographs. It also affects results related to the prediction of ephemeral gully occurrence because there is an uncertainty on the datasets of gullies used for calibration and validation. The solution to avoid human subjectivity in image analysis might be to develop automated approaches to identify and delineate gullies. However, the training and validation datasets required to perform the automated schemes have to be acquired *in situ*. Three solutions can be considered. The first one is to continue working with aerial photographs and to collect as much data as possible on ephemeral gullies in the field at the time of the flights. However, in view of the low density of ephemeral gullies, vast territories have to be covered to obtain sufficient large dataset of field data. Furthermore, flights are not necessarily planned at the most relevant period with respect to gullying. The second solution consists in taking aerial photographs of known ephemeral gullies using UAVs. The automated scheme would be performed based on aerial images acquired through UAV. However, UAV cannot be used to cover vast territories. The automated scheme would be applied to the aerial photographs acquired yearly by the administration across the Walloon region. The automated scheme is expected to be relevant if the UAV aerial images are similar in terms of resolution and spectral characteristics to the aerial photographs acquired by

the administration. The last solution to create the training and validation datasets required to perform the automated scheme would be to order satellite images covering the area of interest of known ephemeral gullies. Ephemeral gullies could then objectively be extracted using the automated scheme on other satellite images. However, for most satellites, the cost of such images is high and the spatial resolution is still too low to allow for a proper gully detection and characterization. Nevertheless, satellites such as Pleiades, Geoye-2 and WorldView-3 currently provide panchromatic images at 50 cm, 34 cm and 31 cm resolution, respectively. In the future, it is expected that satellite images will become available at lower cost and with higher spatial resolution. Stereoscopy or 3D techniques could also be used to decrease the uncertainty when identifying ephemeral gullies. They could bring some useful information on the dimensions of the linear elements identified as potential ephemeral gullies. However, this probably requires high resolution images because ephemeral gullies can be less than 10 cm deep or 50 cm wide.

2) How to improve the prediction of ephemeral gully occurrence?

No ephemeral gully erosion indicator was found to be relevant to predict ephemeral gully occurrence. Currently, except for the unit stream power, all the tested indicators highlight all the runoff flow concentration axes as being potentially prone to gully development. However, gullies will form only if the critical tractive force of the concentrated flow is sufficient. This force depends in part on the quantity of water which results from the combination of land use and rainfall in the upstream area. The discrimination between potential gullied and ungullied flow concentration axes is therefore expected to be improved if the hydrological model to simulate runoff volume is improved. This could be done by integrating additional information on antecedent rainfall, soil moisture or rainfall characteristics (duration, intensity…). More rainfall-runoff volume data are also needed to improve the calibration of the

hydrological model. Furthermore, the prediction could be improved by combining the hydraulic indicators with the related critical soil parameters (e.g., flow shear stress vs. critical shear stress…) in order to take into account soil resistance to concentrated erosion. For that, more reliable and accurate soil data is required but also our knowledge regarding the effects of soil properties such as rock fragment content or clay content on soil resistance to gullying has to be improved.

Besides the improvement of the hydrological model, the prediction of gully occurrence is expected to be significantly improved by taking into account the main linear elements. Currently, the flow direction raster provided by the Walloon administration and used to define the location of the runoff flow concentration axes and the associated drainage areas, does not take into account the impact of linear elements for two main reasons: (i) the smallest landscape linear elements such as ditches, hedges or some banks are not visible given the DEM resolution, (ii) the flow direction raster is forced to pass through the roads while this is not always true. Finally, it is expected that the tillage direction affects gully trajectory and also the location of the ending points in some cases.

Appendix – Derivation of Equation 8-16

For a semi-circular cross-section of radius *r* [m] that is less than half-filled (Figure 8-1), and assuming steady-state flow described by Manning's equation (Equation 8-14), it can be observed graphically that a perfect linear relationship exists between the logarithm of water height H and the logarithm of $(\frac{Q*n}{S^{0.5}})$ (Figure A-1). This relationship is valid for any value of the Manning roughness coefficient *n* and the slope *S*, and can be expressed as Equation A-1:

$$\mathrm{Log(H)} = \mathrm{a(r)} * \mathrm{Log}(\frac{Q*n}{S^{0.5}}) + \mathrm{b(r)} \qquad \text{(A-1)}$$

Knowing the discharge *Q*, the slope gradient *S*, and the Gauckler-Manning coefficient *n*, for any given location, *H* can thus be calculated. However, the *a* and *b* coefficients depend on the value of *r* (Figures A-2 and A-3). The *a* coefficient decreases towards an asymptotic value as a power function (Figure A-2, Equation A-2) whereas the *b* coefficient decreases exponentially (Figure A-3, Equation A-3).

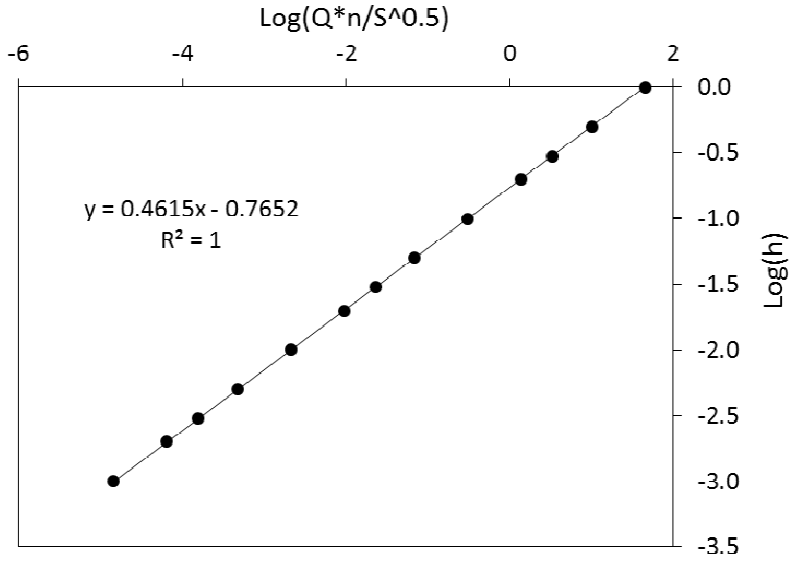

Figure A-1: Relation between log(H) and log($\frac{Q * n}{S^{0.5}}$) for a radius of 1000 m

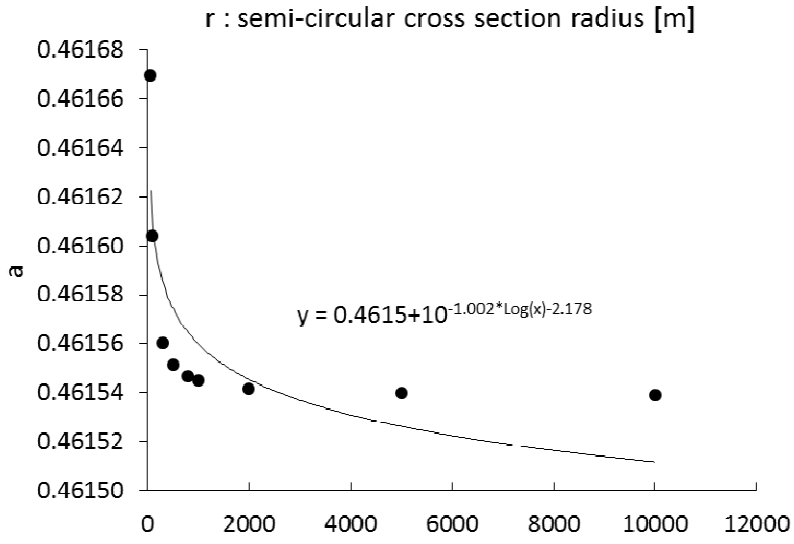

Figure A-2: Relation between the *a* coefficient and the semi-circular cross section radius.

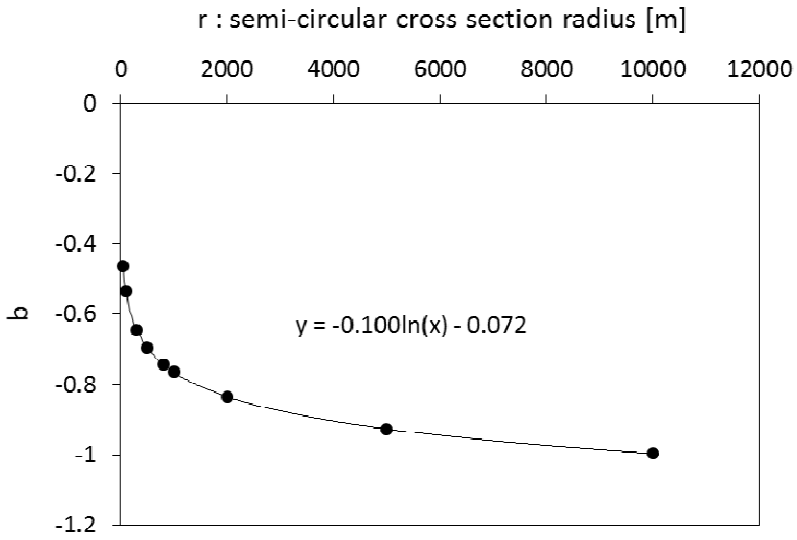

Figure A-3: Relation between the *b* coefficient and the semi-circular cross section radius.

$$a = 0.4615 + 10^{-1.002 * Log(r) - 2.178} \qquad \text{(A-2)}$$

$$b = -0.100 * Ln(r) - 0.072 \qquad \text{(A-3)}$$

Equation A-1 can therefore be rewritten as Equation A-4 which is also the Equation 8-16:

$$Log(H) = (0.4615 + 10^{-Log(r) - 2.178}) \cdot Log(\frac{Q_p \cdot n}{S^{0.5}}) - 0.10 \cdot Ln(r) - 0.072 \qquad \text{(A-4)}$$

Rounding off of Equation A-4 leads to no substantial loss in accuracy :

$$Log(H) = 0.46\ Log(\frac{Q_p \cdot n}{S^{0.5}}) - 0.10 \cdot Ln(r) - 0.072 \qquad \text{(A-5)}$$

For 10 < r < 10 000 m, H is estimated with an accuracy of better than 2% for 0.01 < h < 1 m.

References

Arcement Jr, G.J. and Schneider, V.R., 2008. Guide for Selecting Manning's Roughness Coefficients for Natural Channels and Flood Plains. US Geological Survey.

Baveye, P.C., Laba, M., Otten, W., Bouckaert, L., Dello Sterpaio, P., Goswami, R.R., Grinev, D., Houston, A., Hu, Y., Liu, J., Mooney, S., Pajor, R., Sleutel, S., Tarquis, A., Wang, W., Wei, Q. and Sezgin, M., 2010. Observer-dependent variability of the thresholding step in the quantitative analysis of soil images and X-ray microtomography data. Geoderma, 157(1-2): 51-63.

Bennett, S., Casali, J., Robinson, K. and Kadavy, K., 2000. Characteristics of actively eroding ephemeral gullies in an experimental channel. Transactions of the ASAE, 43(3): 641-649.

Beuselinck, L., Steegen, A., Govers, G., Nachtergaele, J., Takken, I. and Poesen, J., 2000. Characteristics of sediment deposits formed by intense rainfall events in small catchments in the Belgian Loam Belt. Geomorphology, 32(1): 69-82.

Bielders, C.L., Ramelot, C. and Persoons, E., 2003. Farmer perception of runoff and erosion and extent of flooding in the silt-loam belt of the Belgian Walloon Region. Environmental Science & Policy, 6(1): 85-93.

Boardman, J. and Bell, M., 1992. Current erosion on the South Downs: implication for the past. In, Bell, M. and Boardman, J., (eds), Past and present soil erosion: archaeological and geographical perspectives. Oxbow Books Ltd, Oxford pp 9-19.

Brice, J.C., 1966. Erosion and deposition in the loess-mantled Great Plains, Medicine Creek drainage basin, Nebraska. US Government Printing Office.

Bryan, R.B., 2000. Soil erodibility and processes of water erosion on hillslope. Geomorphology, 32(3): 385-415.

Cazier, D.J. and Hawkins, R.H., 1984. Regional application of the curve number method. Proceedings Speciality Conference, Irrigation and Drainage Division, American Society of Civil Enginners. Flagstaff, AZ. abstract p710.

Chaplot, V., Giboire, G., Marchand, P. and Valentin, C., 2005. Dynamic modelling for linear erosion initiation and development under climate and land-use changes in northern Laos. Catena, 63(2-3): 318-328.

Congalton, R.G., 1991. Remote Sensing and Geographic Information System Data Integration: Error Sources and. Photogrammetric Engineering & Remote Sensing, 57(6): 677-687.

Conoscenti, C., Angileri, S., Cappadonia, C., Rotigliano, E., Agnesi, V. and Märker, M., 2014. Gully erosion susceptibility assessment by means of GIS-based logistic regression: A case of Sicily (Italy). Geomorphology, 204: 399-411.

Cade, B.S. and Noon, B.R., 2003. A gentle introduction to quantile regression for ecologists. Frontiers in Ecology and the Environment, 1(8): 412-420.

Casalı, J., López, J. and Giráldez, J., 1999. Ephemeral gully erosion in southern Navarra (Spain). Catena, 36(1): 65-84.

Daba, S., Rieger, W. and Strauss, P., 2003. Assessment of gully erosion in eastern Ethiopia using photogrammetric techniques. Catena, 50(2): 273-291.

Demarcin, P., Degré, A., Smoos, A. and Dautrebande, S., 2009. Projet ERRUISSOL. Cartographie numérique des zones à risque de ruissellement et d'érosion des sols en région wallonne. Rapport final de convention DGO3-FUSAGx. Gembloux, Belgique: Unité d'hydrologie et hydraulique agricole, Faculté universitaire des Sciences agronomiques de Gembloux. 55p.

Demarcin, P., Sohier, C., Mokadem, A.I., Dautrebande, S. and Degré, A., 2011. Essai de cartographie des classes d'infiltrabilité des sols de Wallonie (Belgique). Biotechnol. Agron. Soc, 15: 119-128.

De Ploey, J., 1984. Hydraulics of runoff and loess loam deposition. Earth surface processes and landforms, 9(6): 533-539.

De Santisteban, L., Casalí, J. and López, J., 2005. Evaluation of rill and ephemeral gully erosion in cultivated areas of Navarre (Spain). International Journal of Sediment Research, 20(3): 270.

De Santisteban, L., Casalí, J. and López, J., 2006. Assessing soil erosion rates in cultivated areas of Navarre (Spain). Earth Surface Processes and Landforms, 31(4): 487-506.

Desmet, P. and Govers, G., 1997. Two-dimensional modelling of the within-field variation in rill and gully geometry and location related to topography. Catena, 29(3): 283-306.

Desmet, P., Poesen, J., Govers, G. and Vandaele, K., 1999. Importance of slope gradient and contributing area for optimal prediction of the initiation and trajectory of ephemeral gullies. Catena, 37(3): 377-392.

Dube, F., Nhapi, I., Murwira, A., Gumindoga, W., Goldin, J. and Mashauri, D.A., 2014. Potential of weight of evidence modelling for gully erosion hazard assessment in Mbire District – Zimbabwe. Physics and Chemistry of the Earth, Parts A/B/C, 67-69: 145-152.

Elliot, W. and Laflen, J., 1993. A process--based rill erosion model. Transactions of the ASABE, 36(1): 65-72.

Eustace, A.H., Pringle and M.J., Denham, R.J., 2011. A risk map for gully locations in central Queensland, Australia. European Journal of Soil Science, 62(3): 431-441.

Evrard, O., Bielders, C.L., Vandaele, K. and van Wesemael, B., 2007. Spatial and temporal variation of muddy floods in central Belgium, off-site impacts and potential control measures. Catena, 70(3): 443-454.

Evrard, O., Vandaele, K., Bielders, C. and Wesemael, B.v., 2008. Seasonal evolution of runoff generation on agricultural land in the Belgian loess belt and implications for muddy flood triggering. Earth Surface Processes and Landforms, 33(8): 1285-1301.

Flanagan, D. and Nearing, M., 1995. USDA-Water Erosion Prediction Project: Hillslope profile and watershed model documentation. National Soil Erosion Research Laboratory, West Lafayette, Indiana, Report No 10.

Foster, G., 1982. Modeling the erosion process. In, In Hann C.T. (ed.) Poesen, J. (eds), Hydrologic modeling of small watersheds. ASAE Monograph No.5, St Joseph, Michigan. pp 296-360.

Gallop, R.J., Crits-Christoph, P., Muenz, L.R. and Tu, X.M., 2003. Determination and Interpretation of the Optimal Operating Point for

ROC Curves Derived Through Generalized Linear Models. Understanding Statistics 2(4): 219-242.

Gardin, S., van Laere, S.M., van Coillie, F.M., Anseel, F., Duyck, W., de Wulf, R.R. and Verbeke, L.P., 2011. Remote sensing meets psychology: a concept for operator performance assessment. Remote Sensing Letters, 2(3): 251-257.

Gilleland, M.E., 2012. Verification. R Package Version 1.41, http://www.cran.r-project.org.

Goudenhoofdt, E. and Delobbe, L., 2009. Evaluation of radar-gauge merging methods for quantitative precipitation estimates. Hydrology and Earth System Sciences, 13(2): 195-203.

Govers, G., Everaert, W., Poesen, J., Rauws, G., De Ploey, J. and Lautridou, J., 1990. A long flume study of the dynamic factors affecting the resistance of a loamy soil to concentrated flow erosion. Earth Surface Processes and Landforms, 15(4): 313-328.

Govers, G., 1992. Relationship between discharge, velocity and flow area for rills eroding loose, non-layered materials. Earth Surface Processes and Landforms, 17(5): 515-528.

Gutiérrez, Á.G., Schnabel, S. and Contador, F.L., 2009. Gully erosion, land use and topographical thresholds during the last 60 years in a small rangeland catchment in SW Spain. Land Degradation & Development, 20(5): 535-550.

Hauge, C., 1977. Soil erosion definitions. California Geology 30: 202-203.

Hawkins, R.H. and Khojeini, A.V., 2000. Initial abstraction and loss in the curve number method. proceedings Arizona Hydrological Society. (abstract).

Hawkins, R.H., Ward, T.J., Woodward, D.E. and Van Mullem, J.A., 2009. Curve number hydrology. ASCE publication.

Horton, R.E., 1945. Erosional development of streams and their drainage basins; hydrophysical approach to quantitative morphology. Geological society of America bulletin, 56(3): 275-370.

Hughes, A.O., Prosser, I.P., Stevenson, J., Scott, A., Lu, H., Gallant, J. and Moran, C.J., 2001. Gully erosion mapping for the national land and water resources audit. CSIRO Land and Water.

Imeson, A. and Kwaad, F., 1980. Gully types and gully prediction. Geografisch Tijdschrift, 14(5): 430-441.

Ireland, H.A., Sharpe, C.F.S. and Eargle, D., 1939. Principles of gully erosion in the Piedmont of South Carolina. US Dept. of Agriculture Bulletin 633. 142 pp.

Istanbulluoglu, E., Tarboton, D.G., Pack, R.T. and Luce, C., 2002. A probabilistic approach for channel initiation. Water Resources Research, 38(12): 61-1-61-14.

Jetten, V., Poesen, J., Nachtergaele, J. and Van de Vlag, D., 2006. Spatial Modelling of Ephemeral Gully Incision: a Combined Empirical and Physical Approach. In, Owens, P.N. and Collins, A.J.(eds,.), Soil erosion and sediment redistribution in river catchments: measurement, modelling and management, CABI International, Wallingford pp. 209–220

John, O. and Nduka, E., 2009. Quantile Regression Analysis As a Robust Alternative to Ordinary Least Squares. The Journal of Scientia Africana, 8(2): 61-65.

Kakembo, V., Xanga, W.W. and Rowntree, K., 2009. Topographic thresholds in gully development on the hillslopes of communal areas in Ngqushwa Local Municipality, Eastern Cape, South Africa. Geomorphology, 110(3-4): 188-194.

Knapen, A., Poesen, J. and Debaets, S., 2007a. Seasonal variations in soil erosion resistance during concentrated flow for a loess-derived soil under two contrasting tillage practices. Soil and Tillage Research, 94(2): 425-440.

Knapen, A., Poesen, J., Govers, G., Gyssels, G. and Nachtergaele, J., 2007b. Resistance of soils to concentrated flow erosion: A review. Earth-Science Reviews, 80(1-2): 75-109.

Knight, J., Spencer, J., Brooks, A. and Phinn, S., 2007. Large-area, high-resolution remote sensing based mapping of alluvial gully erosion in Australia's tropical rivers, Proceedings of the 5th Australian Stream Management Conference, pp. 199-204.

Knisel, W.G., 1980. CREAMS: A field-scale model for chemicals, runoff and erosion from agricultural management systems. USDA Conservation Research Report(26).

Knisel, W.G., 1993. GLEAMS: Groundwater Loading Effects of Agricultural Management Systems: Version 2.10. University of Georgia Coastal Plain Experiment Station, Bio. & Ag. Engineering.

Koenker, R. and Bassett Jr, G., 1978. Regression quantiles. Econometrica: journal of the Econometric Society: 33-50.

Koenker, R., 1994. Confidence intervals for quantile regression. In: Proceedings of the Fifth Prague Symposium on Asymptotic Statistics. Physica-Verlag, Heidelberg, pp. 10–20.

Koenker, R. and Hallock, K., 2001. Quantile regression: An introduction. Journal of Economic Perspectives, 15(4): 43-56.

Koenker, R.W., 2012. Quantreg: Quantile Regression. R Package Version 4.76, http://www.cran.r-project.org.

Langran, K., 1983. Potential for monitoring soil erosion features and soil erosion modeling components from remotely sensed data. Proceedings of IGARSS'83, IEEE, San Francisco, CA (1983), pp. 2.1–2.4

Le Bissonnais, Y., Cerdan, O., Lecomte, V., Benkhadra, H., Souchère, V. and Martin, P., 2005. Variability of soil surface characteristics influencing runoff and interrill erosion. Catena, 62(2-3): 111-124.

Leckie, D.G., Gougeon, F.A., Walsworth, N. and Paradine, D., 2003. Stand delineation and composition estimation using semi-automated individual tree crown analysis. Remote Sensing of Environment, 85(3): 355-369.

Legros, J., Kolbl, O. and Falipou, P., 1996. Delimitation d'unites de paysage sur des photographies aeriennes. Etude et Gestion des Sols, 3: 113-124.

Lunetta, RS, Congalton, RG, Fenstermaker, LK, Jensen, JR, McGwire, KC and Tinney LR. 1991. Remote sensing and geographic information system data integration: error sources and research issues Photogrammetric Engineering & Remote Sensing 57 (6), 677-687.

Makanzu Imwangana, F., Dewitte, O., Ntombi, M. and Moeyersons, J., 2014. Topographic and road control of mega-gullies in Kinshasa (DR Congo). Geomorphology, 217: 131-139.

Martınez-Casasnovas, J., 2003. A spatial information technology approach for the mapping and quantification of gully erosion. Catena, 50(2): 293-308.

Maugnard, A., Bielders, C., Bock, L., Colinet, G., Cordonnier, H., Degré, A., Demarcin, P., Dewez, A., Feltz, N. and Legrain, X., 2013. Cartographie du risque d'érosion hydrique à l'échelle parcellaire en soutien à la politique agricole wallonne (Belgique). Etudes et Gestion des Sols, 20: 127-141.

Maugnard, A., Van Dyck, S. and Bielders, C., 2014. Assessing the regional and temporal variability of the topographic threshold for ephemeral gully initiation using quantile regression in Wallonia (Belgium). Geomorphology, 206: 165-177.

Maugnard, A., Cordonnier, H., Degre, A., Demarcin, P., Pineux, N. and Bielders, C.L., 2014. Uncertainty assessment of ephemeral gully identification, characteristics and topographic threshold when using aerial photographs in agricultural settings. Earth Surface Processes and Landforms, 39:1319-1330.

Merkel, W., Woodward, D. and Clarke, C., 1988. Ephemeral gully erosion model (EGEM). Modelling Agricultural, Forest, and Rangeland Hydrology. American Society of Agricultural Engineers Publication 07-88, 315–323.

Momm, H., Bingner, R., Wells, R. and Wilcox, D., 2012. AGNPS GIS-based tool for watershed-scale identification and mapping of cropland potential ephemeral gullies. Applied engineering in agriculture, 28, 1–13

Montgomery, D.R. and Dietrich, W.E., 1988. Where do channels begin? Nature, 336(6196): 232-234.

Montgomery, D.R. and Dietrich, W.E., 1992. Channel initiation and the problem of landscape scale. Science, 255(5046): 826-830.

Moore, I., Burch, G. and Mackenzie, D., 1988. Topographic effects on the distribution of surface soil water and the location of ephemeral gullies. Transactions of the ASAE, 32 (4), 1098–1107.

Morgan, R., Quinton, J. and Rickson, R., 1992. EUROSEM documentation manual. Silsoe College, Silsoe, UK.

Morgan, R.P.C., 2009. Soil erosion and conservation. John Wiley & Sons.

Nachtergaele, J. and Poesen, J., 1999. Assessment of soil losses by ephemeral gully erosion using high-altitude (stereo) aerial photographs. Earth Surface Processes and Landforms, 24(8): 693-706.

Nachtergaele, J., Poesen, J., Steegen, A., Takken, I., Beuselinck, L., Vandekerckhove, L. and Govers, G., 2001. The value of a physically based model versus an empirical approach in the prediction of ephemeral gully erosion for loess-derived soils. Geomorphology, 40(3): 237-252.

Nachtergaele, J., Poesen, J., Sidorchuk, A. and Torri, D., 2002. Prediction of concentrated flow width in ephemeral gully channels. Hydrological Processes, 16(10): 1935-1953.

Nachtergaele, J. and Poesen, J., 2002. Spatial and temporal variations in resistance of loess-derived soils to ephemeral gully erosion. European Journal of Soil Science, 53(3): 449-463.

NRCS, U., 2004. National Engineering Handbook: Part 630—Hydrology. USDA Soil Conservation Service: Washington, DC, USA.

Parkner, T., Page, M.J., Marutani, T. and Trustrum, N.A., 2006. Development and controlling factors of gullies and gully complexes, East Coast, New Zealand. Earth Surface Processes and Landforms, 31(2): 187-199.

Pasqualini, V., Pergent-Martini, C., Clabaut, P., Marteel, H. and Pergent, G., 2001. Integration of aerial remote sensing, photogrammetry, and GIS technologies in seagrass mapping. Photogrammetric Engineering and Remote Sensing, 67(1): 99-105.

Patton, P.C. and Schumm, S.A., 1975. Gully erosion, Northwestern Colorado: a threshold phenomenon. Geology, 3(2): 88-90.

Poesen, J. and Govers, G., 1990. Gully erosion in the loam belt of Belgium: typology and control measures. In, Boardman, J., Foster, I.D.L. and Dearing, J.A. (eds), Soil erosion on agricultural land. Wiley, Chicester. pp 513-530.

Poesen, J., Vandaele, K. and Van Wesemael, B., 1996. Contribution of gully erosion to sediment production on cultivated lands and rangelands. IAHS Publications 236, 251–266.

Poesen, J., Vandaele, K. and van Wesemael, B., 1998. Gully erosion: importance and model implications. In, Boardman, J. and Favis-Mortlock, D.T. (eds.), Modelling Soil Erosion by Water Springer-Verlag, Berlin NATO-ASI Series, I-55:285-311 Modelling soil erosion by water. Springer, pp. 285-311.

Poesen, J., Vandekerckhove, L., Nachtergaele, J., Wijdenes, D.O., Verstraeten, G. and van Wesemael, B., 2002. Gully erosion in dryland environments.In: Bull, L.J. and Kirkby, M.J. (eds.), Dryland Rivers: Hydrology and Geomorphology of Semi-Arid Channels. Wiley, Chichester, UK, pp. 229–262.

Poesen, J., Nachtergaele, J., Verstraeten, G. and Valentin, C., 2003. Gully erosion and environmental change: importance and research needs. Catena, 50(2): 91-133.

Poesen, J., Vanwalleghem, T., de Vente, J., Knapen, A., Verstraeten, G. and Martínez-Casasnovas, J.A., 2006. Gully erosion in Europe. In, Boardman, J., and Poesen, J. (eds), Soil erosion in Europe. Wiley, Chicester. pp 515-536.

Poesen, J., Torri, D. and Vanwalleghem, T., 2011. Gully Erosion: Procedures to Adopt When Modelling Soil Erosion in Landscapes Affected by Gullying. In Morgan R.P.C. and Nearing M.A. (eds.), Handbook of Erosion Modelling, Blackwell Publishing Ltd, Chichester (2011), pp. 360–386

Powell, R. and Matzke, N., 2004. Sources of error in accuracy assessment of thematic land-cover maps in the Brazilian Amazon. Remote Sensing of Environment, 90(2): 221-234.

Riddle, D.L. and Stratford, P.W., 1999. Interpreting validity indexes for diagnostic tests: an illustration using the Berg Balance Test. Physical Therapy 79,:939-950.

Robin, X., Turck, N., Hainard, A., Tiberti, N., Lisacek, F., Sanchez, J. and Müller, M., 2014. pROC. R Package Version 1.7.3, http://www.cran.r-project.org.

Rodzik, J. and Gardziel,Z., 2004. Landscape lay-out of Kazimierz Dolny gullies (in Polish). In Kucharczyk, M. (eds), Present-day problems of landscape protection. ZZ LPK, Lublin. pp 85-92.

Rossi M., 2014. Modeling of landslide phenomena and erosion processes triggered by meteo-climatic factors. PhD Thesis. Università degli Studi di Perugia, Facoltà di Scienze MM. FF. NN - Dipartimento di Scienze della Terra. Dottorato di Ricerca in Scienze della Terra e Geotecnologie. XXVII ciclo – A.A. 2011/2012. DOI: 10.13140/2.1.3835.0404.
https://www.researchgate.net/publication/269111851_Modeling_of_landslide_phenomena_and_erosion_processes_triggered_by_meteo-climatic_factors.

Saito, H., Nakayama, D., Matsuyama, H., 2010. Relationship between the initiation of a shallow landslide and rainfall intensity—duration thresholds in Japan. Geomorphology, 118(1): 167-175.

Sarmento, P., Carrão, H., Caetano, M., Stehman, S.V., 2009. Incorporating reference classification uncertainty into the analysis of land cover accuracy. International Journal of Remote Sensing, 30(20): 5309-5321.

Sidorchuk, A., Litvin, L., Golosov, V. and Chernysh, A. I., 2006. European Russia and Byelorus: chap. 1.8. In, Boardman, J., and Poesen, J. (eds), Soil erosion in Europe. Wiley, Chicester. pp 72-93.

Schumm, S.A., 1979. Geomorphic thresholds: the concept and its applications. Transactions of the Institute of British Geographers: 485-515.

Shruthi, R.B.V., Kerle, N., Jetten, V., 2011. Object-based gully feature extraction using high spatial resolution imagery. Geomorphology, 134(3-4): 260-268.

Smith, H.T.U., 1943. Aerial photographs and their applications. Appleton Century Crofts, New York (1943).

Sohier, C., Degré, A. and Dautrebande, S., 2009. From root zone modelling to regional forecasting of nitrate concentration in recharge flows – the case of the Walloon region (Belgium). Journal of Hydrology 369, 350-359.

Soil Science Society of America., 2001. Glossary of Soil Science Terms, Soil Science Society of America, Madison, WI.

Spitalnic, S., 2004. Test properties 2: likelihood ratios, Bayes' formula, and receiver operating characteristic curves. Hospital Physician, 40(10): 53-58.

Stall, J.B., 1985. Upland erosion and downstream sediment delivery. In, El-Swaify, S.A., Moldenhauer,W.C. and Lo,A. (eds.), Soil Erosion and Conservation. Soil Conservation Society of America, Ankeny, IA, pp. 200–205.

Steegen, A., Govers, G., Takken, I., Nachtergaele, J., Poesen, J. and Merckx, R., 2001. Factors controlling sediment and phosphorus export from two Belgian agricultural catchments. Journal of Environmental Quality, 30(4): 1249-1258.

Takken, I., Beuselinck, L., Nachtergaele, J., Govers, G., Poesen, J. and Degraer, G., 1999. Spatial evaluation of a physically-based distributed erosion model (LISEM). Catena, 37(3): 431-447.

Te Chow, V., 1959. Open channel hydraulics. Mc-Graw Hill, New York .

Thierry, B. and Lowell, K., 2001. An uncertainty-based method of photointerpretation. Photogrammetric engineering and remote sensing, 67(1): 65-72.

Thorne, C., Zevenbergen, L.W., Grissinger, E. and Murphey, J., 1986. Ephemeral gullies as sources of sediment, Proceedings of the Fourth Federal Interagency Sedimentation Conference March 24-27, 1986, Las Vegas, Nevada.

Tiscareno-Lopez, M., Lopes, V., Stone, J. and Lane, L., 1994. Sensitivity analysis of the WEPP watershed model for rangeland applications. II. Channel processes. Transactions of the ASAE, 37(1): 151–158.

Torri, D. and Poesen, J., 2014. A review of topographic threshold conditions for gully head development in different environments. Earth-Science Reviews, 130: 73-85.

Toy, T.J., Foster, G.R. and Renard, K.G., 2002. Soil erosion: processes, prediction, measurement, and control. John Wiley & Sons. New York (2002) 338 pp.

Trimble, S.W., 1999. Decreased rates of alluvial sediment storage in the Coon Creek Basin, Wisconsin, 1975-93. Science, 285(5431): 1244-1246.

Valentin, C., Poesen, J. and Li, Y., 2005. Gully erosion: Impacts, factors and control. Catena, 63(2-3): 132-153.

Vandaele, K., Poesen, J., 1995. Spatial and temporal patterns of soil erosion rates in an agricultural catchment, central Belgium. Catena, 25(1): 213-226.

Vandaele, K. 1996. Temporele en ruimtelijkedynamiek van bodemerosieprocesseninlandelijkestroomgebieden (Midden-Belgie). Unpubl. PhD Thesis, K.U.Leuven.

Vandaele, K., Poesen, J., Govers, G., Wesemael, B.v., 1996. Geomorphic threshold conditions for ephemeral gully incision. Geomorphology, 16(2): 161-173.

Vandaele, K., Poesen, J., Marques da Silva, J., Govers, G., Desmet, P., 1997. Assessment of factors controlling ephemeral gully erosion in

Southern Portugal and Central Belgium using aerial photographs. Zeitschrift fur geomorphologie, 41(3): 273-287.

Vandekerckhove, L., Poesen, J., Oostwoud Wijdenes, D., De Figueiredo, T., 1998. Topographical thresholds for ephemeral gully initiation in intensively cultivated areas of the Mediterranean. Catena, 33(3): 271-292.

Vandekerckhove, L., Poesen, J., Oostwoud-Wijdenes, D., Nachtergaele, J., Kosmas, D., Roxo, M. and Figueiredo, T.d., 2000. Thresholds for gully initiation and sedimentation in Mediterranean Europe. Earth Surface Processes and Landforms 25: 1201–1220.

Van Oost, K., 2003. Spatially distributed modelling of surface runoff. PhD thesis, K.U. Leuven.

Van Oost, K., Govers, G., Cerdan, O., Thauré, D., Van Rompaey, A., Steegen, A., Nachtergaele, J., Takken, I. and Poesen, J., 2005. Spatially distributed data for erosion model calibration and validation: The Ganspoel and Kinderveld datasets. Catena, 61(2): 105-121.

Vanwalleghem, T., Van Den Eeckhaut, M., Poesen, J., Deckers, J., Nachtergaele, J., Van Oost, K. and Slenters, C., 2003. Characteristics and controlling factors of old gullies under forest in a temperate humid climate: a case study from the Meerdaal Forest (Central Belgium). Geomorphology, 56(1): 15-29.

Vanwalleghem, T., Poesen, J., Nachtergaele, J. and Verstraeten, G., 2005a. Characteristics, controlling factors and importance of deep gullies under cropland on loess-derived soils. Geomorphology, 69(1-4): 76-91.

Vanwalleghem, T., Bork, H.R., Poesen, J., Schmidtchen, G., Dotterweich, M., Nachtergaele, J., Bork, H., Deckers, J., Brüsch, B., Bungeneers, J. and De Bie, M., 2005b. Rapid development and infilling of a buried gully under cropland, central Belgium. Catena, 63(2-3): 221-243.

Verstraeten, G. and Poesen, J., 1999. The nature of small-scale flooding, muddy floods and retention pond sedimentation in central Belgium. Geomorphology, 29(3): 275-292.

Verstraeten, G., Poesen, J., Govers, G., Gillijns, K., Bielders, C., Goossens, D., Ruysschaert, G., Van Den Eeckhout, M. and Vanwalleghem, T., 2006. Belgium: chap. 1.30. In, Boardman, J., and Poesen, J. (eds), Soil erosion in Europe. Wiley, Chicester. pp 385-411.

Voloschuk, M.D. and Ionita, I., 2006. Moldavia: chap. 1.15. In, Boardman, J., and Poesen, J. (eds), Soil erosion in Europe. Wiley, Chicester. pp 183-197.

Wantzen, K.M., 2006. Physical pollution: effects of gully erosion on benthic invertebrates in a tropical clear-water stream. Aquatic Conservation: Marine and Freshwater Ecosystems, 16(7): 733-749.

Woodward, D., 1999. Method to predict cropland ephemeral gully erosion. Catena, 37(3): 393-399.

Wu, Y., Cheng, H., 2005. Monitoring of gully erosion on the Loess Plateau of China using a global positioning system. Catena, 63(2-3): 154-166.

Yang, C.T., 1977. The movement of sediment in rivers. Geophysical surveys, 3(1): 39-68.

Yen, B. C., 1992. Hydraulic resistance in open channels, in Channel Flow Resistance: Centennial of Manning's Formula. Water Resour. Publ., Highlands Ranch, Colorado.

Zhou, W., Schwarz, K., Cadenasso, M., 2010. Mapping urban landscape heterogeneity: agreement between visual interpretation and digital classification approaches. Landscape ecology, 25(1): 53-67.

List of publications

Publications in international peer-reviewed journals

- Maugnard, Alexandre, Bielders, Charles, Bock, Laurent ; Colinet, Gilles, Cordonnier, Hélène, Degré, Aurore, Demarcin, Pierre, Dewez, Arnaud, Feltz, Nicolas, Legrain, Xavier, Pineux, Nathalie, Mokadem, Abdel Ilah. Cartographie du risque d'érosion hydrique à l'échelle parcellaire en soutien à la politique agricole wallonne (Belgique). In: Etudes et Gestion des Sols, Vol. 20, no.2, p. 127-141 (September 2013). http://hdl.handle.net/2078.1/134887

- Maugnard, Alexandre, Van Dyck, Senne, Bielders, Charles. Assessing the regional and temporal variability of the topographic threshold for ephemeral gully initiation using quantile regression in Wallonia (Belgium). In: Geomorphology, Vol. 206, p. 165-177. doi:10.1016/j.geomorph.2013.10.007. http://hdl.handle.net/2078.1/134885

- Maugnard, Alexandre, Cordonnier, Hélène, Degre, Aurore, Demarcin, Pierre, Pineux, Nathalie, Bielders, Charles. Uncertainty assessment of ephemeral gully identification, characteristics and topographic threshold when using aerial photographs in agricultural settings. *In:* Earth Surface Processes and Landforms, Vol. 39, no. 10, p. 1279-1420. doi:10.1002/esp.3526. http://hdl.handle.net/2078.1/139532

International conference proceedings

- Maugnard, Alexandre, Cordonnier, Hélène, Degré, Aurore, Demarcin, Pierre, Pineux, Nathalie, Bielders, Charles. Operator-dependance of ephemeral gully characterization when using aerial photographs. 6th International Symposium on Gully Erosion in a

Changing World (ISGE) (Iasi, Romania, 6-12 May 2013). In: Book of abstracts, 2013, p. 36. http://hdl.handle.net/2078.1/128676

- Maugnard, Alexandre, Bielders, Charles, Van Dyck, Senne, Cordonnier, Hélène, Mokadem, Abdel Ilah. Integrating environmental information in gully initiation topographic thresholds: application to three regions of Wallonia (Belgium). 4th International Congress EUROSOIL (Bari, Italy, 2-6 July 2012). In: Proceedings, 2012, p. 163, S04.02a-3. http://hdl.handle.net/2078.1/112594

Internal report

- Bielders, Charles, Feltz, Nicolas, Cordonnier, Hélène, Maugnard, Alexandre, Degré, Aurore, Colard, François, Destain, Marie-France. Convention GISER (Gestion Intégrée Sol Erosion Ruissellement): rapport final, 2011. 181 p. (et annexes). http://hdl.handle.net/2078.1/95322

Summary

Ephemeral gully erosion is responsible for large soil losses in agricultural settings. It contributes to a loss of agronomic value of the soil and causes severe damage to crops. It also induces an increased workload for farmers. By increasing the connectivity in the landscape, the development of ephemeral gullies also enhances sediment delivery to downstream sites. This aggravates off-site effects such as muddy floods and pollution of watercourses by sediment and associated contaminants. In Belgium most studies on ephemeral gully erosion have been performed in the loess belt of Flanders and little information are available for Wallonia. The aim of the thesis was to characterize and predict the occurrence of ephemeral gully erosion in Wallonia in order to improve our understanding of the phenomenon and to suggest relevant mitigation techniques. Gully identification based on interpretation of aerial photographs was shown to be operator-dependent and to affect gully characterization. The number, total length, dominant type as well as topographic conditions leading to gullying were found to vary greatly across Wallonia. A new, more robust method was proposed to characterize the topographic contexts prone to ephemeral gully initiation. The main factors controlling ephemeral gully ending and their spatial variability were also identified. This information may prove useful to manage gully erosion in watersheds sensitive to gullying. The occurrence of ephemeral gully erosion was predicted using a set of topographic or hydraulic indicators. However, their performances were moderate at best. This may be improved in the future by using high resolution DEMs and by ameliorating the hydrological production and transfer functions used. It may also be necessary to integrate information on linear landscape elements and tillage direction.